THE USE OF PSEUDO-RANDOM BINARY SEQUENCES IN GAS CHROMATOGRAPHY

by

GEOFFREY C. MOSS.

A Thesis presented for the degree of Doctor of Philosophy of the University of Warwick, Department of Engineering Science.

February 1971.

ACKNOWLEDGEMENTS

The author would like to express his sincere thanks to all those who have been associated with the various sections of this research programme. In particular, K.C. Ng., B.Sc., Ph.D., is to be warmly thanked for his spirit of encouragement and helpful discussions. The cooperation of Hewlett Packard Ltd., South Queensferry, has been sought at various times and the author is grateful for the facilities extended to him.

February 1971.

To: FRANCES WENDY, my wife.

Thus the prospects open up for the construction of a new method of physical separation of various substances present in organic liquids. The method is based on the ability of soluble substance to mix with various solid mineral and organic substances to form physical adsorption compounds.....

Similarly to light beams in the spectrum the different components of a complex pigment are regularly distributed one after another in the adsorption column and thus lend themselves to qualitative and quantitative analysis. I have called such a multi-coloured preparation a CHROMATOGRAM and the respective method of analysis a CHROMATOGRAPHIC METHOD....

Mikhail Semenovitch Tswett
1872 - 1919.

ABSTRACT.

Techniques of conventional chromatography do not always give convenient results. Analyses are often contaminated with detector noise and baseline drift. Continuous analysis is not possible and anomalous detector response can occur. This report proposes a method which overcomes these difficulties to a certain degree. A pseudo-random sequence controls the injections into a conventional column. Crosscorrelation between input and output yields the chromatogram to within a constant factor. Sample valve and detector must be operated in a linear fashion. The resultant data analysis requires digital computation, but this can be carried out on-line.

INTRODUCTION

In conventional gas or liquid chromatography, a discrete injection gives rise to a sample analysis when one elution time has elapsed. Further analyses require further injections. To obtain the most frequent, separable analyses, one injects once per net settling time. The time separation of each analysis can cause stability problems in associated closed loop control schemes, moreover, simple open loop monitoring becomes difficult. In addition, sources external to the process can cause extraneous noise to appear in the detector outputs. (Industrial chromatographs are particularly prone to noise[1]). Noise can also result from imprecise carrier flow settings, and detector power supply variation. As the lower limit of detection is set by noise levels, this subject is of importance in laboratory work. Accurate analyses also require that the base-line have long term stability, and elaborate procedures are necessary to achieve the low drift rates required[2].

These problems may be somewhat allievated if the injecting sequence is modified. Chapter 2 of this thesis demonstrates that if the input is chosen to be a pseudo-random binary sequence, correlation between input and output yields the desired analysis to within a constant factor. Correlation being an averaging process, this approach has the power to reduce variance in the estimates of sample components. Thus if the detector output is contaminated with noise, correlation enables a more reliable analysis to be made than is possible with a single injection technique. Chapter 2

illustrates this with an analysis of an hydrocarbon sample.

The removal of the effects of base-line drift is discussed in Chapter 2 and requires a slight modification of the basic technique. Chapter 2 also notes that some care is necessary when choosing the apparatus so that the detector is not operated in a non-linear region. The drastic effects of non-linearities in the correlation technique are illustrated with some practical examples. The effect of sample valve non-linearity is also discussed.

Chapter 3 presents several methods of removing the effects of anomalous detector characteristics, first discussed in Chapter 1. The use of one of these methods, (Hadamard-modified sequences) is illustrated by application to analysis of hydrogen in helium, and acetylene in nitrogen. The Katherometer detector characteristic for these cases possesses a turning point, and conventional chromatography gives results which are difficult to interpret. The proposed method allows a useful analysis to be made fairly easily.

Chapter 3 also demonstrates how to extend the basic p.r.b.s. approach so that simultaneous analysis of several independent sample streams may be made with one detector and one column. Another extension of the technique deals with the possibility of analysing samples with time varying concentrations.

Application of correlation techniques requires the

capability of a small computer, but this is not in itself a disadvantage since the method can handle several complete chromatograph systems simultaneously. The number of systems controlled is set only by the number of analogue inputs and the speed of analogue to digital conversion. Approximately 18K of store would be required to service 15 chromatographs and display 500 data points for each. It has been shown[3], that in conventional chromatography, a computer is financially viable when it controls 15-30 chromatography units.

With one system only, 2K of digital computer store is sufficient as long as an interface is available. The computer can be replaced by a pseudo-random binary sequence generator and a digital correlator. Chapter 3 illustrates this possibility with some examples.

REFERENCES

1. Collyer, L.M., Hawkins,L.H.C., Thomson, G.H., Some Hardware Aspects of Computer Aided Gas Chromatography. Paper given at Conf. on Lab.Automation, Middlesex Hospital Medical School, 10-12 November 1970, organised by I.E.R.E.

2. Knox, J.H., Gas Chromatography, pp 66-68, Methuen & Co., Ltd., London 1964.

3. Mitchell, P.,An Automated Laboratory for Gas Chromatography, Column, Spring 1970, Vol.13, No.3.

C O N T E N T S

CHAPTER 2 THE USE OF CORRELATION TECHNIQUES

CHAPTER 1 - THE CONVENTIONAL GAS CHROMATOGRAPH

LIST OF PRINCIPAL SYMBOLS

SUBSCRIPTS	DESIGNATION
r	denotes reference stream
i	denotes i^{th} sample in sample/carrier mixture
io	denotes mixture of i^{th} sample and carrier
o	denotes carrier in sample/carrier mixture

SYMBOLS	INTERPRETATION
S	detector sensitivity in mv/Millimole/ml.
R	detector output in mv.
Q	concentration of subscripted component in Millimoles/ml.
Q_m	minimum detectable concentration in Millimoles/ml.
Q_l	upper limit of concentration on linear portion of detector characteristics in Millimoles/ml.
A	peak area in cm^2.
C	recorder sensitivity in mv/cm of chart.
D	reciprocal of chart speed in mins./cm.

f, E	flow rate of column effluent in mls/min. corrected to detector temperature and pressure.
R.M.R.	Relative Molar Response
w	total weight of sample introduced into the column in mgms.
R_n	peak to peak noise level in detector output.
T_f	temperature of katherometer filament in subscripted gas stream.
q	total katherometer cell heat intake
r_c	internal cell radius
r_f	filament wire radius
L	cell length
C_p	molar heat capacity of subscripted component
$\frac{dN}{dt}$	mole flow rate
Y	mole fraction of subscripted component
b	molecular collison diameter of subscripted component
M	molecular weight of subscripted component
k	thermal conductivity of subscripted component

Z	peak ordinate
Z_{max}	maximum peak ordinate
x	displacement from centre of peak
σ	standard deviation
β_e	peak width at 0.368 of peak height
$\beta_{\frac{1}{2}}$	peak width at half peak height
W	base width of peak found by extrapolating tangents at inflexion points
W'	peak area/peak height
N	number of theoretical plates in a column
H.E.T.P.	height equivalent to a theoretical plate
λ	constant of the order of unity
r	average particle radius
γ	constant of the order of unity
D_g	diffusion coefficient of vapour in gas phase
D_l	diffusion coefficient of vapour in liquid phase
K	partition coefficient
a	average liquid film thickness
ρ	true linear gas velocity at column temperature (^oK) and standard pressure
T	column temperature in ^oK

t	column temperature in ^{o}C
T_a	ambient temperature in ^{o}K
j	pressure correction factor
V_g	gas hold up
V_r	retention volume
V_r'	net retention volume
V_s	specific retention volume
d_1	density of liquid phase
w_1	weight of liquid phase
p	vapour pressure exerted by subscripted component
p^o	vapour pressure of pure subscripted component at given temperature
ν	activity coefficient of pure subscripted component

1. INTRODUCTION

The origins of chromatography are thought to be in the work of a Russian botanist Tswett[1]. His interest lay in examining green leaf pigments he had extracted by a process using petroleum ether. Pouring the petroleum ether-pigment solution into a vertical tube,(column) containing powdered calcium carbonate,(fixed phase) resulted in adsorption of the pigments by the calcium at the top of the column. To wash them down, further petroleum ether was added, causing the components of the mixture to separate into coloured bands as they moved at different speeds down the column. The experiment became known as 'colour writing' generating the title chromatography from the Greek 'chroma' for colour and 'graphein' to write.

The use of a solid fixed phase as adsorber gives the technique the title of 'adsorption chromatography'. The first significant advance was in 1942 when Martin and Synge[2] formulated 'partition chromatography', wherein the fixed phase is a solvent supported on an inert porous packing. Using a second solvent (not completely miscible with the first) as the eluting liquid or mobile phase, samples placed on the column are transported down it. Throughout their progress down the column, sample components continuously transfer from mobile to fixed phase and back again. Since the solubilities of sample components in either phase are characteristic of the components themselves, some com-

ponents remain in the fixed phase longer than others. Since only those molecules of sample in the mobile phase at any instant can move down the column, a gradual separation of components occurs. Molecules aggregate into bands whose velocity is the average velocity of the molecules, and if the process continues for a sufficient time, complete separation occurs.

It is true to say that

$$\text{Fraction of molecules in mobile phase at any instant} = \frac{\text{rate of movement of band}}{\text{rate of movement of mobile phase}}$$

This fraction is determined only by the partition* coefficient, and the weights of the different substances. Substances with different partition coefficients move at different speeds and therefore separate.

The next advance in partition chromatography came in 1952 when James and Martin[3] studied the use of gaseous mobile phases (carrier gas). They were able to separate fatty acids using nitrogen carrier and a column containing silicone oil supported on kieselguhr. However they used automatic titration (an integrating device) for detection, a method which proved to have many practical disadvantages. In 1954 Ray[4] introduced katherometric detection and from then on gas chromatography became a common analytic tool.

---

* see Appendix A1.

Katherometers measure the differential thermal conductivity of the column effluent and a reference stream. As a general detector this method is excellent but the lower limit of detection (1 part in 10^6 of carrier), tended to limit the power of the technique. Thus 1958 saw the invention of two further detectors whose sensitivities are a factor of 10^3 greater. These were the Lovelock argon detector[5] and the McWilliam flame ionization detector[6], both of which ionize the sample gases. This ionization occurs more readily with organic molecules than the usual carrier gases (helium, argon, hydrogen, and nitrogen). It is, therefore, possible to detect much smaller organic samples and use less stationary phase than was possible with earlier detection techniques.

Nowadays gas chromatography is sophisticated enough to handle satisfactorily samples ranging between 10^{-8} and 10^{-2} grammes for analytic work and as large as 100 grammes in preparative work. The analysis time may vary from several hours with complex mixtures to a few seconds using high speed columns. However, analyses to within a 1% tolerance are readily achieved.

2. THE COMPONENTS OF A CHROMATOGRAPHY SYSTEM

A basic chromatography system is shown in Fig. 1. High pressure carrier gas flows through a drying tube and a regulator into an injection device where it collects the sample for analysis. The carrier and sample mixture then passes into the column which separates the sample components. The column effluent flows into a detector whose output is amplified and displayed. Each system component is considered in more detail in the following sections.

2.1 THE DRYING TUBE AND FLOW REGULATOR

The dryer is an essential piece of apparatus since water is a component far from inert, and all gas samples must be dry before they enter the column.

The separation of sample components does not itself require a precise carrier flow since all fluctuations affect all column components to the same extent. However, identification of components by retention volume requires very precise flow regulation. Furthermore, trace components may be easily lost in the noise that results from a variable carrier flow. Thus a precise flow regulator is generally accepted as essential. Such a device usually incorporates pressure reducers to equalise carrier and sample pressures. If equalisation is not performed,

transient pressure spikes can result on injection. To ensure equalisation of flowrates Keulemans[7] recommends the use of a soap film meter for setting up.

2.2 INJECTION DEVICE

The elution peaks, which should be as narrow as possible, are sensitive to injection techniques. In theory there are two limiting ways in which sample vapour can reach the first plate* of the column :-

(a) As a 'plug' without dilution by the carrier which follows with a sharp interface.

(b) Due to mixing of vapour with carrier, as a vapour-carrier mixture with an exponentially increasing sample concentration, which reaches a maximum and then decays exponentially.

It has been shown[8] that column efficiency increases for rising concentration and decreases with increasing sample size. Thus the narrowest elution bands (sharpest separations) are obtained with small, highly concentrated 'plug' injections. In practice the various methods of injection give flow profiles somewhere between the extremes, but one tries to achieve 'plug' flow. The general approach is to trap the sample in a loop which is then flushed through with carrier. The sample tube must be narrow and the column dead space small.

---

* see Section 3

The 'trapping' is achieved by microsyringe or multiport valve although syringes are most common for liquid samples. Syringe volume is usually 1-50µl,[9] the sample being rapidly vapourized in a preheater (50 to 100°C hotter than the column) before being flushed through by the carrier. Multiport valves operate on the principle shown in Fig.2, and as Dal Nogare[9] points out, it is essential to ensure that the valve materials used do not adsorb the sample gases, thereby exhibiting a memory effect, or introducing trailing by desorption of sample components. One manufacturer (LOENCO) quotes the reproductivity of the sample volume as ± 0.5%.

2.3 THERMOSTATTED COLUMN

Columns are constructed using either glass, copper, aluminium or p.v.c. and are 1-2m. long with a 4-6 mm. internal diameter. The tube is bent into a U,W or helix shape, having first been packed with a liquid stationary phase spread over an inert support. Since the aim of the column is to provide a liquid film with as large an interface as possible, the support is chosen with a large specific surface. The liquid film is also required to have a low adsorptive activity so that it does not affect the elution peaks adversely by contributing to the partition process[10]. Unless the sample is gaseous or a very volatile liquid, the column is not normally operated at room temperature. Furthermore the column temperature affects the retention volumes and the flow

rate of the carrier gas e.g for accurate measurements of retention volumes the column temperature must be uniform and steady to within 0.1 degree C[11]. In addition temperature gradients should be avoided, hence columns are placed in stirred air ovens whose set points are adjustable.

2.4.1 DETECTORS

In order to evaluate the performance of a detector some discussion on the concepts of sensitivity and detection limits is warranted. Young[12] and Johnson and Stross[13] have treated these concepts extensively and the following embodies their work. Fig. 3 is a plot of detector response against sample concentration and gives the change ΔR corresponding to the change ΔQ in concentration. Thus for any detector the sensitivity is given by

$$S = \frac{\Delta R}{\Delta Q} \qquad (1)$$

Above a maximum solute concentration Q_1, the global characteristic is non-linear. Q_m is the minimum concentration capable of detection to within a particular confidence level. Dimbat, Porter and Stross[14] propose the alternative expression

$$S = \frac{ACDE}{w} \qquad (2)$$

which has been modified by Rosie and Robinson[15] to incorporate relative molar response factors so that the expression becomes less dependent on experimental conditions[16].

Thus

$$S = \frac{ACDE}{N(R.M.R.)} \qquad (3)$$

Young[12] describes a method of estimating the limit of detection based on the assumption that the noise in the detector output record obeys a guassian distribution. By measurement of the mean square value of the noise, the standard deviation of the distribution is obtained. We arbitrarily chose a detection band of a size greater than two standard deviations of the noise, and give this band size the symbol R_n. The peak to peak excursion of most noise peaks will lie within this band size (i.e. within $-x_{\alpha/2}$ to $x_{\alpha/2}$ in Fig.4). Using the table of the probability integral, this is equivalent to saying that for 95% of the noise peaks

$$\text{peak to peak value} \quad < 2 \times 1.96 \times \sigma$$

Choosing R_n appropriately, the probability of a noise peak exceeding $2R_n$ on one side of the base line is very small and thus such a peak can be said to be a solute peak to within a defined confidence level.

Then $S = 2R_n \times Q_m$ (4) which yields Q_m, whose value depends on the confidence with which R_n is chosen. Appendix A2 shows the variation of Q_m with the fraction of peaks covered by the $2R_n$ band. Young[12] notes that the variation shown is quite acceptable for purposes of detector comparison.

Using the term pQ_m (analogous to ph. measurement) to combat difficulties encountered due to the smallness

of Q_m, Appendix A3 (from Young[12]) shows values of pQ_m for various detectors according to

$$pQ_m = \log_{10} (1/Q_m) = \log_{10} (S/R_n) - \log_{10} 2 \quad (5)$$

Many detectors have been developed for gas chromatography, but only two are of significant practical importance. These are described in some detail in the ensuing sections.

2.4.2 THE THERMAL CONDUCTIVITY CELL (Katherometer)

The thermal conductivity cell (Katherometer), is widely used in gas chromatography owing to its ease of construction, cheapness and general application. It consists of a detector element placed in the stream of column effluent, and a matching element in a reference stream. Each element forms one arm of a Wheatstone bridge, the other arms being dummy elements or matching resistors. The heated detector element is cooled by the carrier stream until a binary, or pseudo-binary mixture of eluted solute and carrier, pass over it. The rate of heat loss by the detector element changes, which causes a change in its resistance. The change of resistance is a function of the instantaneous concentration of sample components in the gas stream.

Following the development of Novak et al[16], the useful detector response is effectively the temperature difference between the times when the detector element is in the pure carrier stream, and that of the chromatographic fraction

$$\text{i.e. } R_i = T_{f_{io}} - T_{f_o}$$

$$= q \log_e \frac{r_c}{r_f} \left[\frac{1}{2\pi L\, k_{io} + \frac{dN}{dt} Cp_{io}/2} - \frac{1}{2L\, k_o + \frac{dN}{dt} Cp_o/2} \right] \quad (6)$$

If $\Delta k = k_{io} - k_o$ and $\Delta Cp = Cp_{io} - Cp_o$

Then

$$T_{fio} = T_{fo} + \frac{1}{1!}\left(\frac{\partial \Delta k}{\partial k_{io}} + \frac{\partial \Delta Cp}{\partial Cp_{io}}\right) T_{fio} + \frac{1}{2!}\left(\frac{\partial \Delta k}{\partial k_{io}} + \frac{\partial \Delta Cp}{\partial Cp_{io}}\right)^2 T_{fio}$$

$$+ \text{----------}$$

Further if we deal with low solute concentrations varying within narrow limits

$$\Delta k \ll k_o \quad \text{and} \quad \Delta Cp \ll Cp_o$$

then $T_{fio} - T_{fo} \approx$

$$\frac{-q \log_e \left(\frac{r_c}{r_f}\right)}{\left(2\pi L + \frac{dN}{dt} Cp_o/2\right)^2} \left[2\pi L\, (k_{io} - k_o) + \frac{dN}{dt}\left(\frac{Cp_{io} - Cp_o}{2}\right) \right] \quad (7)$$

To simplify (7) we need to express k_{io} and Cp_{io} as functions of the concentrations of the components in the column effluent.

The problem of expressing the thermal conductivity of a gaseous mixture in terms of the thermal conductivities of its components, has been dealt with by a number of authors[17-21]. Novak[16] suggests the use of the expression given by Wassiljewa[17]

$$k_{io} = \frac{k_i}{1 + A_{oi}(Y_o/Y_i)} + \frac{k_o}{1 + A_{io}(Y_i/Y_o)} \quad (8)$$

where $A_{io} = \left[(b_i + b_o)/2b_o\right]^2 \sqrt{(M_i + M_o)/2\, M_i}$

A_{oi} is found by interchanging subscripts.

Expanding k_{io} as a series

$$k_{io} = k_o + \frac{1}{1!}\frac{d\,k_{io}}{d\,Y_i}(0)Y_i + \frac{1}{2!}\frac{d^2\,k_{io}}{d\,Y_i^2}(0)\,Y_i^2 + \text{--------}$$

Terminating after the first two terms

$$k_{io} = k_o + \left[ki/Aoi - ko\,Aio\right] Y_i \qquad (9)$$

For Cp_{io} we write

$$Cp_{io} = Cp_i\,Y_i + Cp_o\,Y_o = Cp_o + (Cp_i - Cp_o)\,Y_i \qquad (10)$$

Thus $R_i =$

$$\frac{-q \log_e\left(\frac{r_c}{r_f}\right)}{(2\pi L\,k_o + \frac{dN}{dt}\,Cp_o/2)^2}\left[2\pi L\left(\frac{k_i}{A_{oi}} - k_o\,A_{io}\right) + \frac{dN}{dt}\,\frac{(Cp_i - Cp_o)}{2}\right]Y_i \qquad (11)$$

Novak[16] shows further that the R.M.R.* is given by

$$\text{R.M.R.} = \frac{2\pi L\,(k_i/A_{oi} - k_o\,A_{io}) + \frac{dN}{dt}\left(\frac{Cp_i - Cp_o}{2}\right)}{2\pi L\,(kr/A_{or} - k_o\,A_{ro}) + \frac{dN}{dt}\left(\frac{Cpr - Cp_o}{2}\right)}$$

Rosie and Grob[22] used benzene as the reference substance assigning it a relative value of 100. This practice is still followed with the result that the R.M.R. of a number of compounds (in Helium) are known. Within a homologous series there is a linear relationship between the R.M.R. and the molecular weight[22]. The empirical equation is R.M.R. = A + B.M where A and B are constants. Hence members of a homologous series can be determined quantita-

---

* See Appendix A1 for definition of R.M.R.

tively from area per cents without the use of response factors.

2.4.3 ANOMALIES IN THE KATHEROMETER RESPONSE

Some authors[16;24] have noted that for light carrier gases (helium, hydrogen), the thermal conductivity of the sample-carrier mixture varies linearly with sample concentration. Van de Craats[25], using n-Butane sample demonstrated this to be true over a concentration range 0-10 mole %. In the case of the heavier nitrogen carrier however, linearity was poor even below 0.5 mole %. Thus in cases such as the latter, equation (9) has restricted validity (if any). For (9) to hold, implying a linear detector characteristic, the literature[23,25,26] suggests that sample and carrier must have widely differing thermal conductivities. The use of tailored carrier gases has also been proposed[27]. These latter are a mixture of gases so chosen that the overall molecular properties such as mass, collision diameter and intermolecular constants, match those of the sample. Such carrier gases give linear detector characteristics over the normal range concentrations used in chromatography.

Even assuming a linear detector characteristic, examination of (11) shows that there is a possibility of peak polarity reversal, when operating over a range of

temperatures. If at one temperature ki/Aoi > Aio ko, it may be that at another temperature ki/Aoi < Aio ko. If in equation (11), the thermal conductivity and thermal capacity factors are comparable at one temperature, then at the second, the detector response changes sign. Peak reversal occurs without any distortion of the peak. Further, if reversal occurs, then there exists a temperature at which the response of the given configuration is very small or zero.

Bohemen and Purnell[28] have noted that the inverted peaks they obtained were distorted. However, since they used nitrogen carrier, it is unlikely that operation within the detectors' linear regime was possible at any temperature, i.e. all peaks would be distorted. Novák[29] suggests that if a peak becomes distorted on inversion, distortion occurs because of a curtailing of the range of detector linearity by the temperature change. Harvey and Morgan[30] show this effect for a methanol vapour-nitrogen mixture.

For some mixtures the detector characteristic is seen to exhibit a turning point. Under such conditions(9) does not hold because the Wassiljewa equation (8) is not applicable. The literature contains many examples of such behaviour including :-

(i) helium in hydrogen[26,31]

(ii) acetylene in nitrogen[24]

(iii) methanol in argon[32]

(iv) carbon dioxide in nitrogen[33]

Operating in such a regime causes the chromatographic peaks to be partially inverted to give M or W shapes[26,30,34,35,36,37], which are analytically uninterpretable[27].

In the particular case (i), the turning point is at 8 mole % hydrogen in helium, so Purcell and Ettre[35] have suggested the use of an helium/hydrogen mixture (91.5% helium and 8.5% hydrogen) as carrier. A single negative peak results for a hydrogen in helium sample but the range of linearity is limited. Panson and Adams[36] suggest the use of small samples, and other authors[38] consider that extensive calibration surmounts the problem. None of these approaches are particularly convenient.

2.4.4 THE FLAME IONIZATION DETECTOR (F.I.D.)

McWilliam and Dewar[6] designed this instrument which consists simply of a jet and a collector with a potential applied across the two. Column effluent mixed with either hydrogen or hydrogen/nitrogen mixture is burnt in an excess of air at the metal jet. This process leads to ionization of the molecules in the column effluent by mechanisms not fully understood. However, by carefully choosing the applied potential, ion collection is at a maximum, and thus the detector responds. Organic molecules

ionize much more readily than do those of the normal carrier gases, hence the detector is used generally in hydrocarbon analysis. The hydrogen and air streams are filtered to remove alkali salts and carbon compounds, which produce ion avalanches as they pass through the flame, and result in detector noise.

The preferential response to organic substances results in an ionization efficiency of one ion in 10^5 organic molecules, whereas for hydrogen the figure is as low as one ion in 10^{12} molecules. Hence it is normally said that the detector has no response to hydrogen. Purnell[39] lists a number of substances to which there is little or no response, and this includes hydrogen.

In general the detector response is proportional to carbon content, but this is not so for oxygenated and nitrogen containing compounds. These give a lower response than expected; thus extensive calibration is necessary. It should also be noted that the F.I.D. responds not to concentration changes, but to quantity of sample per unit time, since samples are actually consumed by the flame.

The detector reaction volume is of the order 5µl, the background current 10^{-12} amp and noise levels 10^{-14} amp. The minimum detectable amount of organic material is approximately 1 part in 10^9 of hydrogen, but a linear response can be obtained up to a concentration

of 0.5% by volume. These figures give a dynamic range of the order 10^7 which is confirmed by a recent study[40].

2.4.5 ANOMALIES IN F.I.D. RESPONSE

Peak inversions have been noticed for concentrations by volume of 0.65% propane and butane in nitrogen[41], and 0.03% carbon disulphide in nitrogen[42]. This latter is interesting since carbon disulphide is one of those gases to which the F.I.D. is said to be insensitive; unfortunately this has not been explained. Some modes of F.I.D. construction use a cathode electrode other than the jet[9]. The position of this cathode was seen to influence the propane and butane inversion[41], and also to limit linearity in the range of small concentrations. McWilliam[42] shows further that the upper electrode spacing can influence linearity for high concentrations. Sternberg[43] reasons that the 10^7 range of linearity is only achieved if the ion collection is complete, which implies an adequate voltage gradient between electrodes. Other experiments[44] have shown that the reproducibility of the peak height is poor if the air supply is insufficient.

3. THE KINETICS OF GAS CHROMATOGRAPHY

Any sharp band injected into a column spreads as it passes down the column, the extent of the spreading being a measure of the inefficiency of the chromatographic process. A real column can be considered to behave as a series of distinct units or plates joined together. Initially all plates are connected and a plug dv of carrier is added to the first plate. This causes the gas phase to move as a plug a short distance down the column, and an amount dv to emerge from the last plate. As this happens, a small fraction of the contents of each plate is transferred to each succeeding one. The plates are then disconnected long enough for equilibrium to be established in each plate, and then reconnected for the process to be repeated. If the sample vapour is added to the first plate, addition of further small quantities of carrier gas elutes the sample down the column until it emerges from the last plate. During this elution, the amount of band spreading which occurs depends solely on the number of plates in the column, if dv is small enough. The amount of observed spreading in any real column is used to calculate the number of plates in a hypothetical plate column which would give the same degree of spreading. This leads to the H.E.T.P. as defined in Appendix A1. Assuming the partition coefficient to be independent of the concentration of the solute, Knox[11] gives the elution curve of the substance as the guassian distribution

$$Z = Z_{max}\, e^{-x^2/2\sigma^2} \qquad (13)$$

The situation is illustrated by Fig.5. The process is characterised by the following relations.

$$\begin{aligned} \beta_e &= 2\sqrt{2}\ \sigma \\ \beta_{\frac{1}{2}} &= 2.36\ \sigma \\ W &= 4\sigma \\ W' &= \sigma\sqrt{2\pi} \\ N &= (\frac{V_r}{\sigma})^2 = 8\ (\frac{V_r}{\beta_e})^2 = 16\ (\frac{V_r}{W})^2 \\ &= 5.54(\frac{V_r}{\beta_{\frac{1}{2}}})^2 = 2\pi\ (\frac{V_r}{W'})^2 \end{aligned} \qquad (14)$$

An alternative approach taking into consideration the contributions of the several separate effects in elution gives,(for a packed column)

$$\text{H.E.T.P.} = 4\lambda r + 2\gamma D_g/p + \frac{8K\, a^2 \rho}{\pi^2(1+K)^2 D_1} \qquad (15)$$

which is often written

$$H = A + \frac{B}{\rho} + C\rho \qquad (16)$$

The first term represents the effects due to mixing caused by unequal paths around the particles and is often called the eddy diffusion term. Longitudinal diffusion in the gas phase gives rise to the second term,and the third is due to the slowness of mass transfer between the liquid and gas phases.

In graphical form (16) appears as Fig.6, but

note that the optimum is generally quite flat. However, it is desirable to work as close to the optimum as possible since this gives the minimum H.E.T.P. and makes full use of the separating power of the column. For nitrogen or argon as carrier, the optimum is in the region of 3-6 cm/sec and 10-20 cm/sec for hydrogen or helium.

3.1 THE EFFECT OF TEMPERATURE ON COLUMN PERFORMANCE

As far as (16) is concerned the major affect of temperature is through the variation in partition coefficient. As temperature increases, K decreases, causing an increase of C and thereby decreasing the column efficiency. However the specific retention volume* varies with temperature according to[10]

$$\log_e V_s = D + \frac{F}{t+G} \qquad (17)$$

where D,F and G are constants. Hence although low temperatures give highest column efficiencies, they also cause longer retention times, and some compromise must be made.

3.2 THE EFFECT OF SOLUTE CONCENTRATION ON ELUTION PEAKS

In section 3, the partition coefficient is assumed to be independent of concentration, however

---

* see Appendix A1 for definition of specific retention volume

there are conditions under which such an assumption is not valid. A volatile component of a solution exerts a vapour pressure above the solution which is expressed by

$$p_1 = \nu_1 Y_1 p_1^{\circ} \qquad (18)$$

the mole fraction Y_1 referring to the solute in solvent. If the activity coefficient is unity, (18) becomes Henrys' law. Thus for a binary mixture which obeys Raoult's law (ν = constant)

$$p_1 = Y_1 p_1^{\circ} \quad ; \quad p_2 = (1 - Y_1)p_2^{\circ}$$

$$\therefore \quad p = p_1 + p_2 = p_2^{\circ} + Y_1 (p_1^{\circ} - p_2^{\circ}) \qquad (19)$$

the total vapour pressure p then varies with mole fraction according to Fig. 7a. However most real solutions deviate from Raoult's law and as shown in Fig.7b and Fig.7c, these deviations can be positive or negative. The deviations for components of a binary mixture are always of the same sign, with positive deviations the more common. Fig. 8 shows the situation for components in two solutions, one exhibiting a positive and the other a negative deviation. In the region of very dilute solution, the curve is well approximated by its tangent at the origin. In this region (18) holds with a constant activity coefficient, and this is the region of interest in gas-liquid chromatography. For a constant activity coefficient, the partition coefficient is independent of concentration and symmetrical elution peaks result. If the partition coefficient varies, the elution peaks become asymmetrical[10].

4. APPENDICES

APPENDIX A1.

GLOSSARY OF GAS CHROMATOGRAPHIC TERMINOLOGY

1.	MOLE	A 'mole' of sample is the mass of sample numerically equal to its molecular weight.
2.	MOLE-FRACTION	The 'mole fraction' of a component is the ratio of the number of moles of that component to the number of moles of mixture.
3.	PARTITION COEFFICIENT (K)	The 'partition coefficient' of a two phase system is the ratio of the concentrations of solute in the liquid phase and in the gas phase, in a theoretical plate.
4.	PRESSURE CORRECTION FACTOR (j)	Owing to the compressibility of the carrier gas, the average flow rate of the carrier is not the same as measured at the column exit, they are related by

$$\frac{fav}{fo} = \frac{po}{p_{av}} = \frac{3}{2}\left[\frac{(pi/po)^2 - 1}{(pi/po)^3 - 1}\right] = j \qquad A1.(1)$$

5.	GAS HOLD-UP	After injection at time 0 of Fig.5, a substance not adsorbed by the stationary phase breaks through the column at A. The

distance OA converted to the total volume of gas which has flowed in the time interval, is known as the gas hold-up of the column. It is physically equal to the 'dead' volume of the column and connecting tubes.

6. RETENTION VOLUME

The volume of gas eluted out of the column between the injection at O and the appearance of the sample maximum at B is the retention volume of the substance.

7. NET RETENTION VOLUME (V_r')

$$V_r' = V_r - V_g \qquad \text{Al.(2)}$$

Note that V_r and V_g in Al.(2) are not the raw experimental values which are calculated on the basis of an outlet flow rate measured at ambient temperature and pressure, thus

$$V_r - V_g = j \frac{T}{Ta} \left[V_{r\ \text{experimental}} \quad V_{g\ \text{experimental}} \right] \qquad \text{Al.(3)}$$

8. SPECIFIC RETENTION VOLUME (V_s)

The specific retention volume is the net retention volume divided by the weight of stationary phase reduced to 0 °C

$$\text{i.e. } V_s = \frac{V_r' 273}{w_1 T} \qquad \text{Al.(4)}$$

The specific retention volume is related to the partition coefficient by

$$K = \frac{V_s \, d_1 \, T}{273} \qquad \text{A1.(5)}$$

9. PEAK WIDTH

The peak width can be measured in three ways

(a) at the inflexion points (β_e)

(b) at the half peak height ($\beta_{\frac{1}{2}}$)

(c) by extrapolation of tangents at inflexion points (W)

10. HEIGHT EQUIVALENT TO A THEORETICAL PLATE (H.E.T.P.)

The H.E.T.P. =

$$\frac{\text{length of column}}{\text{No. of Theoretical Plates for a particular elution}} \qquad \text{A1.(6)}$$

11. R.M.R. Relative Molar Response.

APPENDIX A2.

PROBABILITY OF A NOISE PEAK EXCEEDING TWICE THE NOISE DETECTION BAND

% of Noise Peaks included in detection band	Probability of Noise exceeding 2xband width on one side of baseline	Relative Q_m value
99.9	< 1 in 10^{15}	1.28
99.0	< 1 in 10^{11}	1.00
95.0	< 1 in 10^{9}	0.76

APPENDIX A3.

SENSITIVITY AND LIMIT OF DETECTION OF SOME DETECTORS

	DETECTOR	S	R_n	Q_m	pQ_m
1.	L & N therm. cond.cell	40,000	0.001	5×10^{-8}	7.3
2.	Hot wire therm.cond. cell	40,000	0.01	5×10^{-7}	6.3
3.	Thermistor	25,000	0.01	8×10^{-7}	6.1
4.	Ionisation Gauge	2.5×10^{6}	0.02	1.6×10^{-8}	7.8
5.	Flame ionisation	7.4×10^{10}	0.07	1.9×10^{-12}	11.7
6.	Electric Discharge	2×10^{10}	20	2×10^{-9}	8.7
7.	Beta ionisation	55,000	0.0125	5×10^{-7}	6.3

5. REFERENCES

1. Tswett,M., Ber.deut.botan.Ges., 24,316,384(1906)
2. Martin,A.J.P., Synge,R.L.M., Biochem.J.(London), 35, 1358(1941)
3. James,A.T., Martin,A.J.P.,Analyst,77,915,(1952)
4. Ray,N.H., J.Appl.Chem. 4,21,82.(1954)
5. Lovelock,J.E., J.of chromatog.1,35,(1958)
6. McWilliam,I.G., Dewar,R.A., Gas Chromatography 1958, ed. Desty,D.H.,London (Proc.of 2nd Symposium on Gas Chromatography, Amsterdam,May 1958).
7. A.I.M., Keulemans, Gas Chromatography, Reinhold pub.corp; New York (1959),(second edition).
   p.59. (Soap film meter)
8. Deemter,J.J.Van, Zuiderweg,F.J., Klinkenberg,A., Chem.Eng.Sci. 5,271,(1956).
9. Dal Nogare, S., Juvet,R.S., Gas Liquid Chromatography Theory and Practice, Interscience Pub. (1963) (second edition).
   p.177 (Sample size)
   p.177 (Valve design)
   p.218 (F.I.D.Cathode)
10. Ambrose, D., Ambrose,B.A., Gas Chromatography, Geo.Newnes,(1963) (second edition)
    p.109 (Asymmetrical peaks)
    p.85 (Effect of Temperature on Elution)
11. Knox, J.H.,Gas Chromatography, Methuen,London, 1962(first edition)
    p.96 (Temperature tolerance)
    p.13 (Elution curve)

12. Young,I.G., Gas Chromatography, ed. Noebels, H.J., Wall, R.F., Brenner,N., Academic Press, New York,(1961)

13. Johnson, H.W., Stross, F.H., Gas and Liquid Elution Chromatography, Quantitative Detector Evaluation. Anal.Chem, 31,7, July 1959.

14. Dimbat,M., Porter, P.E., Stross,F.H., Apparatus Requirements For Quantitative Application of Gas-Liquid Partition Chromatography, Anal. Chem. 28, 3, 1956.

15. Robinson, D.W., Rosie, D.M., Paper No.2 presented at the Pittsburgh Conference on Anal. Chem., March 1964.

16. Novák,J., Wičar, S., Janák, J., Prediction of the Katherometer Relative Molar Response I. Coll.Czech. chem. commun. Vol.33, 1968.

17. Wassiljewa,A., Physik Z., 5, 737, (1904)

18. Hirschfelder, J.O., Curtiss, C.F., Bird,R.B., Molecular Theory of Gases and Liquids, Wiley, London (1954).

19. Srivastava, B.N., Saxena, S.C., Thermal Conductivity of Binary and Ternary Rare Gas Mixtures. Proc.Phys.Soc.(London) 70B (1957) pp.369-378.

20. Tsederberg, N.V., Thermal Conductivity of Gases and Liquids, M.I.T. Press, Cambridge, Mass. 1965, pp.144-165 inc.

21. Lindsay, A.L., Bromley, L.A., Thermal Conductivity of Gas Mixtures. Ind. and Eng. Chem.42,8,(1950).

22. Rosie, D.M., Grob, R.L., Thermal Conductivity Behaviour, Anal. chem. 29, 9, (1957)

23. Lawson, A.E., Miller, T.M., Thermal Conductivity Detectors in Gas Chromatography, J. of G.C. Aug.1966. pp273-284

24. Keulemans, A.I.M., Kwantes, A., Rijnders, G.W.A., Quantitative Analysis with Thermal Conductivity Detection in Gas Liquid Chromatography, Analytica Chimica Acta Vol 16, 29, 1957.

25. Van De Craats, F., Some Quantitative Aspects Of The Chromatographic Analysis Of Gas Mixtures Using Thermal Conductivity As Detection Method. Gas Chromatography 1958, ed. Desty, D.H., Academic Press, New York.

26. Schmauch, L.J., Dinnerstein, R.A., Response Of Thermal-Conductivity Cells In Gas Chromatography, Anal.Chem., 32, 3, (1960)

27. Jordan, J., Kebbekus, B.B., Mixed Carrier Gases for Quantitative Chromatography: A New Approach For Linearizing Thermal Conductivity Based on Kinetic Theory. Anal.Chem. 37,12,(1965)

28. Bohemen, J., Purnell, J.H., The Behaviour Of Katherometers For Gas Chromatography In Carrier Gases Of Low Thermal Conductivity, J. Appl. Chem. 8, 1958.

29. Novák, J., Janák, J., Prediction Of The Katherometer Relative Molar Response II, Coll.Czech, Chem.Commun. Vol 35, 1970.

30. Harvey, D., Morgan, G.O., Factors Affecting Thermal Conductivity Detectors In Vapour Phase Partition Chromatography, Vapour Phase Chromatography, 1956, ed. Desty, D.H., Academic Press, New York.

31. Hansen, R.S., Frost, R.R., Murphy, J.A., The Thermal Conductivity Of Hydrogen Helium Mixtures, Jour. Phys. Chem., 68,7 (1964).

32. Bennet, L.A., Vines, R.G., Thermal Conductivities Of Organic Vapour Mixtures, Jour. Chem. Phys., 23, 9, (1955).

33. Rothman, A.J., Bromley, L.A., High Temperature Thermal Conductivity Of Gases, Ind.Eng.Chem.,47, 5, (1955).

34. Baker, W.J., Zinn, T.L., Wise, K.V., Wall, R.F., Observations On The Anomalous Chromatographic Behaviour Of Hydrogen. Nat.Instr,Soc.Am. Symposium on Instrumental Methods Of Analysis, Houston, Texas, May 1958, ISA Proc.4.

35. Purcell, J.E., Ettre,L.S., Analysis Of Hydrogen With Thermal Conductivity Detectors, J.of G.C. 3, 69, (1965)

36. Panson, A.G., Adams, L.M., Complete Gas Chromatographic Analysis Of Hydrogen In Fixed Gases And Hydrocarbons Using One Detector And Helium As Gas Carrier, J. of G.C., May 1964.

37. Miller, J.M., Lawson, A.E., Gas Chromatographic Detector Response Using Carrier Cases Of Low Thermal Conductivity, Anal.Chem., 37,11,(1965).

38. Castello, G., Biagani,E., Munari,S., The Quantitative Determination of Hydrogen in Gases by Gas Chromatography with Helium as the Carrier Gas. J.Chromatog., 20, (1965).

39. Purnell, H., Gas Chromatography, Wiley, 1962, p.306 (Gases to which F.I.D.insensitive) p.302 (large samples and F.I.D.)

40. Oster, H., Opperman, F., Linearity or Unlinearity of the F.I.D., Chromatographia, 2, 1969.

41. Novák, J., Janák, J., The Non-linearity of Signal Response and the Inversion Effect in the F.I.D., J. Chromatg., 4, (1960).

42. McWilliam, I.G., Linearity and Response Characteristics of the F.I.D., J.Chromatog., 6,(1961)

43. Sternberg, J.C., Gas Chromatography, ed. Brener, N., Callen, J.E., Weiss, M.D., Proc. of Third Int. Symp. of Inst. Soc. of America, Academic Press, New York. p.542.(contribution to discussion)

44. Batt, L., Cruickshank, F.R., Irreproducibility in the Quantitative Calibration of a Flame Ionisation Detector, Journ. of Chromatog., 21 (1966).

6. ILLUSTRATIONS FOR CHAPTER 1.

THE BASIC CONVENTIONAL CHROMATOGRAPHY SYSTEM

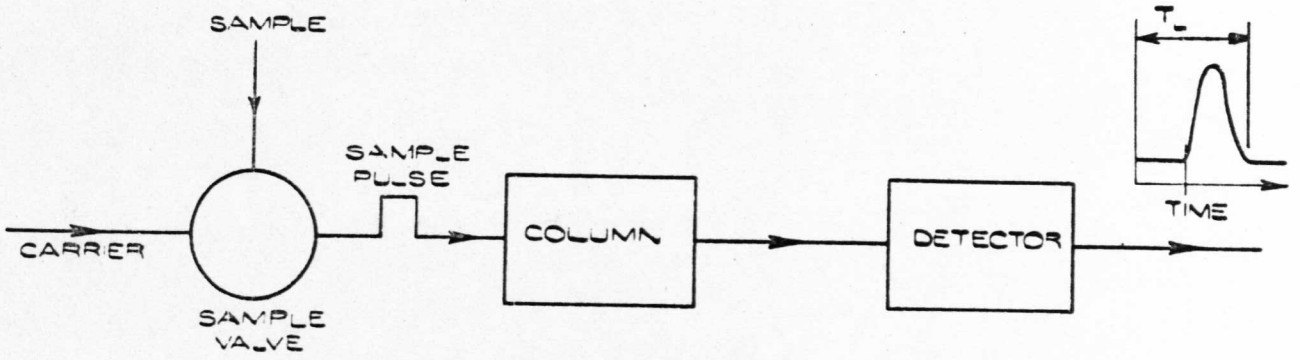

FIG. 1

FIG. 2a

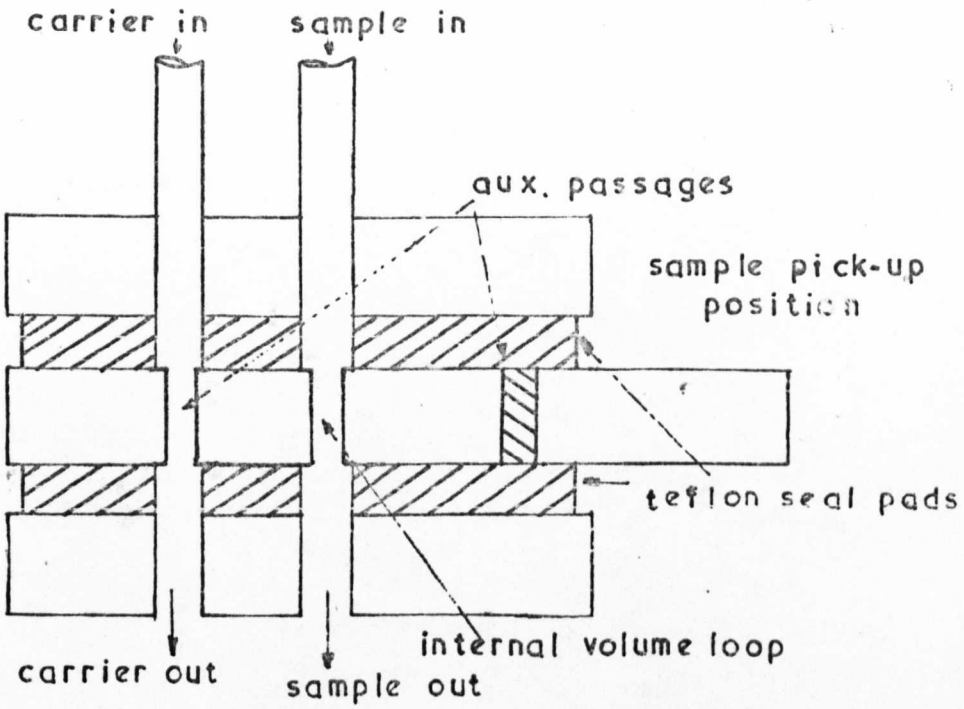

ACTION OF LOENCO MULTIPORT VALVE

FIG. 2b

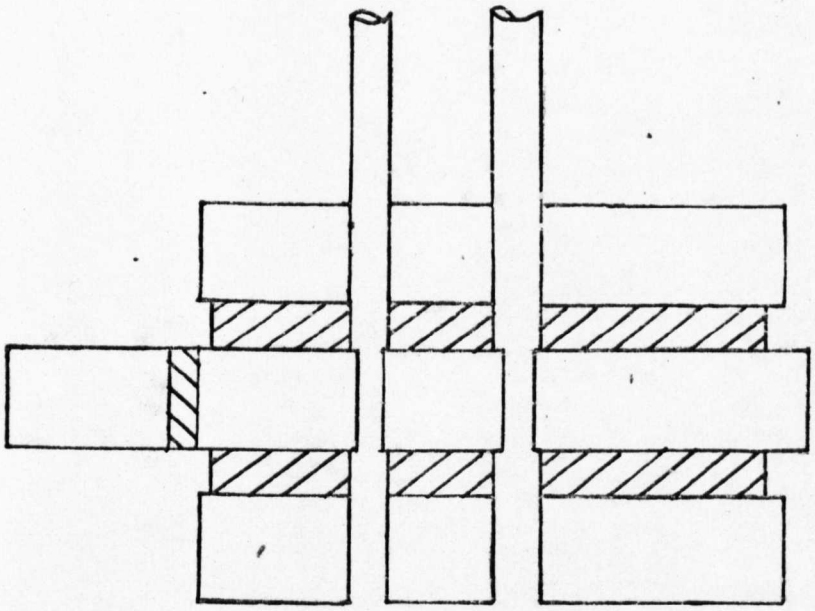

TYPICAL DETECTOR CHARACTERISTIC

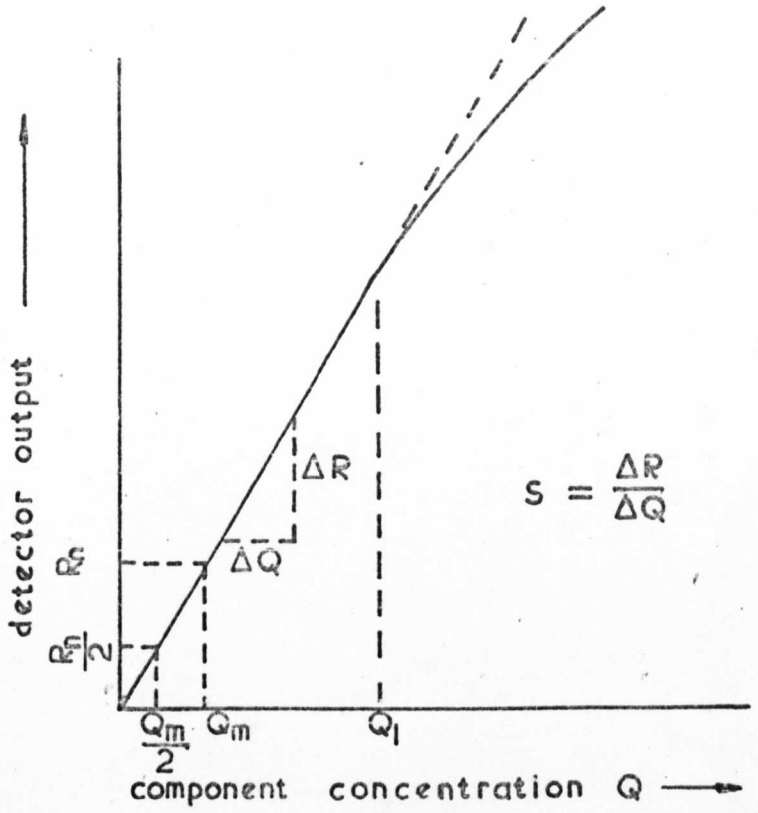

FIG. 3

Probability Distribution of Noise in Detector Output

$x_{\alpha/2} = 1.96\sigma$ for 95 % confidence

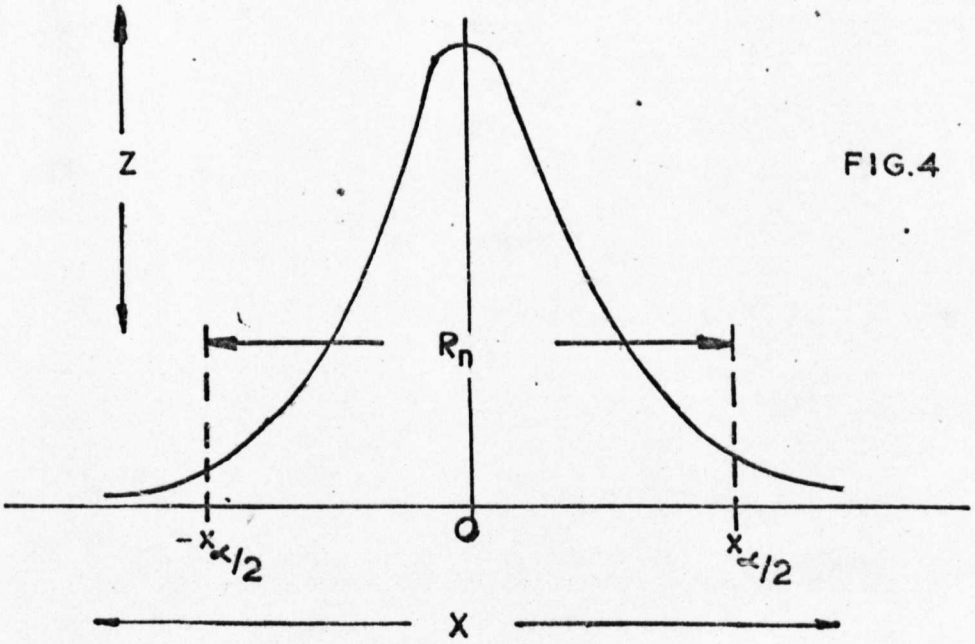

FIG.4

ELUTION CURVE

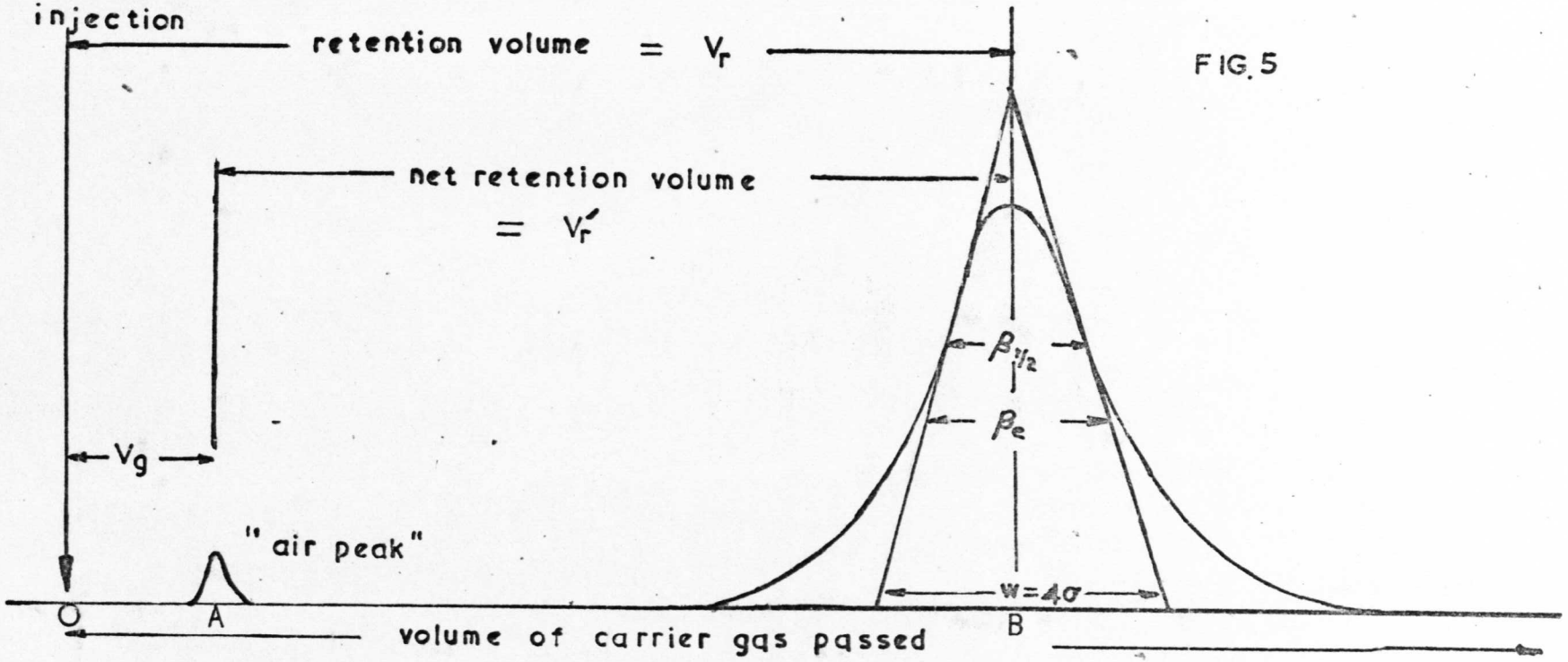

FIG. 5

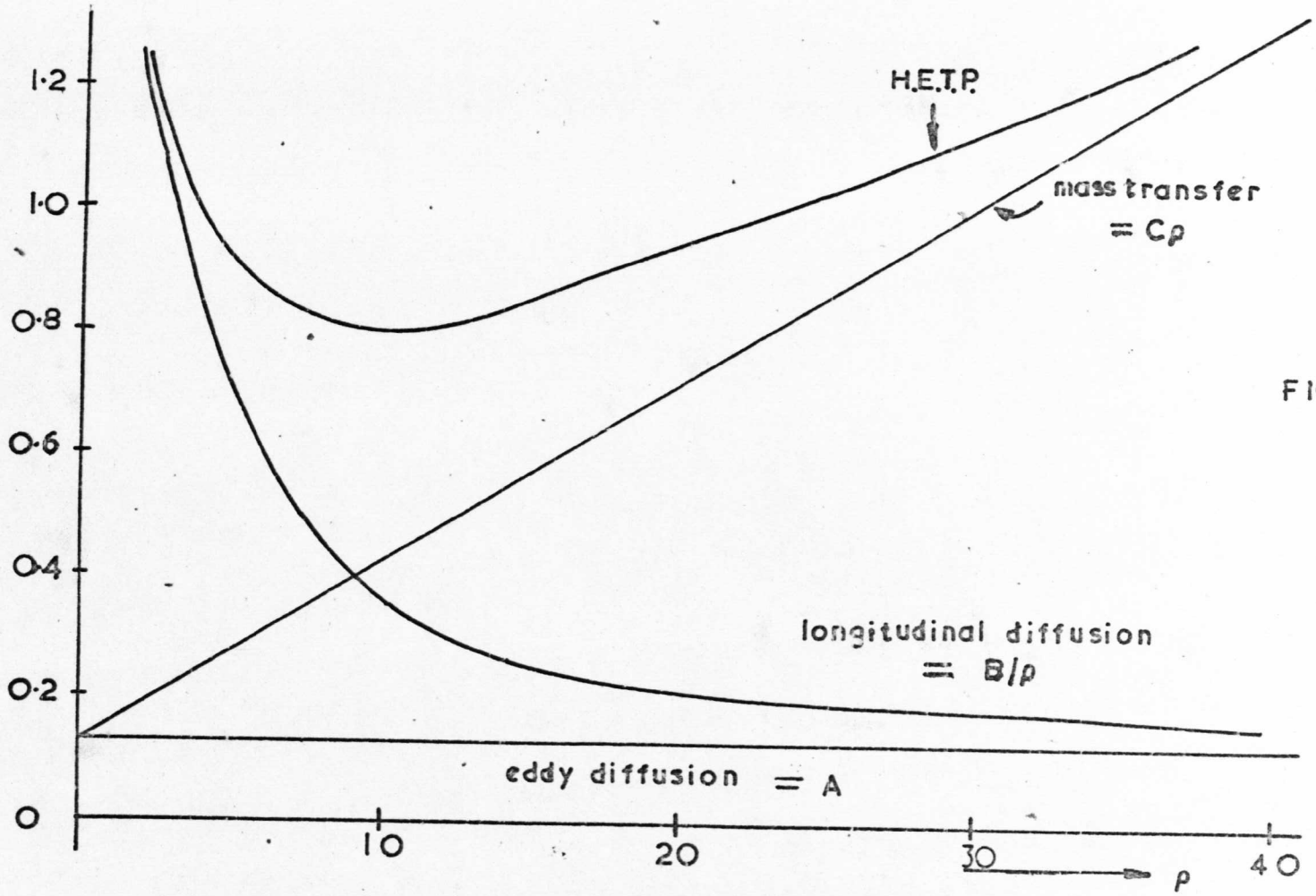

FIG 6

THE DEPENDENCE OF H.E.T.P. ON FLOW RATE

THE VARIATION OF VAPOUR PRESSURE WITH CONCENTRATION

FIG. 7a

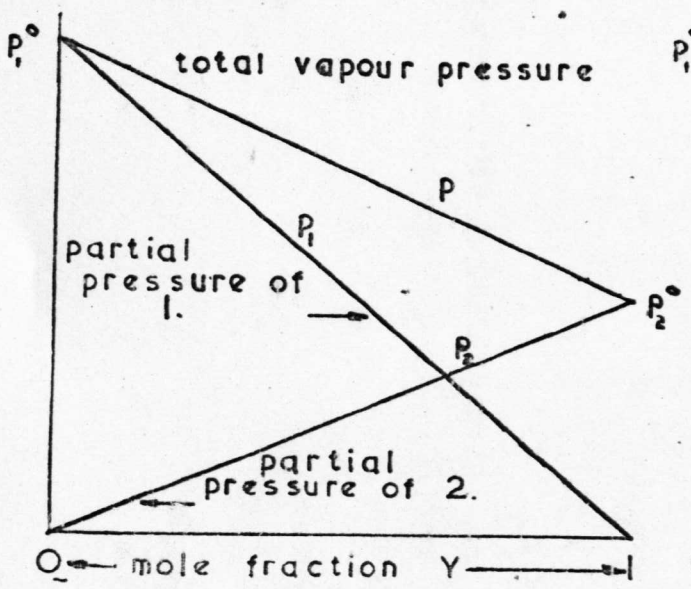

ideal solution i.e. Raoults' law obeyed.

FIG. 7b

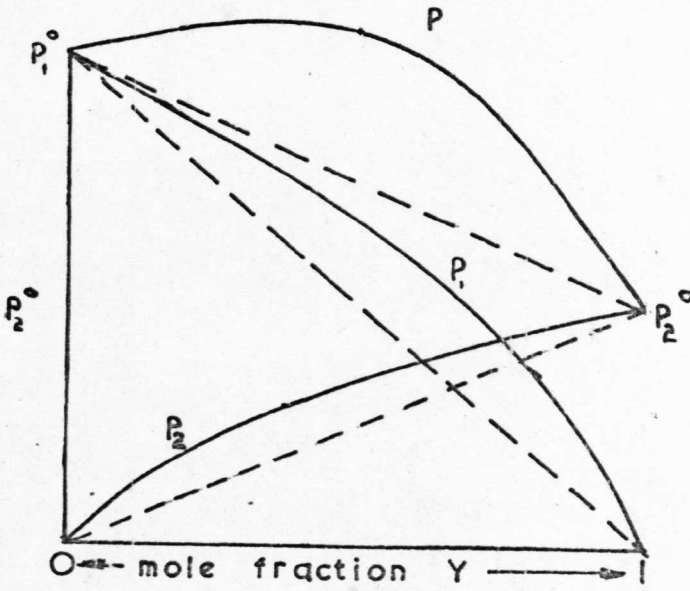

non ideal solution with +ve deviations from Raoults' law

FIG. 7c

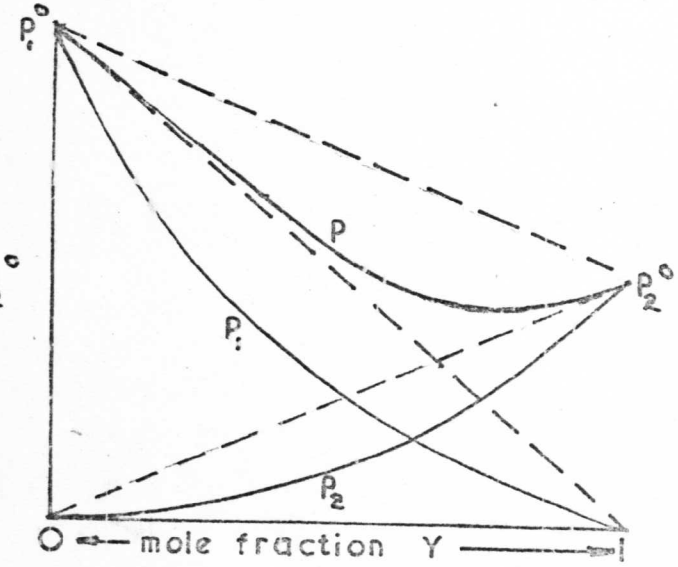

non ideal solution with -ve deviations from Raoults' law

FIG. 8

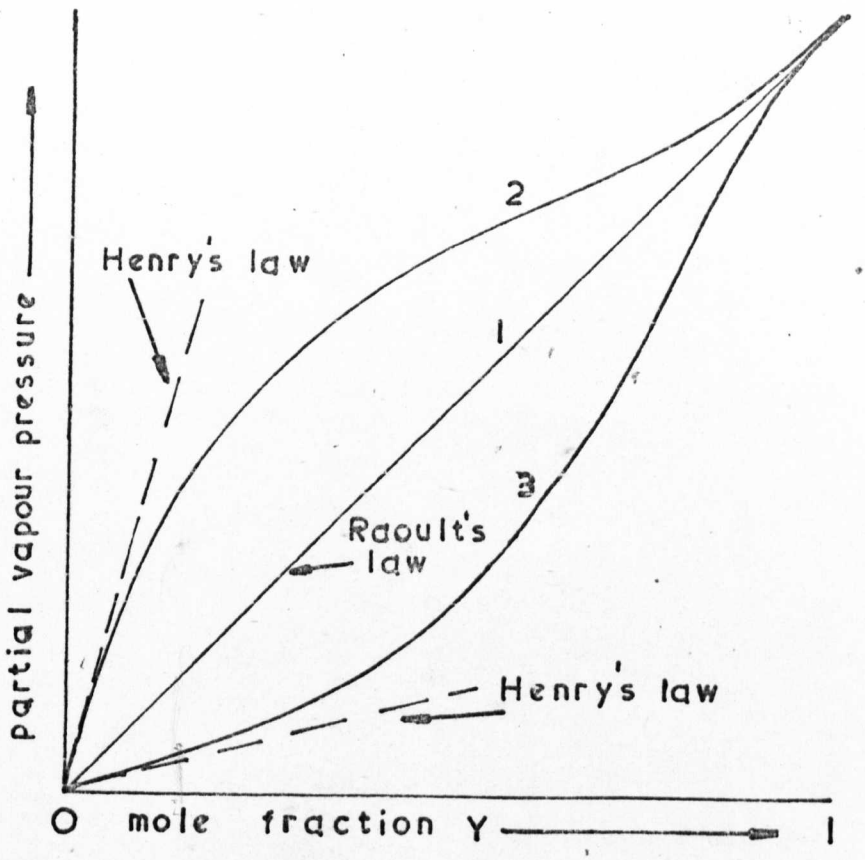

partial vapour pressure of one component

1, Raoult's law obeyed

2, +ve deviations from Raoult's law

3, -ve deviations from Raoults law

DEVIATIONS FROM RAOULT'S LAW FOR REAL SOLUTIONS

CHAPTER 2 - THE USE OF CORRELATION TECHNIQUES

LIST OF PRINCIPAL SYMBOLS

SYMBOLS	INTERPRETATION
t, g	time variables
τ, ε	shift variables
$x(t)$	system input before any level modification
*	the transformation 0 = -1, 1 = +1.
$y(t)$	linear system output
$n(t)$	noise at output
$z(t)$	measurable output
T	period of input
p.r.b.s.	pseudo-random binary sequence
L	number of bits in p.r.b.s.
n	number of register stages used to generate the p.r.b.s.
λ	minimum time interval between changes of state of p.r.b.s., i.e. p.r.b.s. clock interval
b	amplitude of transducer output
$\delta(t)$	delta function
k	impulse strength
$c(t)$	actual system input
$h(\tau)$	system impulse response
$\hat{h}(\tau)$	estimated impulse response
$\hat{h}_d(\tau)$	estimated impulse response in presence of drift
τ_p	shift at which impulse responce has maximum amplitude

ϕ_{xy}	crosscorrelation function between input and linear, noise free output
ϕ_{xx}	autocorrelation function of x
ϕ_{xz}	crosscorrelation function between x and measurable output z
ϕ_{nn}	autocorrelation function of noise at output
$\Phi_{nn}(f)$	noise spectral density
b_n	bandwidth of output noise in c.p.s.
σ_n	standard deviation of output noise
σ_1	standard deviation of estimates obtained by correlation
σ_2	standard deviation of estimates obtained by impulse testing
T_c	integrator time constant
M_j	j^{th} time moment of p.r.b.s.
M	order of base line drift
$P_i\ t^i$	i^{th} component of base line drift
$\xi(\tau)$	error term due to presence of base line drift
W	weighting function
w_i	i^{th} weight
^FC_f	binomial coefficient
A_1	area over which opening air pressure acts
A_2	area over which closing air pressure acts
μ	'on'delay expressed as a fraction of the p.r.b.s. bit interval

ψ	'off'delay expressed as a fraction of the p.r.b.s. bit interval
e(t)	error sequence
q	value of shift variable τ at which extra peaks are predicted for unequal 'on' and 'off' delays
N	number of theoretical plates in column
V_r	retention volume
β_e	peak width at 0.368 of peak height
t_{col}	temperature of column in ^oC
T_{col}	temperature of column in ^oK
T_{amb}	ambient temperature in ^oK
T_L	elution plus settling time of last eluted component
H.E.T.P.	Height equivalent to a theoretical plate
E,F,G	constants
a_i	i^{th} coefficient in detector characteristic
T_f	filter bandwidth,(3dB)
S	Laplace variable
D	Delay Operator

1. INTRODUCTION

In conventional chromatography the injection device places a measured quantity of sample in the form of a single pulse onto the column, and at the detector output, a series of multiple pulses are observed. This type of analytic procedure is akin to using a pulse input to determine linear system dynamics. If the pulse width is small it can be regarded as an impulse, and the output the impulse response. Generally this method cannot be applied directly to most linear systems since the noise levels demand the test impulse to be so large as to be totally impracticable. Thus other methods of determining the impulse response have been developed. The particular approach of interest in this chapter uses a continuous injection sequence of defined form instead of single pulses. Data analysis of the detector output yields the required chromatogram.

Inherent in this technique is considerable noise rejection. The desirability of this in realistic sample analysis is illustrated with practical examples. Several other advantages of using this approach are enumerated. Early experiments with the technique were not particularly conclusive since the system is easily forced into a non-linear regime. This can have drastic and unfortunate consequences with the approach proposed here. Examples of such behaviour are given. Fortunately it is possible to overcome such difficulties, by careful choice of commer-

cially available equipment, as shown in this chapter. The effects of temperature and carrier flow rate are also illustrated for an adsorption column.

2. IMPULSE RESPONSE ESTIMATION

The use of impulses has been mentioned in 1. An indirect and more practical method for determining the impulse response function is available and is now briefly described.

Consider a 'white noise' input applied to a linear, time invariant system, and the resultant output. We can define a crosscorrelation function between input and output as :-

$$\phi_{xy}(\tau) = \lim_{T\to\infty} \frac{1}{2T} \int_{-T}^{T} x(t-\tau)y(t)dt \qquad (1)$$

By the convolution integral

$$y(t) = \int_{-\infty}^{\infty} h(\tau_1)x(t-\tau_1)d\tau_1 \qquad (2)$$

$$\therefore \quad \phi_{xy}(\tau) = \int_{-\infty}^{\infty} \phi_{xx}(\tau-\tau_1)h(\tau_1)d\tau_1 \qquad (3)$$

$$\text{where } \phi_{xx}(\tau) = \lim_{T\to\infty} \frac{1}{2T} \int_{-T}^{T} x(t)x(t-\tau)dt \qquad (4)$$

is the autocorrelation function of the input. Since the the autocorrelation function of 'white noise' is impulsive

$$\phi_{xy}(\tau) = k\hat{h}(\tau) \qquad (5)$$

where k is the strength of the impulse. Thus by varying τ in (5), the impulse response is estimated to within a constant.

Although this technique is simple in concept, certain practical difficulties make it less attractive than appears at first sight. These difficulties are:-

(i) The statistics of 'white noise' are defined over an infinite length of record

(ii) 'White noise' is difficult to generate and delay

(iii) The stationarity of a 'white noise' generator is difficult to ensure

(iv) In many instances it would not be possible to find a transducer suited to a 'white noise' input

The difficulties associated with the use of 'white noise' may be overcome by choosing the input from a special class of periodic, deterministic signals. These are the pseudo-noise signals whose autocorrelation function approximates to the ideal impulsive form. Owing to their periodicity noise free measurements can be made over finite time. Of these classes of pseudo-noise signals, the maximal length binary sequences are of interest here. A sequence and its

delayed versions are easily generated from a set of interconnected feed-back shift-register stages, the resultant output being a chain of pulses with a period equal to $L\lambda$,

where $L = 2^n - 1$

The autocorrelation function of such a sequence is given by the relations,

$$\phi_{xx}(\tau) = 1 - \frac{|\tau|}{\lambda}\left(\frac{L+1}{L}\right) \text{ for } |\tau| \leq \lambda$$

$$\phi_{xx}(\tau) = -\frac{1}{L} \text{ for } |\tau| > \lambda,$$

and is illustrated by Fig.1. Note that since the sequences are binary, a suitable input transducer is not difficult to find.

A fuller discussion of these sequences and their generation is given in the literature[1,2,3]. Using these pseudo-random binary sequences (p.r.b.s.) the integration inherent in the crosscorrelation process need only be carried out over one period. However, the system itself must be in the steady state before crosscorrelation begins. This is discussed further in (vi) of the next section.

3. CROSSCORRELATION APPLIED TO GAS CHROMATOGRAPHY

The application of the technique of cross-correlation to gas chromatography is now clear. Samples are introduced into the column during the "1" state of a p.r.b.s., carrier alone being injected in the "0" state. The sequence length must be greater than the longest elution time and the bit interval chosen to give the required resolution . Fig. 2 shows the mechanisation of the process in block diagram form together with a typical input p.r.b.s. and the resultant detector output.

There are two alternative methods of introducing samples onto the column :-

(i) Direct injection into the carrier stream for the whole or part of the "1" bits of the p.r.b.s.

(ii) Trapping the sample in a bypass loop of known volume and sweeping the loop out with carrier during each "1" bit.

Conventional analysis techniques use method (ii) only,since (i) does not give the reproducibility required. Thus, in the work described in this thesis, injection method (ii) is used except when stated otherwise.

The p.r.b.s. approach can be expected to have several advantages :-

(i) If each sample injection is the same size as a single injection in the conventional approach, greater accuracy may be achieved. However, column flooding could occur as the total sample size is now (L+1)/2 as large as a single injection.

(ii) The detector output is no longer a chromatogram but of the form shown in Fig.2. The detector operates on one range only as widely differing peak heights will not occur. (This also means that range changing is not applied so that all components are detected with the same sensitivity).

(iii) The cross correlation process would necessarily be carried out by a computer and a series of ordinates would result, which when plotted give the chromatogram. This will aid peak area evaluation if the resolution has been correctly chosen.

(iv) If the detector output is contaminated with random noise, the variance in the estimates of the ordinates of the chromatogram is reduced by correlation so that the signal to noise is improved according to

$$\frac{[\text{Signal/Noise}]\ \text{by correlation technique}}{[\text{Signal/Noise}]\ \text{by conventional technique}} = \left(\sqrt{Tb_n}\right)/2 \qquad (6)$$

For a proof of this result see Appendix B1. If the variance in the estimates is still too high, correlation can be averaged over several periods of the sequence so that the variance is reduced by a factor $\sqrt{\text{Number of averaging periods}}$

(v) Base line drift during the experiment can be represented as a further polynomial noise term at the output. Appendix B2 shows that the effects of such baseline drift on impulse response estimates can be removed by correlating over two periods and weighting the estimates according to the rules given there.

(vi) After commencing sample injections with a p.r.b.s., the detected output should not be recorded before the system reaches its steady state. This does not occur until the last sample peak has been eluted. The p.r.b.s. should be chosen so that its period is equal to or greater than this time. Sampling the output at each succeeding bit, the input-output crosscorrelation function yields

a reliable sample analysis after a further L bit intervals have elapsed. Thus for a minimum period p.r.b.s., the first useful analysis is not available before two sequence periods have elapsed. This analysis is also one period out of date

If the sample composition remains constant, the analysis is recomputed every bit interval, and it is to be noted that

$$\lambda \ll T_L.$$

If the sample composition varies, a further two sequence periods after the change are normally required before a new quantitative analysis is obtained. However, the input-output crosscorrelation function heralds the change as soon as it is recorded at the output. Applying the techniques outlined in Chapter 3 section 4 quantitative analysis would also be possible at the same instant. Moreover a continuously varying sample concentration can be tracked. Thus using p.r.b.s. continuous analysis of samples with varying concentration is possible.

4. BRIEF REVIEW OF EARLY EXPERIMENTS BY OTHER WORKERS

The correlation technique has been applied by other authors[4,5], but with limited success in all cases. Early work by Izawa and Furuta[4] in 1967 was directed at analysing a mixture of oxygen and nitrogen with helium carrier on a molecular sieve column(adsorption chromatography). Their results obtained using katherometer detectors showed the two components fairly well separated. Also in evidence however were several supplementary peaks of heights up to 4% of the major peak height. The presence of these extra peaks was not explained. If they do not correspond to trace components, it is doubtful if such a correlogram would be acceptable to an analyst. Since little was known with regard to the performance of the technique, two further investigations were initiated[5,6].

Godfrey and Devenish[5] attempted to analyse a sample of air using argon carrier with a 300µl sample valve, and a thermal conductivity detector. The major components of the air sample were discernible but again, many supplementary peaks of up to ±25% of the major peak height appeared. Changing to helium carrier gave similar results. The excellent reproducibility of these results (±0.5%) suggested that such behaviour could only be explained by the presence of a nonlinearity somewhere within the system. This was substantiated when by reducing the sample to 10µl, the base-

line ripple was reduced to ≈±6%. Though encouraging, this result is still unacceptably large when compared with the figure of less than 1% variance on the baseline of conventional chromatographs.

5. BRIEF REVIEW OF INITIAL ANALYSES CONDUCTED BY THE AUTHOR

Concurrently but independently of Godfrey and Devenish[5], the author began work[(a)] in the field which was subsequently submitted as an M.Sc. thesis in 1968[6]. Some of the results of that work are described in this section.

5.1 HYDROCARBON ANALYSIS

Using conventional techniques and injection method (i), a sample of 5% hydrocarbon mixture[(b)] in helium yields the chromatogram of Fig.3. Helium carrier and a 20% weight by weight methoxy-ethyl adipate on 6' by $\frac{1}{8}$" o.d. 60-80 mesh chromasorb P, column operated at room temperature, were used. Detection was by a Servomex Mk. 158 microkatherometer. Note that this is an example of gas-liquid chromatography.

The corresponding chromatogram using the p.r.b.s. approach and injection method (i) is shown in Fig.4. This shows supplementary peaks up to 13% of the major peak height. Reducing the hydrocarbon concentration to 1% in helium reduces the magnitude of these supplementary peaks to 3.5% as seen in Fig. 5. In common with the observations of Godfrey and Devenish[5], this behaviour suggests that one or more portions of the system were non-linear. The non-linearity could have been in either the sample valve, the column or

---

(a) This work was carried out with the cooperation of Hewlett Packard Ltd. at their South Queensferry research and development section.

(b) Hydrocarbon mixture by volume: 90% Propylene, 8% Propane, 2% C 2's.

the detector, or even a combination of these.

The possible existence of non-linearity in each of these components is investigated in the next section.

6. CONSIDERATION OF NON-LINEARITIES

In order to isolate the nonlinearity each of the system components was examined separately in the following order.

6.1 SAMPLE VALVE NON-LINEARITY

The sample valve (I.C.I.patent number 800,212) was designed so that the gas supply to the column could be derived either from carrier or sample reservoirs depending on the position of a piston. Attached to this piston is a flange, over an area A_1 of which pressurized air acts, so that the piston is in such a position that carrier gas normally flows into the column. To inject samples, a second stream of air at the same pressure is directed onto an area A_2 on the opposite side of the same flange. Providing the ratio $A_1:A_2 = \frac{1}{2}:1$, then the net force to move the piston to the inject position, equals the net force to return when the second air stream is removed and hence the 'ON' and 'OFF' time constants would be equal.

By measurement however $A_1/A_2 = \frac{1}{2.48}$ suggesting that the 'ON' and 'OFF' time constants of the valve would be different, and in the ratio

$$\frac{\text{'ON' TIME CONSTANT}}{\text{'OFF' TIME CONSTANT}} = (A_1/A_2)\ \text{actual} \Big/ (A_1/A_2)\ \text{desired}$$

$$= 2/2.48$$

$$\approx 0.8$$

To check this, a step response of the form Fig.6*was obtained by injecting pure nitrogen directly through the sample valve into the detector.(i.e. the column was omitted) At the flow rate used (10 ml/min), the effects of diffusion in the katherometer would be negligible, since the cell volume was only 2µl. Thus Fig.6 is effectively the responce of the sample valve above.

Approximating the behaviour of Fig.6 to the step response of a first order system then

$$\frac{\text{'ON' TIME CONSTANT}}{\text{'OFF' TIME CONSTANT}} = \frac{0.799}{1.052} \simeq 0.8$$

Godfrey et al [7,8,9] have made a study of the effects of such non-linearities. They show that with such a non-linearity in the system, each peak in the true impulse response will give rise to a single extra peak in the resultant correlation function. The location of these extra peaks with respect to their 'parent' peaks is known, and their areas depend on the difference in the time constants. Furthermore the 'parent' peaks are themselves distorted. In the case of Figs. 4 and 5, bit intervals of one second were used, but Fig.6 suggests that the minimum transport time was two seconds. The results of Godfrey et al [7,8,9] therefore, may not be directly applied to interpret Figs. 4 and 5, since they considered only the case of a transducer

---

* Figs.6,7,8 taken from M.Sc.thesis

reaching its final valve within the bit interval.

The present practical case is better studied by a digital simulation of a non-linear filter,(time constants equal to those of the sampling valve) applied to a p.r.b.s. of length 127 and λ = one second. The output of the simulated filter for this sequence and the corresponding autocorrelation function are shown in Fig.7 and Fig. 8 The general results are the same as those of Godfrey et al[7,8,9] with the extra peak in the same region, but with an increased baseline ripple.

The effects of the unequal 'ON' and 'OFF' delay times (see Fig.6) are similar to those of unequal time constant (see Appendix B3). In particular the extra peaks for the two cases appear within one bit of each other. Since the extra peaks predicted from Fig. 8 do not coincide with those of Figs. 4 and 5, sample valve non-linearity does not appear to have been the dominant source of trouble.

6.2 COLUMN NON-LINEARITIES

In Chapter 1, section 3.2, it is noted that gas-liquid chromatography is normally used with low sample concentrations for which Raoult's law is obeyed during elution. If gross samples are loaded onto a column, the partition coefficient varies with concentration and Raoult's law no longer holds. Using p.r.b.s. to estimate the chromatogram, the effect would be similar to that of a distributed non-linearity down the column. To establish whether such behaviour could account for the non-linearity evident in section 5, chapter 2,

a sample gas was chosen from the range of gases not adsorbed by the stationary phase. Such gases pass through the column without partition. The column serves only as a volume to flow through.

The particular column used in section 5, Chapter 2, behaves in this way with nitrogen sample. Injecting pure nitrogen in the conventional manner, a single peak results with a flat base line. Using p.r.b.s. Fig.9a is obtained. Subsidiary peaks of up to ±7% of the nitrogen peak are again present. The bypass volume is 40µl and at a flow rate of 1/6 ml./sec.,the concentration of nitrogen in helium at the column input is 23 mole%, for each 1 second injection.

6.3 DETECTOR NON-LINEARITIES

Since the column could not have contributed significantly to the non-linear effects in Fig.9a, it appears that the dominant source of non-linearity lay in the detector. Equation (8), section 2.4.2,Chapter 1, relates the thermal conductivity of a mixture of gases to their concentration in the mixture. This equation shows that at high concentrations, the relationship is non-linear. A figure of 23 mole% nitrogen in helium would be considered high, and thus the detector output under such conditions would be related to nitrogen concentration by

$$z(t) = a_0 + a_1 y(t) + a_2 y^2(t) + a_3 y^3(t) + \ldots \qquad (7)$$

where y (linear system output) in this case is the nitrogen

concentration at the detector input. In a correlation scheme the presence of indices greater than unity in (7) cause errors in the estimated impulse response and give rise to supplementary peaks. If the input sequence is modified so that it is inverse-repeat*, then the effect of even power indices on the impulse response is removed. Performing such an experiment yields Fig.9b where the supplementary peaks have been reduced to ±2% of the major peak height. A reduction of supplementary peak height using inverse repeat sequences was also noted by Godfrey and Devenish[5].

To demonstrate conclusively that the distribution of supplementary peaks in Fig.9a could be explained by a detector characteristic such as (7), the chromatography system was simulated by analogue and digital components. For the purposes of this simulation it was meaningful to lump the sample valve non-linearity as an overall delay in 'ON' time, (see Appendix B3). The transport lag in the column was simulated by an artificial delay in the input perturbations, and the flow dynamics by five identical first order lags in cascade and a high pass filter. (The purpose of the filter was to improve the symmetry of the response peak). Approximating the detector characteristic to a cubic polynomial following the dynamics, the system model is then as shown in Fig.10. On this model an un-

---

* A fuller discussion of the effects of non-linearities on process crosscorrelations is given in Chapter 3.

modified p.r.b.s. input gives the crosscorrelation of Fig. 11.

The degree of sample valve non-linearity controls the area under the negative excursion immediately prior to the major peak, and the order of the polynomial detector characteristic the position of the supplementary peaks. Although the model correlogram does not exactly fit the chromatograph response (Fig.9a), they are sufficiently alike to suggest that the model is a valid representation of the system.

If the detector is assumed to be non-linear, the behaviour of the results of section 5 when analysing hydrocarbons, as well as the effects noted by Godfrey and Devenish[5], can be explained. It might also be noted from Chapter 1, section 2.4.3, that one prerequisite for a linear katherometer response is that sample and carrier must have widely differing thermal conductivities. In some of the work of Godfrey and Devenish[5] argon carrier was used when analysing air samples. Since argon and air have comparable thermal conductivities, the presence of supplementary peaks indicating a non-linear detector response is not surprising.

7. EXPERIMENTS USING MODIFIED APPARATUS

Since it was seen that the nitrogen sample size was so large as to force detector operation into the non-linear region, a modified set of apparatus, to allow injection of very small samples (down to 0.3µl) was assembled. This consists of a Servomex GC 203 chromatograph with a Loenco LSV220 sliding plate valve. In the LOENCO valve the sample gas is trapped in a bypass volume, the size of which can be chosen from one of several values (0.3,1.0,3.0, 10.0 and 20.0µl). The same katherometer (Servomex MK 158) is used but the column packing is changed to porous polymer beads (Porapak 'Q'). The column dimensions are 8'x$\frac{1}{8}$"o.d.

In this column separations occur through the mechanisms of gas-solid chromatography, which enables operation over a greater range of temperature than with the partition column. The only effect of note due to the change in column length and packing material is the increase in retention times.

The laboratory in which the apparatus is situated is insufficiently shielded from external sources radiating considerable noise power. Thus the detector outputs are contaminated with random fluctuations. Furthermore, to facilitate the interface between katherometer and digital computer, some d.c. amplification is required. The amplifier outputs are seen to contain considerable high frequency noise levels, so they are passed through a low pass filter

$$\left[\frac{1}{(1+ST_f)^2},\ \text{B.W.} = 3\ \text{c/s}\right].$$

In all the work that follows in this thesis, the amplifier and filter are incorporated in the detection system. It will be seen however, that the noise levels which remain are still too high to allow conventional analysis of the hydrocarbon samples under test. This situation could easily arise in an industrial environment.

To ensure that this apparatus will allow operation of the detector in a linear mode, initial tests were carried out by using nitrogen sample,(not absorbed by Porapak 'Q') before realistic tests were carried out on hydrocarbon samples.

7.1 NITROGEN SAMPLES

Using a 1.0µl slider and a helium carrier flow rate of 1/6 ml/sec., the chromatogram of Fig. 12 is obtained with p.r.b.s. The reduction of sample size results in a lower nitrogen concentration (0.6 mole %) at the column input and allows operation within the linear regime of the detector. Consequently the baseline ripple has been reduced to ±0.5 % of the peak height. The sample valve is known to be linear. The residual ripple is possibly due to some remnant non-linearity in the detector, but is more likely to be caused by quantisation effects in the correlation routine. Since the baseline ripple is less than

1% of the peak height, such a correlogram would be acceptable for quantitative analysis purposes.

7.2 HYDROCARBON SAMPLES

Fig.13 is the chromatograph obtained by conventional analysis of a representative hydrocarbon sample at 20 °C with helium carrier, and a single 10µl injection. High background noise levels prevent even a qualitative analysis. The sample is known to be a 1% hydrocarbon mixture in helium, the hydrocarbon composition being approximately 90% propylene, 8% propane and 2% ethane.

Using the continuous (p.r.b.s.) approach under the same experimental conditions, all three components become easily identifiable as shown in Fig. 14. The extra nitrogen peak is probably due to a small amount of the gas resident in the apparatus. A comparison of the results in Figs. 13 and 14 illustrates the significant noise rejection properties of the correlation technique. These could be particularly useful in trace analysis.

Assuming that the volume concentration can be estimated by calculating area percentages without applying any response factors, use of Simpson's rule on Fig. 14 gives the hydrocarbon analysis as propylene 91%, propane 7.1%, ethane 1.8%.

Continuous analysis of the hydrocarbon sample at 60% yields Fig. 15. It is noticed that by increasing the temperature from 30 to 60 ^{o}C decreases the longest retention time by 14.1%,and reduces the separation between the component peaks. This effect is discussed in the next section.

8. THE EFFECT OF EXPERIMENTAL CONDITIONS ON COLUMN PERFORMANCE

Chapter 1, section 3 introduces the concept of H.E.T.P. as a measure of column efficiency and shows its dependence on the flow rate of the mobile phase. The theoretical development referred to there applies specifically to gas-liquid chromatography, although the literature suggests that the approach can be extended to gas-solid chromatography. However, such an analysis could not be found in the standard texts. It was decided to measure the equivalent H.E.T.P.-flow rate characteristic of the Porapak 'Q' column for propylene.

It has been noted[10,11] that carrier impurities are eluted in the normal way as if they were present in the sample, but that they yield a negative detector response. Thus their presence may not be a disadvantage. Furthermore, in our case if the impurity is nitrogen, measurement of the retention volume of the negative peak gives the gas hold up of the column. Such a carrier (nitrogen impurity in helium) was readily available from the waste product of other experiments, and was used in the following, for the sake of economy.

In addition, it was seen that analysis of the 1% hydrocarbon sample was impossible by conventional chromatography, since the high background noise levels masked everything

except the negative impurity peak. The noise rejection properties of the correlation approach have already been demonstrated, so this method was used exclusively in the work described in the sections following.

8.1 THE EFFECT OF FLOW RATE ON H.E.T.P.

Average flow rates were computed from the expression

Average flow rate = output flow rate x pressure correction factor (8)

and the number of theoretical plates from equation (14) Chapter 1, i.e.

$$N = 8\left(\frac{V_r}{\beta_e}\right)^2 \qquad (9)$$

Since H.E.T.P. $\propto \frac{1}{N}$, a plot of 1/N versus average flow rate shows the dependence of H.E.T.P. on that parameter. The results are presented in Fig. 16.

8.2 THE EFFECT OF TEMPERATURE ON RETENTION

To examine the validity of the expression relating retention time to temperature, viz

$$\log_e(\text{specific retention volume}) = E + \frac{F}{t_{col}+G} \qquad (10)$$

for this column, an experiment was conducted to measure the

variation of propylene retention volume with column temperature. Now

$$\text{propylene retention volume} = \frac{T_{col}}{T_{amb}} \left(\frac{\text{propylene retention time}}{\text{nitrogen retention time}} \right) \text{Vol. of column} \quad (11)$$

Thus a graph of $\log_e \frac{T_{col}}{T_{amb}} \left(\frac{\text{propylene retention time}}{\text{nitrogen retention time}} \right)$ against $\frac{1}{T_{col}}$ $(G=273)$ would show the validity of (10)

Note that $T_{col} = t_{col} + C$.

Fig.17 shows the result of such an experiment, from which we conclude that(10) is a good approximation to the experimental behaviour of the porapak 'Q' column.

In 7.2 the increase of column temperature from 30 to 60 ^{o}C was seen to reduce the retention time by 14.1%. Using Fig. 17, it is possible to predict the decrease in retention time if the nitrogen retention times are known. For the same temperature change, this procedure predicts a decrease of 13.3%. Thus increase of column temperature reduces analysis time.

There are other aspects to be considered, however, since such increases of temperature cause the peaks to crowd together and decrease their resolution. Thus, one limit to which column temperature can be raised is set by peak resolution. Components are said to be just resolved when the peak of one falls on the trough of the other. This is the case for propane and propylene in Fig. 15, and hence

further temperature increases in an effort to reduce analysis time, would result in unresolved peaks.

9. APPENDICES

APPENDIX B.1.

IMPULSE RESPONSE ESTIMATES FROM NOISY DATA

If we assume that the system output is corrupted with random noise as shown in Fig. 18, then crosscorrelation between input and measurable output yields an estimate of the system impulse response

$$\text{i.e. } \hat{h}(\tau) = \frac{1}{T_c}\int_0^T z(t)x(t-\tau)dt \qquad \text{B.1.(1)}$$

$$\text{where } z(t) = y(t) + n(t) \qquad \text{B.1.(2)}$$

$$\therefore \hat{h}(\tau) = \frac{1}{T_c}\int_0^T\int_0^\infty h(\tau_1)c(t-\tau_1)x(t-\tau)d\tau_1 dt + \frac{1}{T_c}\int_0^T n(t)x(t-\tau)dt \qquad \text{B.1.(3)}$$

where the actual system input c(t) is +b and 0, rather than ±1

$$\text{i.e. } c(t) = \frac{b}{2}\left[x(t) + 1\right]$$

$$\therefore E\left[\hat{h}(\tau)\right] = \frac{b}{2T_c}\int_0^T\int_0^\infty h(\tau_1)E\left[x(t-\tau_1)x(t-\tau)+x(t-\tau)\right]d\tau_1 dt + \frac{1}{T_c}\int_0^T E\left[n(t).x(t-\tau)\right]dt \qquad \text{B.1.(4)}$$

$$\doteq \frac{bT}{2T_c}\int_0^\infty \phi_{xx}(\tau-\tau_1)h(\tau_1)d\tau_1 + \frac{1}{T_c}\int_0^T \bar{n}.\bar{x}.dt + \frac{bT}{2T_c}\int_0^\infty h(\tau_1)d\tau_1 \qquad \text{B.1.(5)}$$

N.B. In this Appendix bar signs indicate averaging.

i.e. $\bar{x} = \frac{1}{T}\int_0^T x(t)dt.$

$$\therefore\ \hat{h}(\tau)-E[\hat{h}(\tau)] = \frac{b}{2T_c}\int_0^T\int_0^\infty h(\tau_1)[x(t-\tau_1)x(t-\tau)+x(t-\tau)]d\tau_1 dt$$

$$+\frac{1}{T_c}\int_0^T n(t)x(t-\tau)dt - \frac{b}{T_c}\int_0^\infty \phi_{xx}(\tau-\tau_1)h(\tau_1)d\tau_1 dt - \frac{bT}{2T_c}\int_0^T h(\tau_1)d\tau_1$$

$$-\frac{1}{T_c}\int_0^T \bar{n}.\bar{x}dt \qquad \text{B.1.(6)}$$

$$\text{i.e. } \hat{h}(\tau)-E[\hat{h}(\tau)] \simeq \frac{b}{2T_c}\int_0^T\int_0^\infty h(\tau_1)[x(t-\tau_1)x(t-\tau)+x(t-\tau)$$

$$-\phi_{xx}(\tau-\tau_1)-1]d\tau_1\, dt$$

$$+\frac{1}{T_c}\int_0^T n(t)x(t-\tau)dt - \frac{1}{T_c}\int_0^T \bar{n}.\bar{x}.dt \qquad \text{B.1.(7)}$$

If we assume that x(t) is a p.r.b.s. with zero mean* then the first and last terms are zero. Now

$$\text{variance in estimate} = \sigma_1^2 = E\left[\hat{h}(\tau)-E[\hat{h}(\tau)]\right]^2$$

$$\text{i.e. } \sigma_1^2 = E\left[\frac{1}{T_c^2}\int_0^T\int_0^T n(t_1)n(t_2)x(t_1-\tau_1)x(t_2-\tau_1)dt_1\ dt_2\right]$$

$$\simeq \frac{1}{T_c^2}\int_0^T\int_0^T \phi_{nn}(t_1-t_2)\phi_{xx}(t_1-t_2)dt_1\ dt_2 \qquad \text{B.1.(8)}$$

which can be transformed to

$$\sigma_1^2 = \frac{2}{T_c^2}\int_0^T (T-g)\phi_{nn}(g)\phi_{xx}(g)dg \qquad \text{B.1.(9)}$$

If we assume that the bandwidth b_n of the noise is very much greater than that of the signal x(t), then the auto-correlation function of the noise may be approximated by an

---

*x(t) will have zero mean if its levels are $(1-\frac{1}{L})$ and $-(1+\frac{1}{L})$

impulse function. Then since

$$\phi_{nn}(f) = \int_{-\infty}^{\infty} \phi_{nn}(\tau)\exp(-j2\pi f)\, d\tau$$

$$\phi_{nn}(0) = \int_{-\infty}^{\infty} \phi_{nn}(\tau)d\tau = \frac{\sigma_n^2}{2b_n} \qquad \text{B.1.(10)}$$

$$\therefore \quad \phi_{nn}(\tau) = \frac{\sigma_n^2}{2b_n}\,\delta(\tau) \qquad \text{B.1.(11)}$$

If x has zero mean level, $\phi_{xx}(0) \simeq 1$, so B.1.(9) can be evaluated as

$$\sigma_i^2 \simeq \frac{2}{T_c^2} \cdot T \cdot \frac{\sigma_n^2}{2b_n} = \frac{\sigma_n^2\, T}{T_c^2 b_n} \qquad \text{B.1.(12)}$$

Thus from the correlation experiment the signal to noise ratio is given by

$$\simeq \frac{\frac{bT\lambda}{2T_c}\,\hat{h}(\tau)'}{\frac{\sigma_n}{T_c}\sqrt{\frac{T}{b_n}}} \qquad \text{B.1.(13)}$$

where the dash signifies that the impulse response estimates depend on the extent of the approximation involved in assuming that the autocorrelation function of a p.r.b.s. is impulsive at the origin.

If we now attempt to measure the impulse of the system by stimulating it with an approximate impulse of

strength $b\lambda$,

$$z(t) = b\lambda\hat{h}(\tau) + n(t).$$

$$\therefore \quad E\left[\hat{h}(\tau)\right] = h(\tau) + \frac{1}{b\lambda} E\left[n(t)\right]$$

$$\text{thus Var}\left[\hat{h}(\tau)\right] = \sigma_2^2 = \frac{\sigma_n^2}{b^2\lambda^2} \qquad \text{B.1.(14)}$$

Thus the signal to noise ratio in the latter experiment

$$= \frac{\hat{h}(\tau).b\lambda}{\sigma_n}$$

Thus the ratio of signal to noise ratios from the two experiments

$$\approx \frac{b\lambda\,\hat{h}(\tau)\sqrt{T\,b_n}}{2\,\sigma_n} \quad \frac{\sigma_n}{h(\tau)\,b\lambda}$$

$$\approx \left(\sqrt{T\,b_n}\right)/2 \qquad \text{B.1.(15)}$$

This expression gives the improvement in signal to noise ratio when using correlation, but depends upon the assumption that the noise bandwidth is wide compared to that of the signal.

APPENDIX B.2

THE EFFECT OF BASE-LINE DRIFT ON IMPULSE RESPONSE ESTIMATES

To understand the effects of base line drift on impulse response estimates consider n(t) of Fig.18 to be the polynomial

$$n(t) = \sum_{i=0}^{M} P_i \, t^i \qquad \text{B.2.(1)}$$

If correlation is performed between the p.r.b.s. x and the measurable output z,

$$\phi_{xz}(\tau) = \frac{1}{T} \int_0^T [n(t+\tau) + y(t+\tau)]x(t)dt \qquad \text{B.2.(2)}$$

$$= \frac{1}{T} \int_0^T n(t+\tau)x(t)dt + \phi_{xy}(\tau)$$

$$\text{i.e. } \phi_{xz}(\tau) = \hat{h}(\tau) + \zeta(\tau) \qquad \text{B.2.(3)}$$

where $\zeta(\tau)$ is an error term due to drift and is dependent on τ. Early workers[12,13] noted that $\zeta(\tau)$ is a sum of time moments of the m sequence defined as

$$M_j = \int_0^T t^j \, x(t+\tau)dt \qquad \text{B.2.(4)}$$

M_o is zero if the levels of x at the correlator are chosen so that the code has zero mean level over one period.

Ream[14] has examined p.r.b.s. and found that there exists a 'reference phase' such that if x(t) has such a phase

it is uncorrelated with constant and linear signals. Starting x with the reference phase, M_1 is identically zero. Furthermore M_2 is a constant(i.e. independent of τ) for the same x. Thus by careful choice of x the effects of quadratic drift can be minimised[15]. However this approach is of little value in chromatography where continuous analysis is required, since the p.r.b.s. will not always have the same phase.

A more useful approach has been formulated[16] and is applicable to continuous analysis. If the observations start at time $t=s+T_1$,

$$\hat{h}_d(\tau) = \frac{1}{T}\int_0^T x(t+T_1+s)\, z\,(t+T_1+s+\tau)dt \qquad \text{B.2.(5)}$$

Since in B.2.(5), the estimate $h_d(\tau)$ depends on s if drift is present, the dependence is emphasised by writing $\hat{h}_d(\tau)$ as $\hat{h}_d(T_1+s)$.

Davies and Douce[16] also postulate a weighting function $W(T_1)$ and form weighted sums of estimates according to

$$h\,(\tau) = \frac{\int_0^T W(T_1)\,\hat{h}_d\,(T_1+s)d\,T_1}{\int_0^T W(T_1)d\,T_1} \qquad \text{B.2.(6)}$$

The weighting function can then be chosen so that

$$\int_0^T W(T_1)\left[\int_0^T n(t+T_1+s+\tau)x\,(t+T_1+s)dt\right]d\,T_1 = 0 \qquad \text{B.2.(7)}$$

and then the drift term does not influence the final estimate of impulse response. Davies and Douce[16] show that B.2.(7) is satisfied if $W(T_1)$ is a polynomial in T_1, the coefficients of which depend solely on the order of the drift. These polynomials however are not orthogonal and all coefficients must be recalculated on adding further terms to the series n(t). It is also to be noted that (6) implies crosscorrelation over two periods of the m sequence, and that a large amount of off-line computation is required to arrive at $W(T_1)$.

Brown[17] gives a method which employs inverse repeat sequences which have the property

$$x(t+T) = -x(t) \qquad (T=L\lambda)$$

and are of length 2L.

Redefining B.2.(2) so that

$$\phi_{xz}(\tau) = \frac{1}{T}\int_0^T [n(t)+y(t)]x(t-\tau)dt \qquad \text{B.2.(8)}$$

and noting that z(t) also has the inverse repeat property Brown[17] shows

$$T\left(\sum_{i=0}^{M+1} w_i\right)\phi_{xz}(\tau) \doteq \sum_{i=0}^{M+1}\int_{iT}^{(i+1)T} w_i\, x(t-\tau)z(t)dt \qquad \text{B.2.(9)}$$

where w_i are arbitrary weights associated with the respective half periods of the crosscorrelation. In the presence of drift

$$T\left(\sum_{i=0}^{M+1} w_i\right)\phi_{xy}(\tau) = T\left(\sum_{i=0}^{M+1} w_i\right)\phi_{xz}(\tau) + \sum_{i=0}^{M+1}\int_0^T w_i(-1)^i \times (t-\tau)\mathbf{n}(t+iT) \qquad \text{B.2.(10)}$$

By correct choice of the w_i in B.2.(10), the drift term can be made identically zero. Brown[17] notes that this can be done independent of the coefficients of the drift, and shows that the w_i are binomial weightings.

A point to notice with the use of this method is that to remove M^{th} order drift one needs to cross-correlate over (M+2) half periods of the inverse repeat sequence. Thus the measurement time increases with the order of the drift. Besides this objection, Brown[18] himself notes in a later paper, that the method of Davies and Douce[16] is superior on the basis of its noise rejection properties.

Macleod[19] has proposed a method requiring just two periods of an m sequence to eliminate drift of order up to L-2. Using a sequence of levels ±b, an estimate of impulse response in a drift free environment can be obtained from

$$\hat{h}(\tau) = \frac{L}{b^2(L+1)\lambda}\left[\phi_{xy}(\tau) - \phi_{xy}(0)\right] \qquad \text{B.2(11)}$$

which in the presence of drift becomes

$$\hat{h}_d(\tau) = \hat{h}(\tau) + \frac{L}{b^2(L+1)\lambda}\left[\phi_{xn}(\tau) - \phi_{xn}(0)\right] \qquad \text{B.2.(12)}$$

Using the binomial coefficient defined as

$$ {}^{F}C_{f} = \frac{F!}{f!(F-f)!} \qquad \text{B.2.(13)} $$

We can form a new input-output crosscorrelation according to

$$ \phi'_{xz}(\tau) = \frac{L}{b^2(L+1)} \left[\frac{1}{L} \sum_{r=0}^{L-1} \left[\sum_{f=1}^{F} (-1)^f \, {}^{F}C_{f} (z_{r+f} - z_{r}) \right] x_{r-\tau} \right] $$

If F = M+1, the effect of the base line drift is eliminated and

$$ \phi'_{xz}(\tau) = \sum_{f=1}^{F} (-1)^f \, {}^{F}C_{f} [\hat{h}(q+\tau) - \hat{h}(\tau)] \qquad \text{B.2.(14)} $$

B.2.(14) gives a set of (L-1) linearly independent equations from which the required unknowns can be estimated.

From the point of view of continuous analysis the choice of drift compensation lies between the methods of Macleod[19], Davies and Douce[16] and Brown[17]. Macleod's method seems to be the most applicable since only two periods of output data are required to remove high order drift effects, and the resultant equation set is easy to program digitally. This procedure may also benefit from the existence of transport lags (zeroes in impulse response function) in chromatography experiments.

APPENDIX B.3.

THE ESTIMATION OF ERRORS CAUSED BY UNEQUAL DELAY TIMES IN THE INPUT TRANSDUCER

Assume a system of the form of Fig.18. Consider the case of negligible output disturbance n(t), so that y(t) = z(t). The actual system input c(t) is derived from x(t) by a non-ideal transducer. Postulating the case of a transducer with negligible time constants but significant 'ON' and 'OFF' delay times, c(t) is a much distorted version of x(t) when these delay times are unequal. There are two cases :-

(a) Zero off delay, non zero on delay so that

'ON' delay : bit interval = μ : 1 B.3.(1)

(b) Zero on delay, non zero off delay so that

'OFF' delay : bit interval = ψ : 1 B.3.(2)

Note that the case of non zero and unequal 'ON' and 'OFF' delays can be reduced to either case (a) or case (b).

First consider case (a). We have

$$\phi_{x*z}(\tau) = \int_0^T h(\tau_1)\phi_{cx*}(\tau-\tau_1)d\,\tau_1 \qquad \text{B.3.(3)}$$

where the * denotes the transformation 0=-1,1=+1.
Further if c(t) is a sequence of 1's and 0's

$c(t) = x(t) \oplus e(t)$ where e(t) is an error sequence.

equivalently $e(t) = x(t) - c(t)$ B.3.(4)

$$\therefore \quad \phi_{cx}(\tau) = \phi_{xx}(\tau) - \phi_{ex}(\tau) \qquad \text{B.3.(5)}$$

Now e(t) is a sequence which has zeroes everywhere except at the beginning of a run of ones in x(t), where it has a single one. The situation for a 15 bit sequence is illustrated in Fig. 19a. The area of a single pulse in e(t) is μ, thus e(t) can be replaced by a sequence of pulses of width unity and height μ. The following equation will thus be seen to generate e(t) from x(t)

$e(t) = \mu[\bar{x}\ (t-\lambda).\ x(t)]$ (bar denotes inversion) B.3.(6)

$$= \mu[1 \oplus x(t-\lambda)].\ x(t)$$

$$= \mu[x(t) \oplus x(t-\lambda).x(t)] \qquad \text{B.3.(7)}$$

$$\therefore \quad \phi_{ex}(\tau) = \frac{\mu}{T} \int_0^T x(t-\tau)\ e\ (t)dt$$

or if we use the * transformation

$$\phi_{e^*x^*}(\tau) = \frac{\mu}{T} \int_0^T x^*(t-\tau)\ e^*(t)dt$$

$$= \frac{\mu}{T} \int_0^T x^*(t-\tau)[x(t) \oplus x(t-\lambda).\ x(t)]^*dt \qquad \text{B.3.(8)}$$

$$\text{i.e.} \quad \phi_{e^*x^*}(\tau) = \frac{\mu}{T} \int_0^T \overline{[x^*(t-\tau)x^*(t)][x(t-\lambda)x(t)]}^*dt \qquad \text{B.3.(9)}$$

$$\therefore \quad \phi_{e^*x^*}(\tau) = \frac{\mu}{T} \int_0^T \overline{[2x(t-\tau)-1][2x(t)-1][2x(t-\lambda)x(t)-1]}dt$$

B.3.(10)

Note that in this Appendix unlike Appendix B.1, bars indicate inversion. Hence if x(t) is a sequence of 1's and 0's, $\bar{x}(t)$ is a sequence of 0's and 1's.

Since $x(t).x(t) = x(t)$, this becomes

$$\phi_{e^*x^*}(\tau) = -\frac{\mu}{T}\int_0^T [4x(t-\tau)x(t-\lambda)x(t)-2x(t)x(t-\lambda)-4x(t)x(t-\tau) +2x(t-\tau)+2x(t)-1]dt$$

$$= -\frac{\mu}{T}\int_0^T 4x(t-\tau)x(t-\lambda)x(t)dt - \mu[-2\phi_{xx}(\lambda)-4\phi_{xx}(\tau) -1+\frac{4}{T}\int_0^T x(t)dt] \qquad \text{B.3.(11)}$$

Using the expression $x(t) = \frac{1}{2}(x^*(t)+1)$, the first term in B.3.(11) can be written as

$$-\frac{\mu}{2}\left[\frac{1}{T}\int_0^T [D^0 \oplus D^\lambda \oplus D^\tau]x^*(t)dt + \phi_{x^*x^*}(\tau) + \phi_{x^*x^*}(\lambda) + \phi_{x^*x^*}(\tau-\lambda) +1 +\frac{3}{T}\int_0^T x^*(t)dt\right]$$

which is equivalent to

$$-\frac{\mu}{2}\left[\frac{1}{T}\int_0^T [D^0 \oplus D^\lambda \oplus D^\tau]x^*(t)dt + \phi_{x^*x^*}(\tau) + \phi_{x^*x^*}(\tau-\lambda) +\frac{L+2}{L}\right] \qquad \text{B.3.(12)}$$

Similarly the second term in B.3.(11) becomes

$$-\mu\left[-\frac{(L+1)}{2L} -4\,\phi_{xx}(\tau) -1 + 4\,\frac{(L+1)}{2L}\right]$$

$$= \mu\left[4\phi_{xx}(\tau) - \frac{(L+3)}{2L}\right] \qquad \text{B.3.(13)}$$

Using B.3.(12) and B.3.(13) we can determine $\phi_{e^*x^*}(\tau)$ from B.3.(11) at various τ, to give the following :-

	τ	$\phi_{e^*x^*}(\tau)$
	0	$\mu\frac{(L-1)}{2L}$
	λ	$-\mu\frac{(L+3)}{2L}$
	$q\lambda$	$\mu\frac{(L-1)}{2L}$
all other	τ	$-\frac{\mu}{L}$

Note that in evaluating $\phi_{e^*x^*}(\tau)$ for $\tau = q\lambda$, use has been made of $D^0x \oplus D^\lambda x = D^{q\lambda}x$ where q is a constant for a sequence and the relationship holds for all sequences.

Noting that
$\phi_{c^*x^*}(\tau) = \phi_{x^*x^*}(\tau) - \phi_{e^*x^*}(\tau) - \frac{1}{L}$, the effects of transducer non-linearity can be calculated from B.3.(3).

Consider now case (b), the equivalent expression of B.3.(4) is

$$e(t) = c(t) - x(t) \qquad \text{B.3.(14)}$$

$$\therefore \quad \phi_{cx}(\tau) = \phi_{xx}(\tau) + \phi_{ex}(\tau) \qquad \text{B.3.(15)}$$

e(t) is a sequence with a single one at the beginning of a run of zeroes in x(t), and zeroes elsewhere. A typical case for x(t) a 15 bit m sequence is illustrated in Fig. 19b. As for case (a)

$$e(t) = \psi[\bar{x}(t).x(t-\lambda)] \qquad \text{B.3.(16)}$$

where the bar denotes inversion

$$= \psi\left[x(t-\lambda) \oplus x(t).\ x(t-\lambda)\right] \qquad \text{B.3.(17)}$$

$$\therefore \quad \phi_{e^*x^*}(\tau) = -\frac{\psi}{T}\int_0^T 4x(t-\tau)x(t-\lambda)x(t)dt + 2\psi\ \phi_{xx}(\lambda)$$

$$+ 4\ \psi\ \ \phi_{xx}(\tau-\lambda) + \psi(1-\frac{4}{T}\int_0^T x(t)dt) \qquad \text{B.3.(18)}$$

This equation can be evaluated at various τ to give the following

τ	$\phi_{e^*x^*}(\tau)$
0	$-\frac{\psi(L+3)}{2L}$
λ	$\frac{\psi(L-1)}{2L}$
$q\lambda$	$\frac{\psi(L-1)}{2L}$
all other τ	$-\frac{\psi}{L}$

Noting that in this case

$$\phi_{c^*x^*}(\tau) = \phi_{x^*x^*}(\tau) + \phi_{e^*x^*}(\tau) + \frac{1}{L} \text{ the}$$

effects of the transducer non-linearity can similarly be calculated from B.3.(3).

The effect of a non ideal transducer on a simulated system is shown in Fig. 20. The case (a) transducer causes the effect of 20(b) and the case (b) transducer, those of Fig. 20(c).

For L = 63, q = 58; the theory above predicts

a secondary peak q bits from the true peak.

i.e. a peak at $(46+58)_{mod63} = 41$. This is confirmed in Fig.20. The theory also predicts that the maximum height of this secondary peak is

$$= \mp \frac{(L-1)}{2L} \cdot (\psi \text{ or } \mu) \cdot h(\tau_p)$$

i.e. $\mp$ 56 in this case. The actual maximum heights are -54 and +55.

The work of Godfrey et al[7,8,9] is concerned with the case of zero delay times but unequal time constants, in the input transducer. Inasmuch as their results demonstrates the possibility of secondary peaks appearing, and the distance between maxima of parent and secondary to be (q-1) bits, the two cases give similar results. It is also evident that by choice of delays and time constants, the two agencies of error can be made to reinforce or counteract one another.

10. REFERENCES

1. Peterson,W.W., Error Correcting Codes, M.I.T. Tech Press,1961.
2. Everett,D., Periodic Digital Sequences With Pseudo-Noise Properties, G.E.C.Journal, Vol.33, No. 3, P115, 1966.
3. Briggs, P.A.N., Hammond,P.H., Hughes,M.T.G., Plumb, G.O., Correlation Analysis of Process Dynamics Using Pseudo-Random Binary Test Perturbations, Proc.I.Mech.E.,Vol.179,3H,P37,1964.
4. Izawa, K., Furuta,K., Application of Correlation Technique for the Measurement of Transfer or Transport Lag, I.M.E.K.O., Warsaw,1967.
5. Godfrey, K.R.,Devenish,M., An Experimental Investigation of Continuous Gas Ghromatography Using Pseudo-random Binary Sequences, Measurement and Control (U.K.), 2, pp 228-233,1969.
6. Moss,G.C., The Use of Pseudo-random Binary Sequences in Gas Chromatography, Report Submitted in Partial Fulfilment of Requirements for the award of M.Sc., Sept.1968, Univ.of Warwick.
7. Godfrey, K.R., Murgatroyd,W., Input-Transducer Errors in Binary Crosscorrelation Experiments, Proc.I.E.E.,Vol.112, No.3, March 1965.
8. Godfrey, K.R., Everett,D., Bryant,P.R., Input-Transducer Errors in Binary Crosscorrelation Experiments -2, Proc.I.E.E., Vol.113, No.1, Jan.1966.
9. Godfrey, K.R., Input-Transducer Errors in Binary Crosscorrelation Experiments -3, Proc. I.E.E., Vol. 113, No.6, June 1966.

10. Willis,V., Analysis by Gas Chromatography of a 'Pure' Sample with an 'Impure' Carrier, Nature, June 20,1959, Vol.183, p1754.

11. Castello,G., D'Amato,G., Negative Peaks In Gas Chromatography: Vacancy Chromatography as the Cause of Anomalous Response of Thermal Conductivity Detectors, J.Chromatog., 32,(1968),pp 625-634.

12. Douce, J.L., Ng,K.C., Walker, A.E.G., System Identification in the Presence of a Ramp Disturbance, Electronics Letters, Vol.3, No.2, p 243, July 1966.

13. Davies, W.D.T., Simple Method of Measuring Output Drift with Particular Reference to Identification Using Chain Codes, Electronics Letters, Vol.3, No.2, p 72, Feb.1967.

14. Ream,N., Proof of the Drift Resistant Property of Binary m Sequences, Electronics Letters, Vol.4, No. 18, pp 38o-381, Sept. 1968.

15. Barker, H.A., Choice of Pseudorandom Binary Signals for System Identification, Electronics Letters, Vol. 3, No. 11, pp 524-526, Nov.1967.

16. Davies, W.D.T., Douce, J.L., On Line System Identification in the Presence of Drift, Proc. of I.F.A.C. Symp. on Identification, Prague 1967.

17. Brown, R.F., Drift Correlation in Periodic Cross-correlation Schemes, Electronics Letters, Vol.4, No. 22, pp 478-479, Nov. 1968.

18. Brown, R.F., Review and Comparison of Drift-Correction Schemes for Periodic Crosscorrelation, Electronics Letters, Vol.5, No.9, pp 179-181, May 1969.

19. Macleod, C.J., Drift Elimination in System Identification Using Binary m Sequences, Electronics Letters, Vol.5., No.6, pp 112-113, March 1969.

11. ILLUSTRATIONS FOR CHAPTER 2

Fig.1 The Autocorrelation Function of a P.R.B.S.

Fig.2 Chromatograms By Correlation.

Fig.3 Conventional Chromatograph of a 5% Hydrocarbon Mixture in Helium.

Fig.4 Correlogram 1.

Fig.5. Correlogram 2.

Fig.6 Step Response of Valve Detector Combination.

Fig.7 Input and Output of Non-Linear Filter.

Fig.8 A.C.F. of Output From Non-Linear Filter

Fig.9a Nitrogen Analysis with I.C.I. Sample Valve

Fig.9b and P.R.B.S.

Fig.10 System Simulation.

Fig.11 Impulse Response Estimates of Simulated System.

Fig.12 Nitrogen Analysis Using Modified Apparatus and P.R.B.S.

Fig.13 Conventional Injection of Hydrocarbon Mixture.

Fig.14 Analysis of Hydrocarbon Mixture Using P.R.B.S. at 30°C.

Fig.15. Analysis of Hydrocarbon Mixture Using P.R.B.S. at 60°C.

Fig.16 The Effect of Flow Rate on 'H.E.T.P.'

Fig.17 The Effect Column of Temperature on Retention.

Fig.18. System with Noise at Output.

Fig.19a, Fig.19b } The Effect of Unequal Transducer Delay Times on a 15 bit P.R.B.S.

Fig.20(a), Fig.20(b), Fig.20(c) } The Effect of Unequal Transducer Delay Times on Impulse Response Estimates.

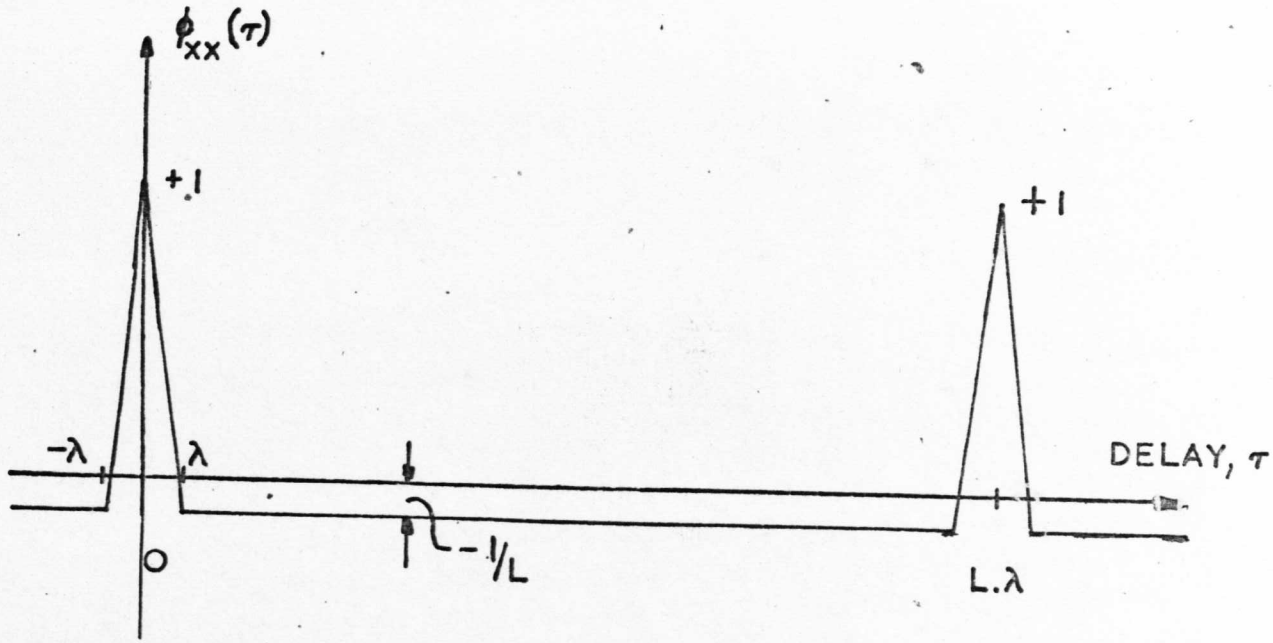

FIG.1. AUTOCORRELATION FUNCTION OF A P.R.B.S. x(t).

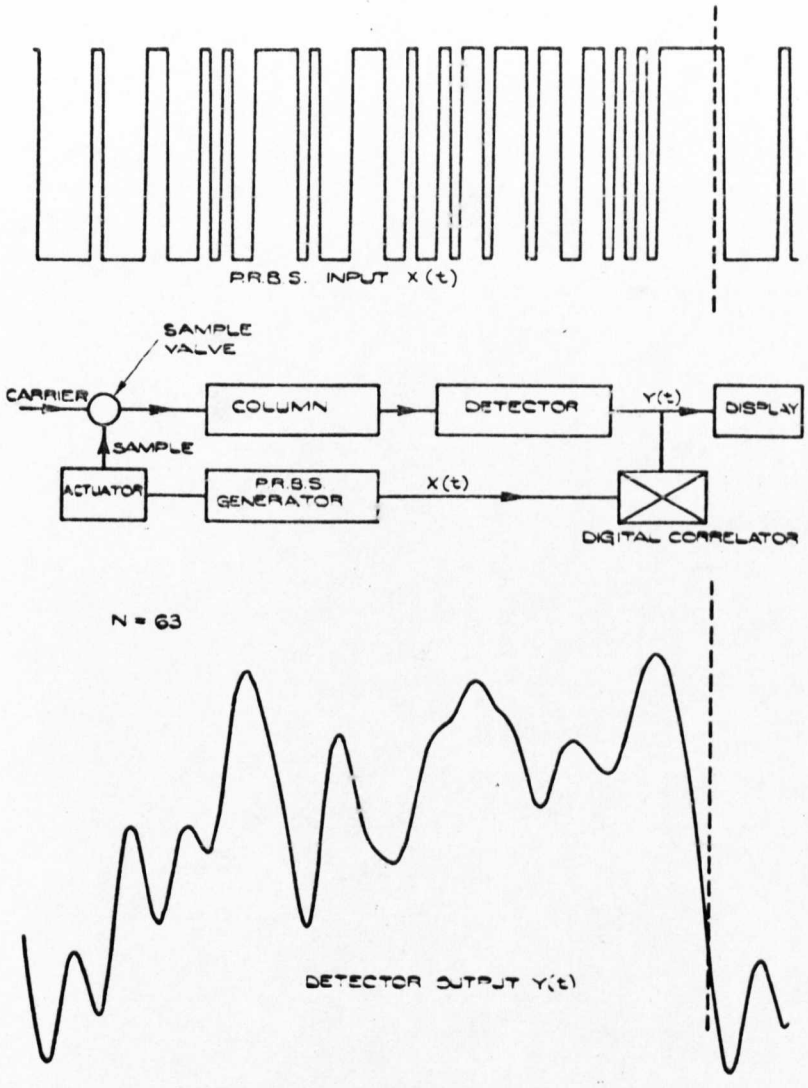

FIG. 2

CHROMATOGRAMS BY CROSSCORRELATION

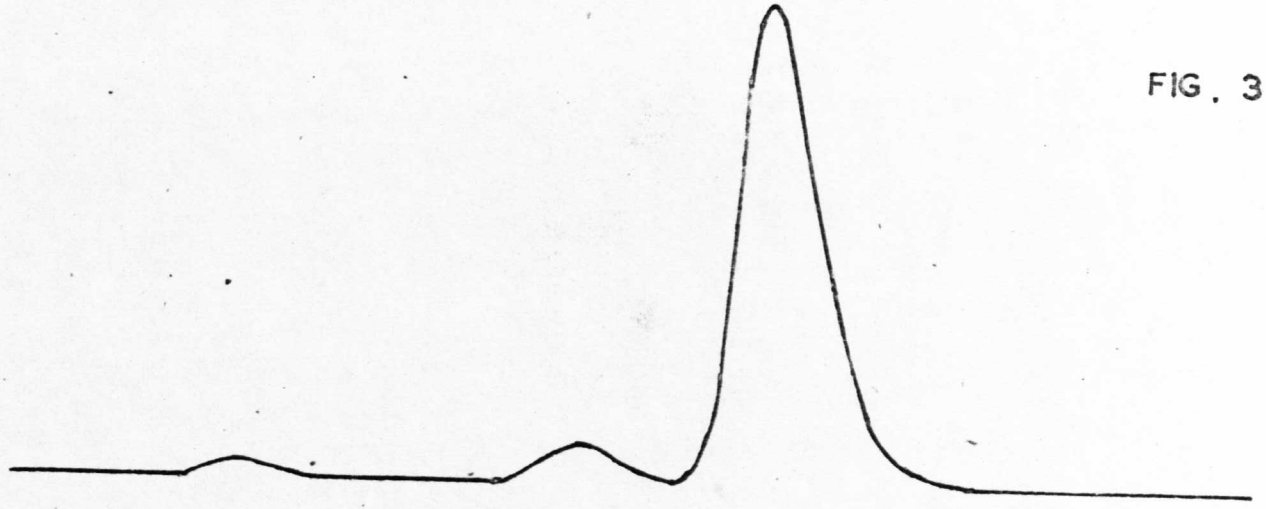

FIG. 3

A CONVENTIONAL CHROMATOGRAPH OF A 5% HYDROCARBON IN HELIUM MIXTURE

CORRELOGRAM I.

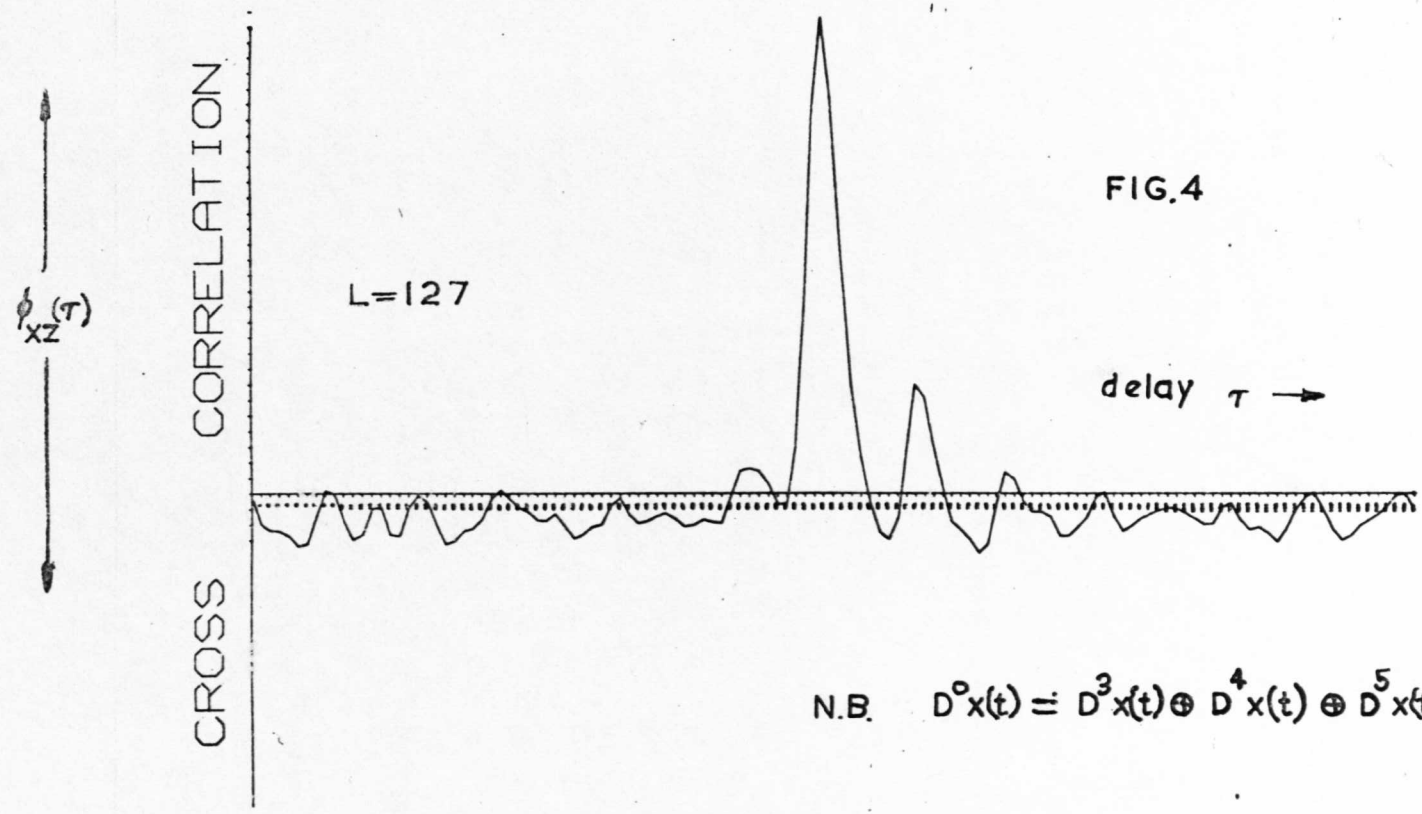

FIG.4

N.B. $D^0x(t) = D^3x(t) \oplus D^4x(t) \oplus D^5x(t) \oplus D^7x(t)$

CORRELOGRAM 2

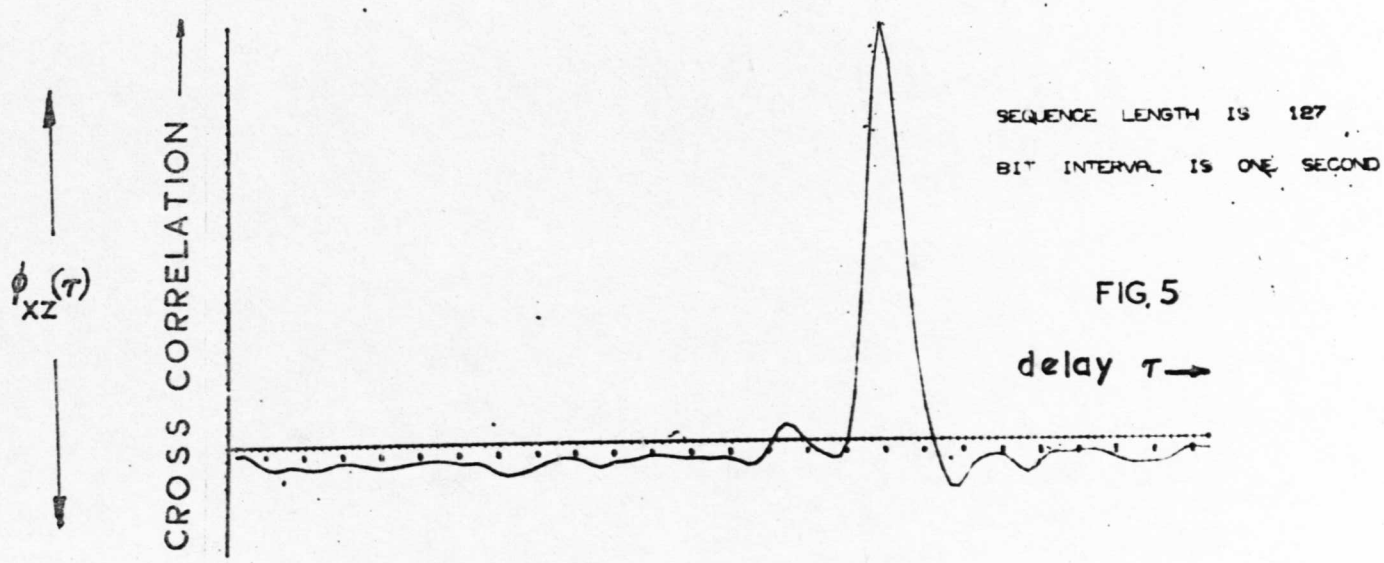

FIG. 5

N.B. $D^0x(t) = D^3x(t) \oplus D^5x(t) \oplus D^4x(t) \oplus D^7x(t)$

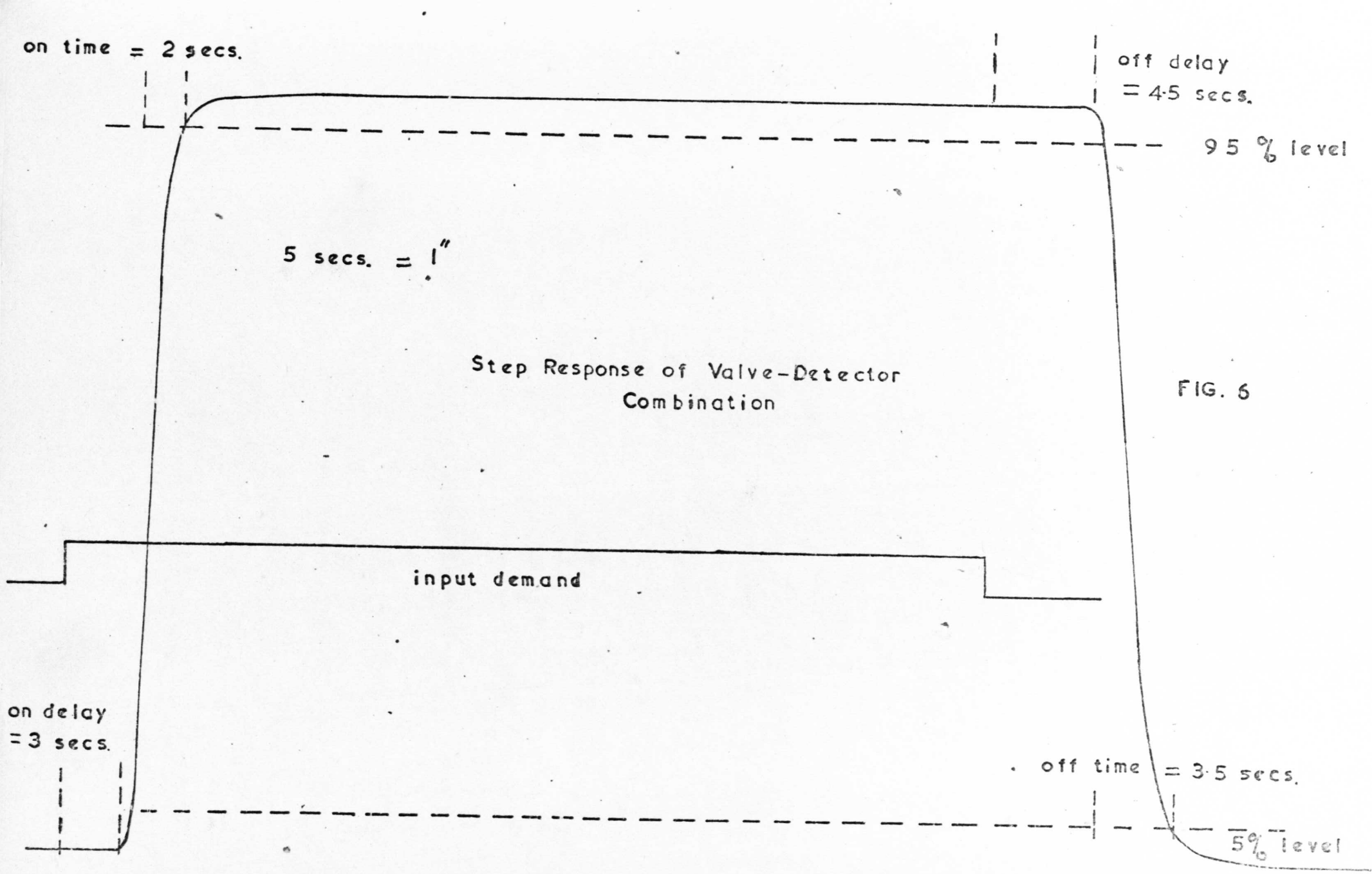

Step Response of Valve-Detector Combination

FIG. 6

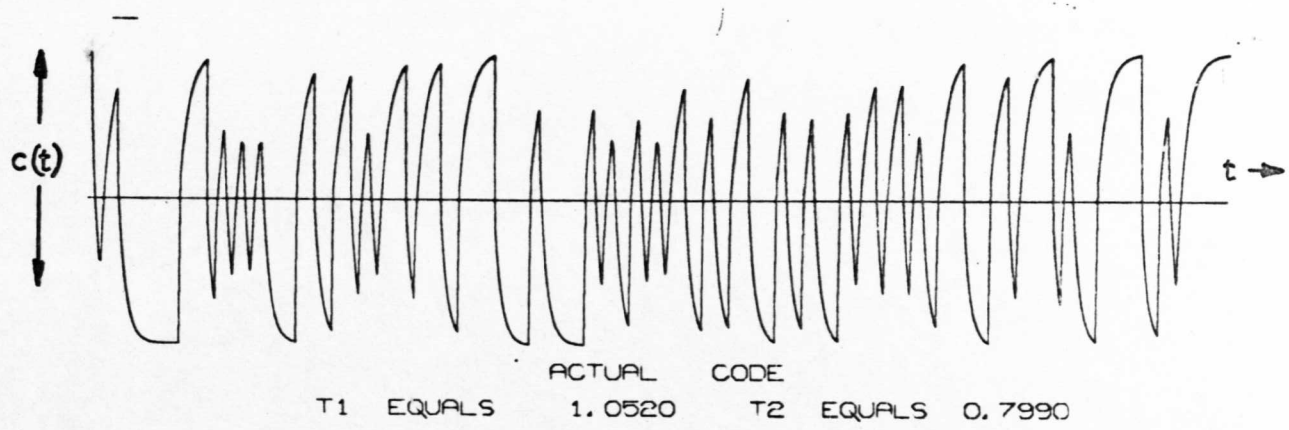

L = 127

FIG. 7

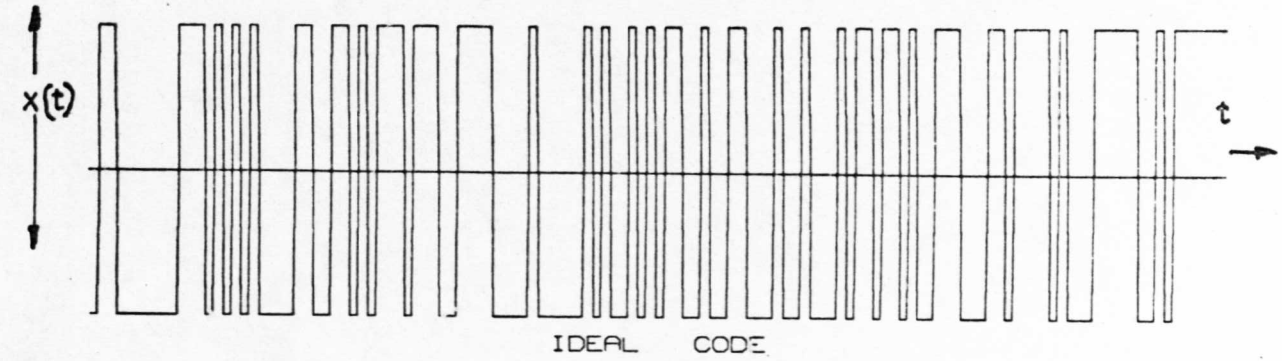

INPUT AND OUTPUT OF NON-LINEAR FILTER

N.B. $D^0x(t) = D^3x(t) \oplus D^4x(t) \oplus D^5x(t) \oplus D^7x(t)$

A.C.F. OF OUTPUT FROM NON-LINEAR FILTER

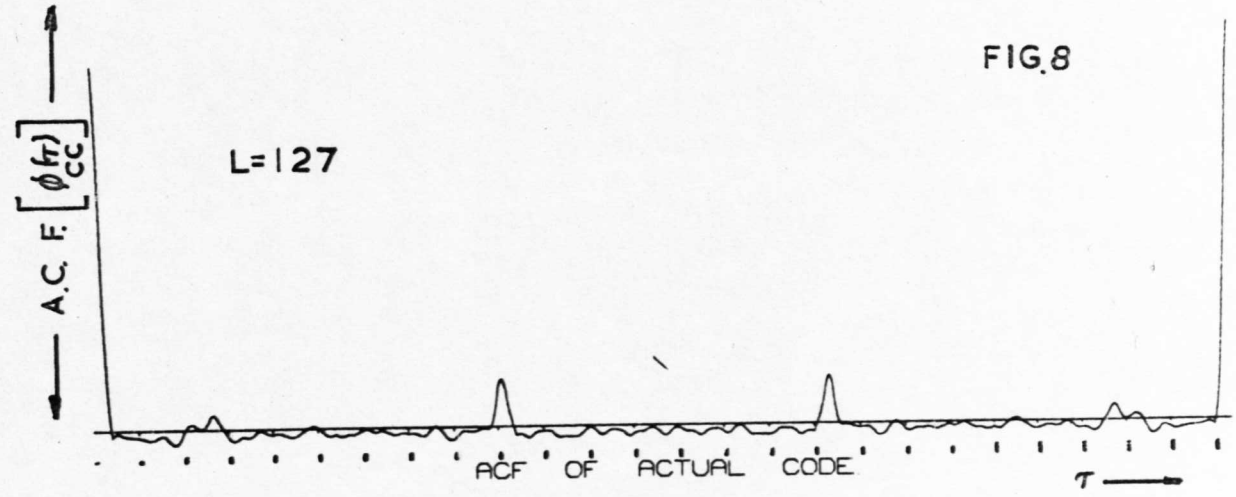

FIG.8

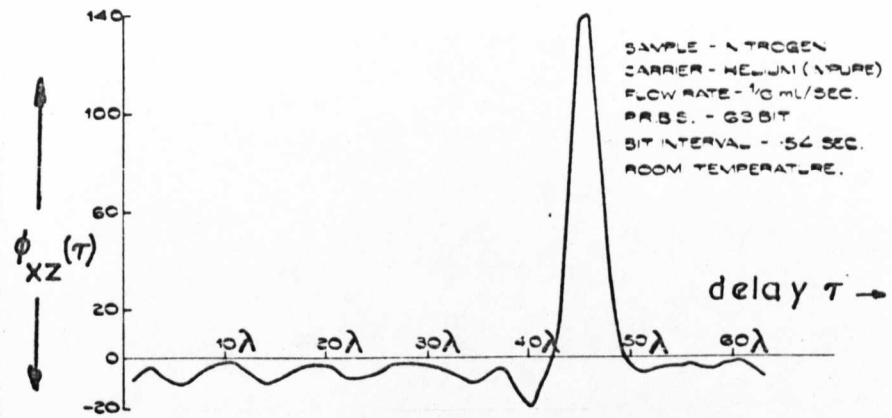

FIG. 9a

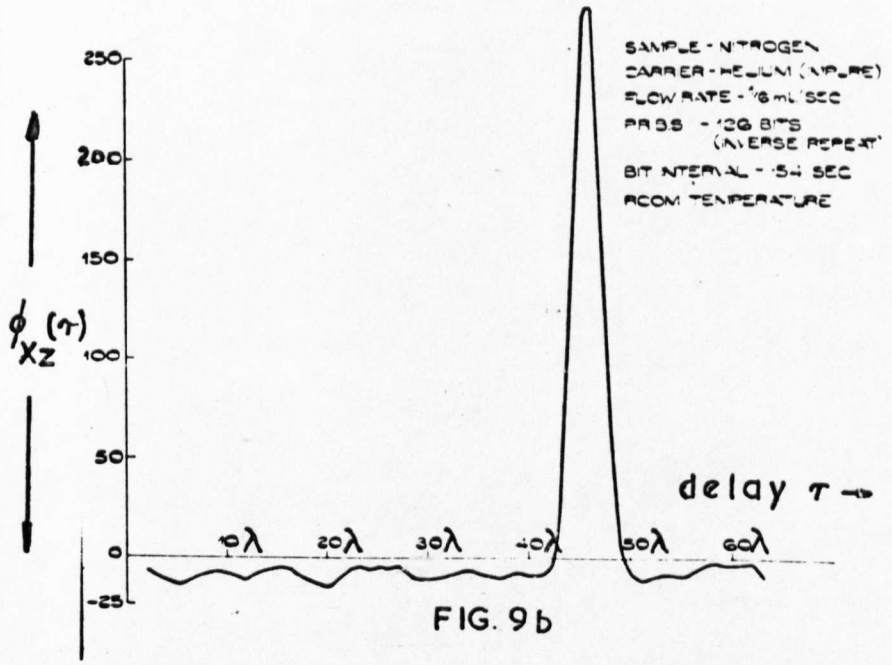

FIG. 9b

NITROGEN ANALYSIS USING I.C.I. SAMPLE VALVE AND P.R.B.S.

N.B. $D^0 x(t) = D^5 x(t) \oplus D^6 x(t)$

• SYSTEM SIMULATION

FIG. 10a

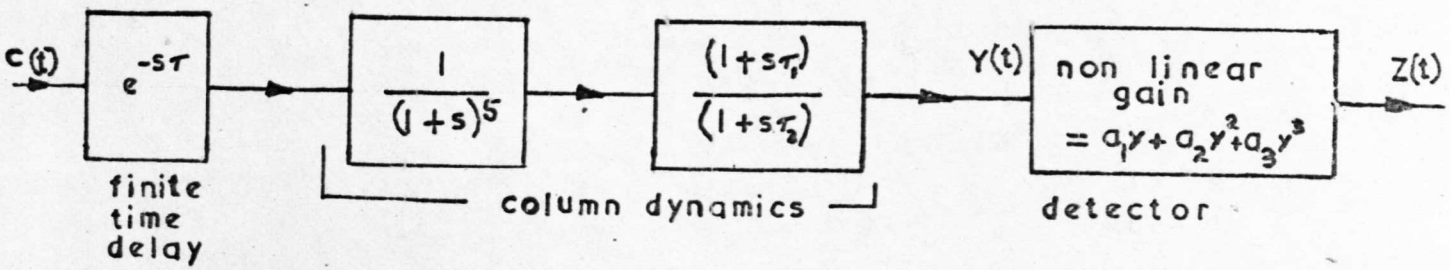

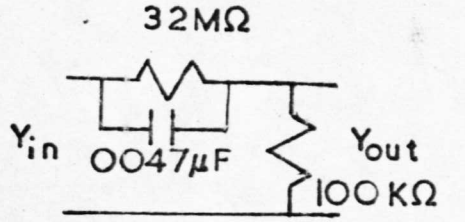

PHASE ADVANCE N/W.

FIG 10b

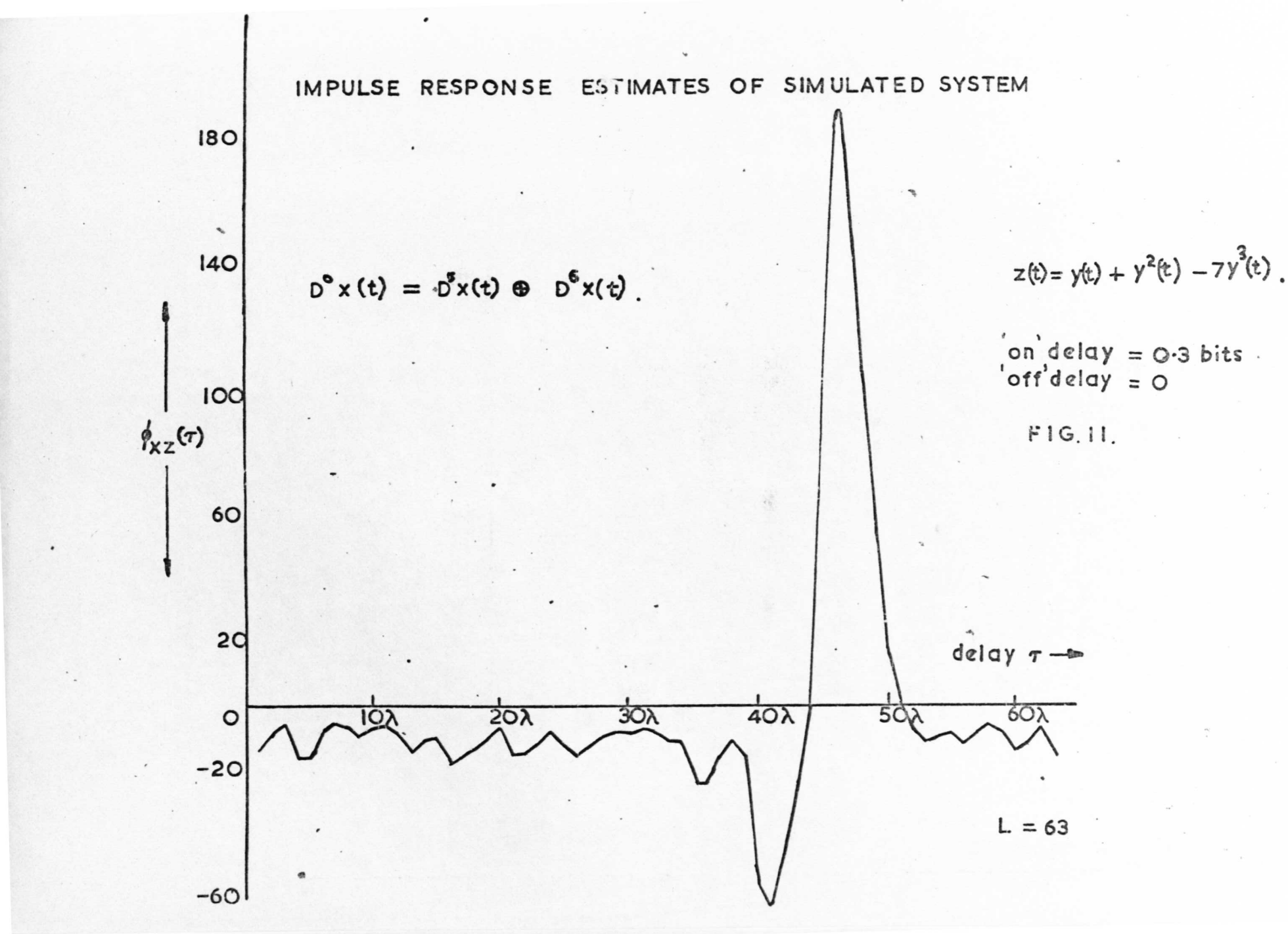
IMPULSE RESPONSE ESTIMATES OF SIMULATED SYSTEM
180
140
100
60
20
0
-20
-60
$\phi_{xz}(\tau)$
$D^0x(t) = D^5x(t) \oplus D^6x(t)$.
$z(t) = y(t) + y^2(t) - 7y^3(t)$.
'on' delay = 0·3 bits
'off' delay = 0
FIG. 11.
delay τ →
10λ
20λ
30λ
40λ
50λ
60λ
L = 63

NITROGEN ANALYSIS USING MODIFIED APPARATUS AND P.R.B.S.

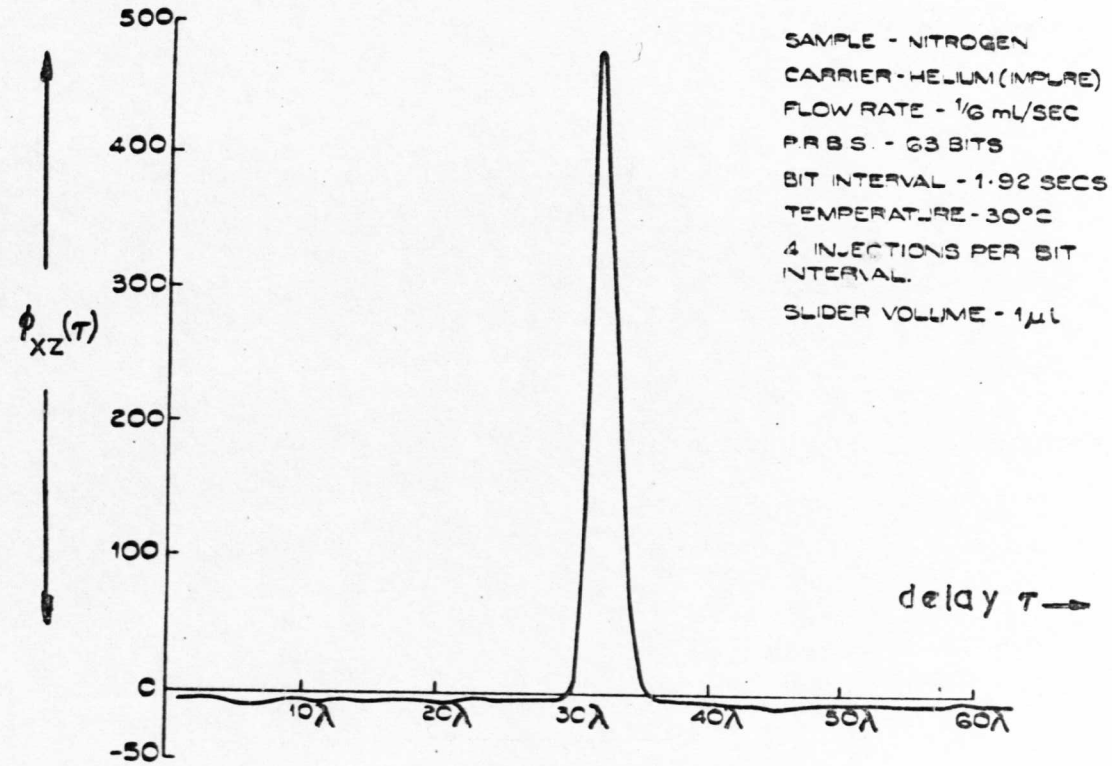

FIG. 12

N.B. $D^0x(t) = D^5x(t) \oplus D^6x(t)$.

CONVENTIONAL INJECTION OF HYDROCARBON MIXTURE (a)

CARRIER = HELIUM (PURE)
FLOW RATE = 1/3 ml/SEC.
TEMPERATURE = 30°C
SLIDER VOLUME = 10μl
FILTER IN
Y SENSITIVITY = 0·1 VOLT/cm
X SENSITIVITY = 10 SECS/cm
AMPLIFIER GAIN = 10^4
BRIDGE VOLTAGE SUPPLY = 5·75 VOLTS
INJECTION TIME = 1 SECOND

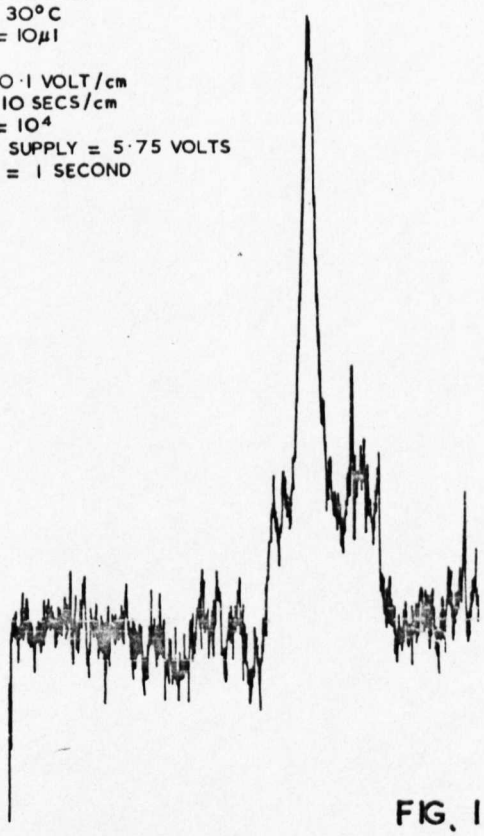

FIG. 13

ANALYSIS OF HYDROCARBON MIXTURE AT 30°C USING P.R.B.S.

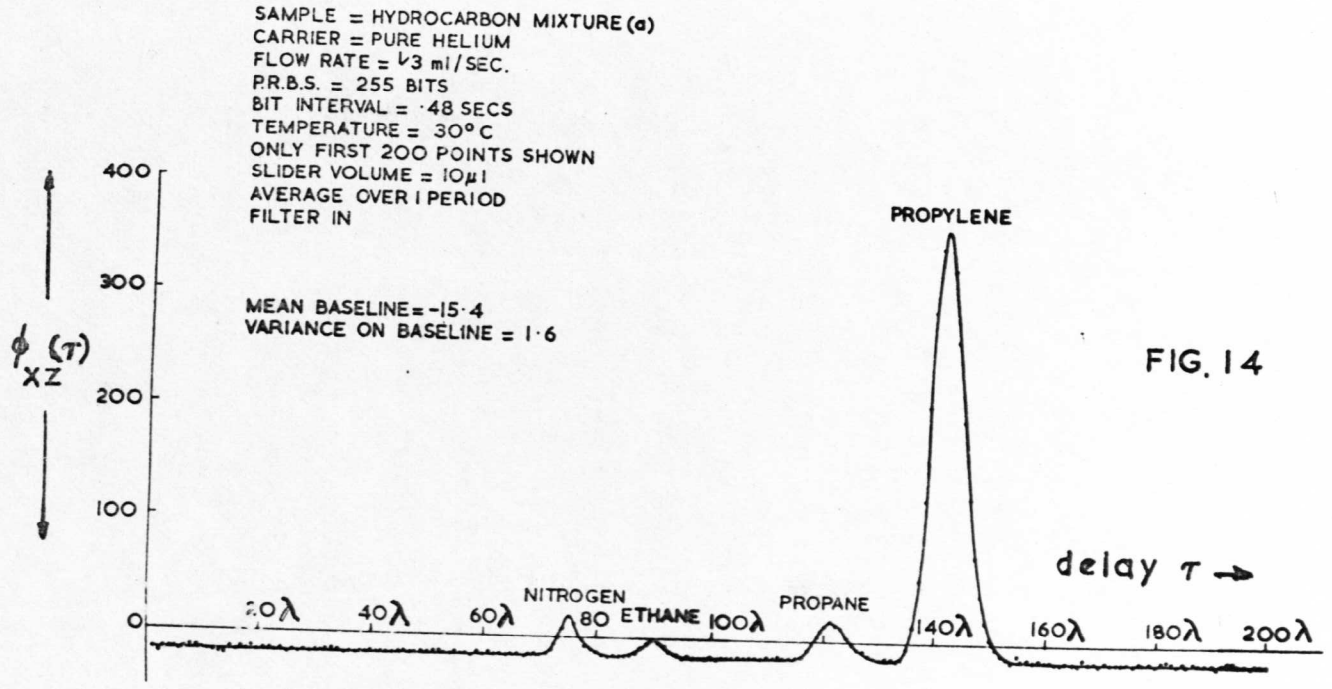

FIG. 14

N.B. $D^0x(t) = D^3x(t) \oplus D^5x(t) \oplus D^7x(t) \oplus D^8x(t)$

ANALYSIS OF HYDROCARBON MIXTURE AT 60°C USING P.R.B.S.

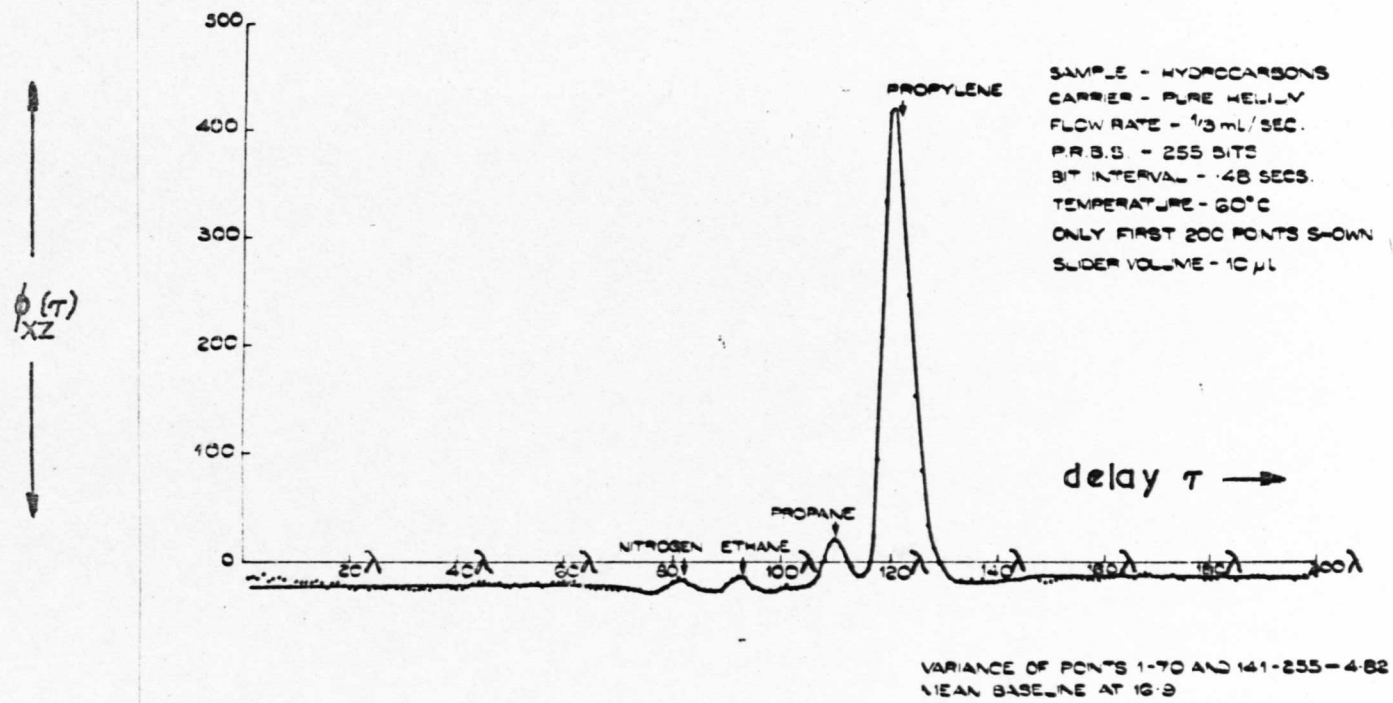

FIG.15

N.B. $D^0x(t) = D^3x(t) \oplus D^5x(t) \oplus D^7x(t) \oplus D^8x(t)$

FIG. 16.

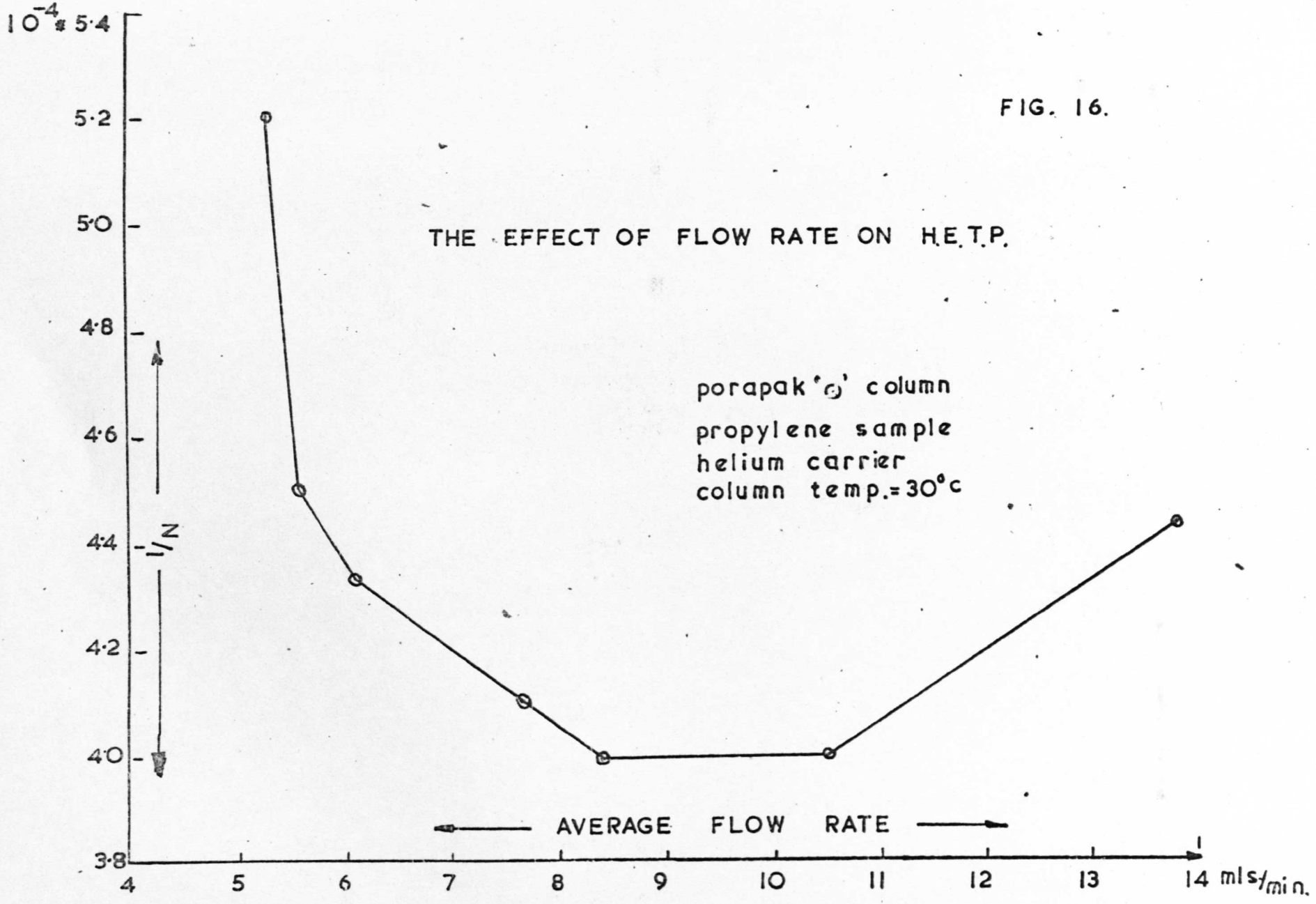
THE EFFECT OF FLOW RATE ON H.E.T.P.
porapak 'Q' column
propylene sample
helium carrier
column temp.= 30°c
10^{-4} x 5·4
5·2
5·0
4·8
4·6
4·4
4·2
4·0
3·8
1/N
AVERAGE FLOW RATE
4
5
6
7
8
9
10
11
12
13
14 mls/min.

FIG.17.

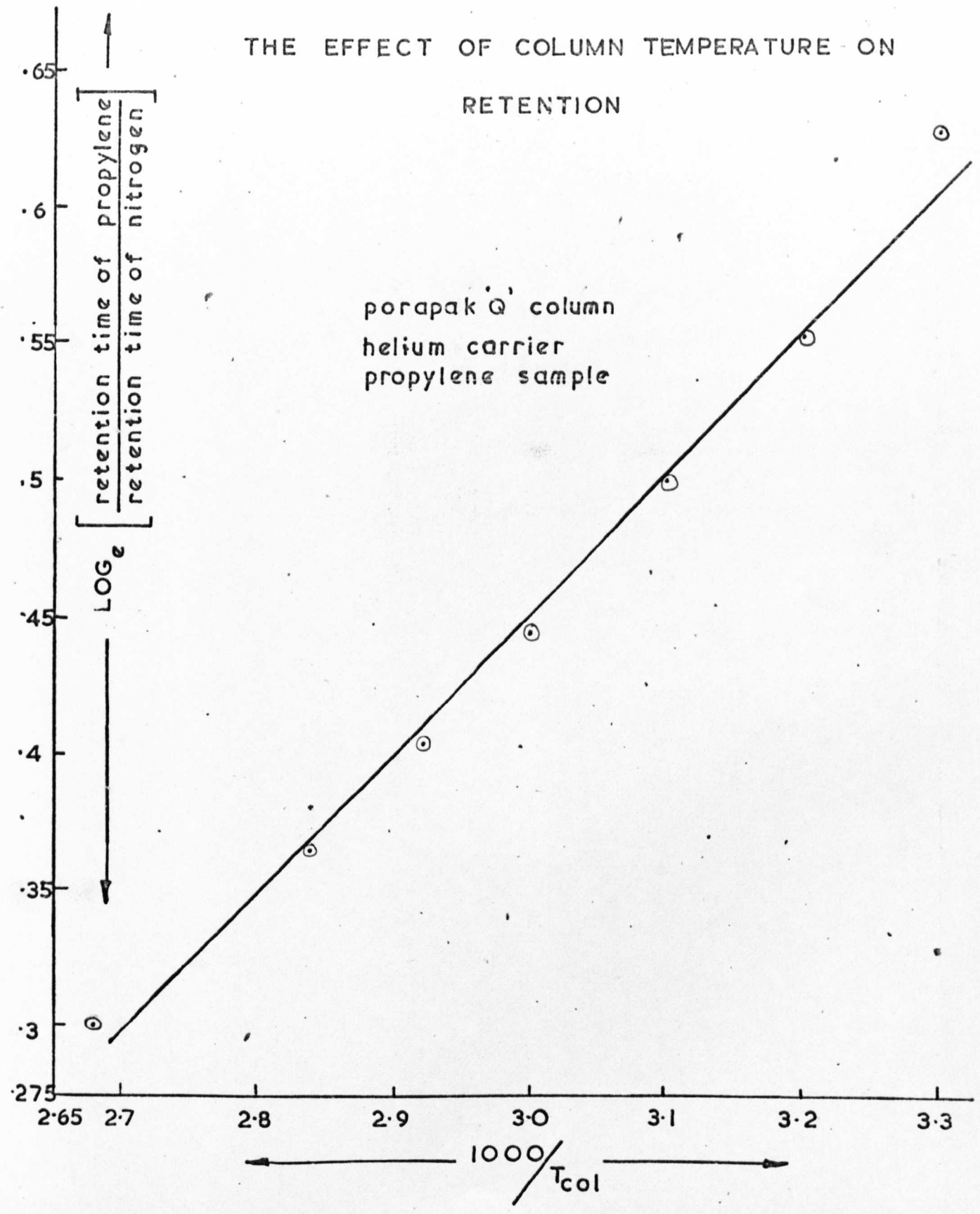
THE EFFECT OF COLUMN TEMPERATURE ON RETENTION
porapak 'Q' column
helium carrier
propylene sample
LOG$_e$ [retention time of propylene / retention time of nitrogen]
·65
·6
·55
·5
·45
·4
·35
·3
·275
2·65
2·7
2·8
2·9
3·0
3·1
3·2
3·3
1000/T$_{col}$

FIG. 18

SYSTEM WITH NOISE AT OUTPUT

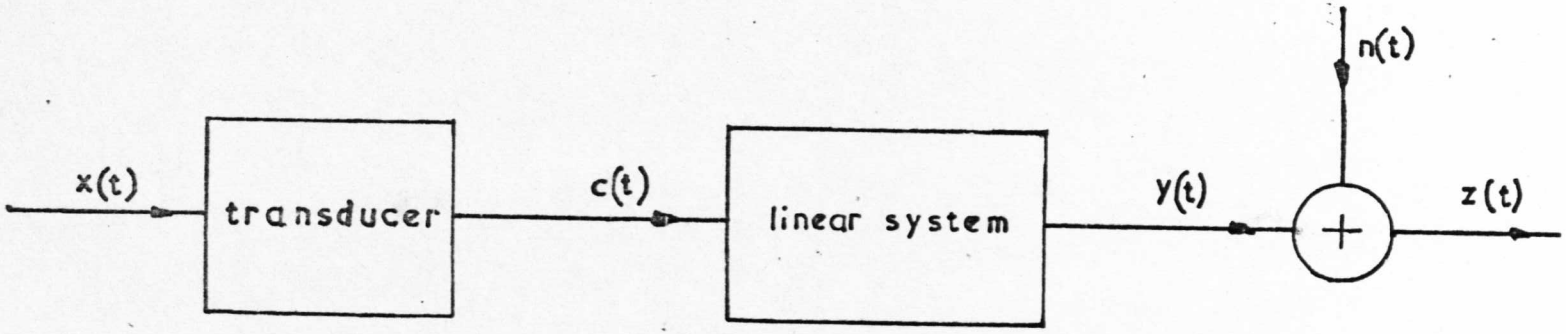

THE EFFECT OF UNEQUAL, INPUT TRANSDUCER DELAYS ON A 15 BIT P.R.B.S.

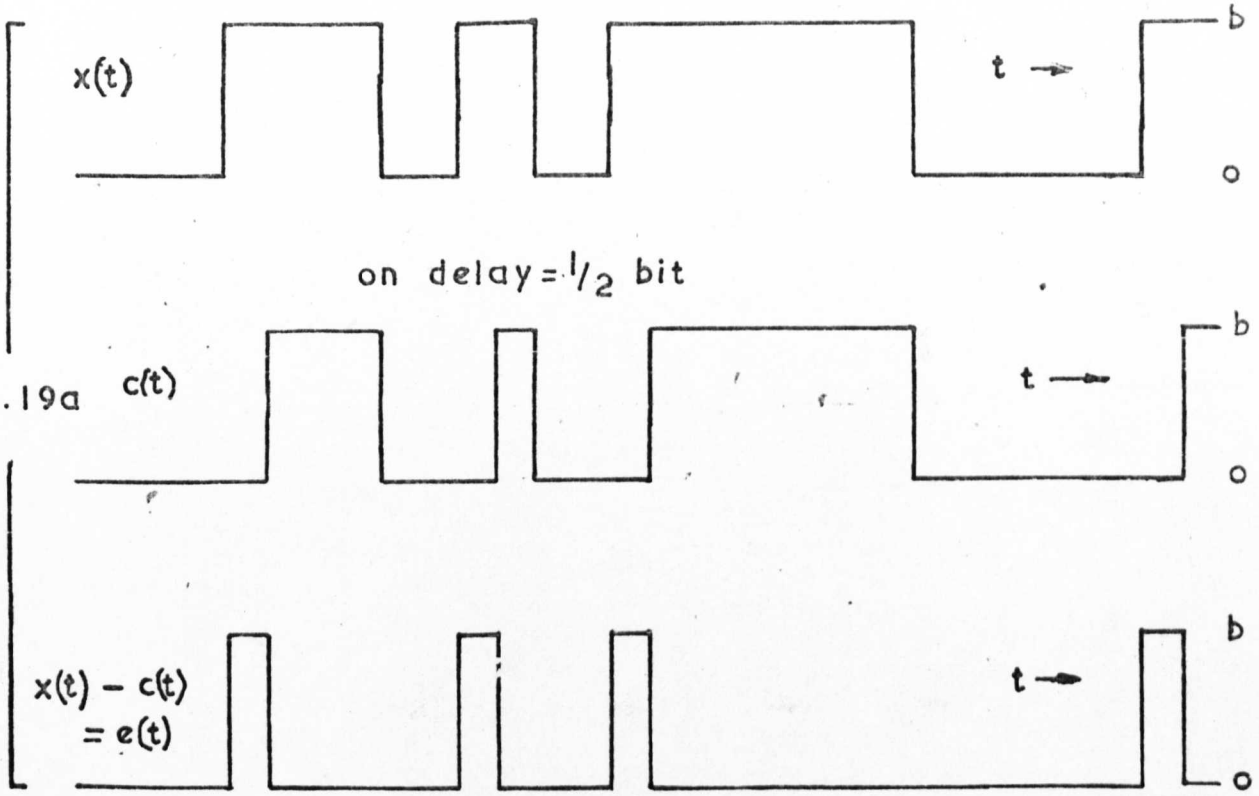

FIG. 19a

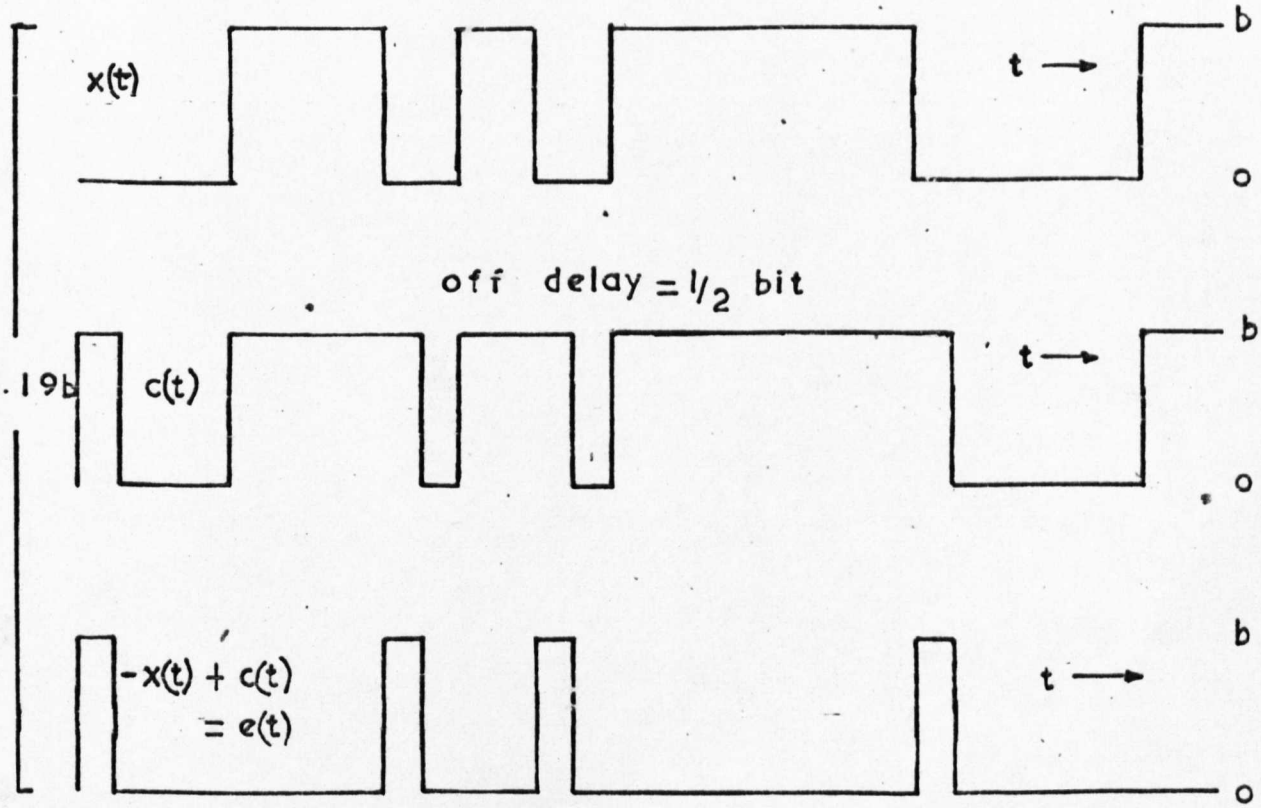

FIG. 19b

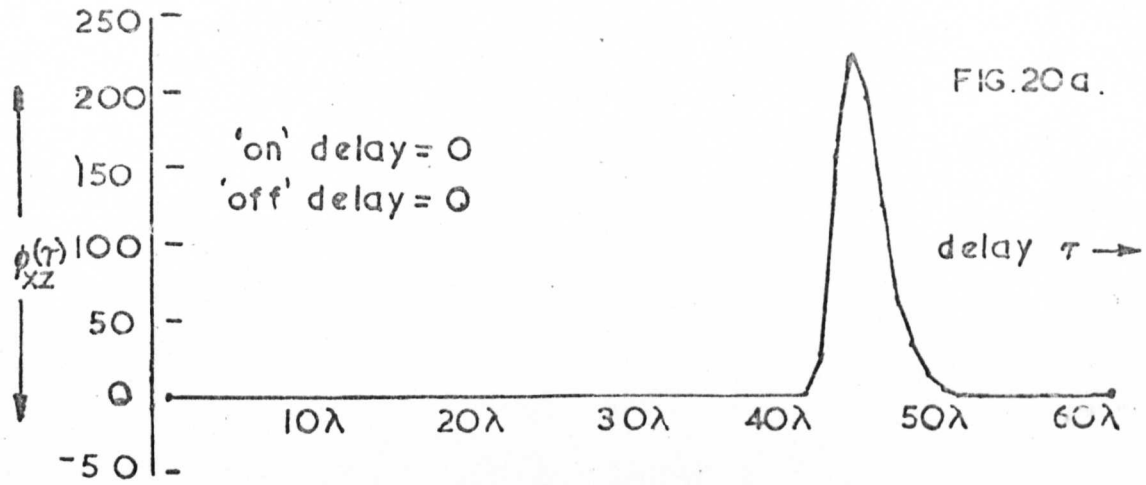

FIG. 20a.

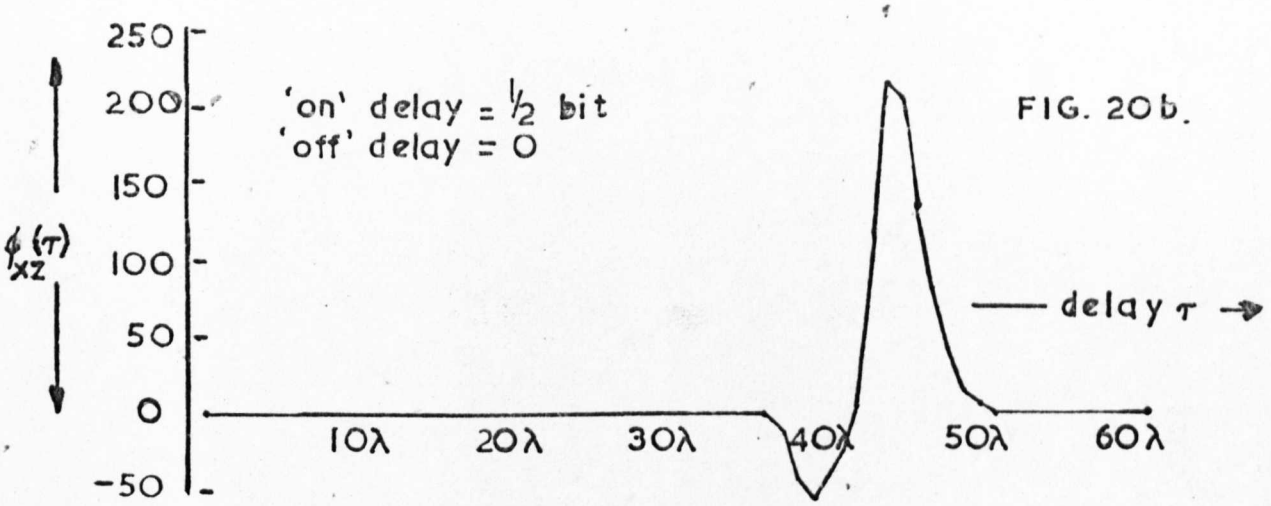

FIG. 20b.

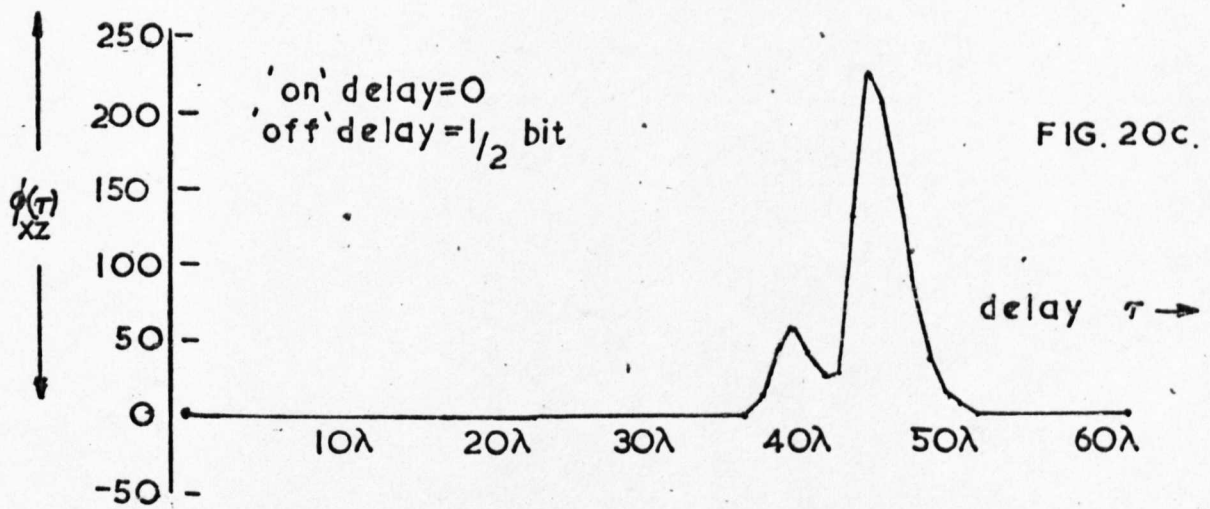

FIG. 20c.

N.B. (1) D.C. bias removed from all correlograms
(2) $D^0x(t) = D^5x(t) \oplus D^6x(t)$
(3) system in all cases = $\frac{1}{(1+s)^5} \cdot e^{-s\tau}$

THE EFFECT OF UNEQUAL, INPUT TRANSDUCER DELAYS ON IMPULSE RESPONSE ESTIMATES

CHAPTER 3 - ADVANCED STUDIES WITH P.R.B.S. IN CHROMATOGRAPHY

LIST OF PRINCIPAL SYMBOLS

t	time variable
$\tau, \tau_{12}, \mu, \psi$	shift variables
p.r.b.s.	pseudo-random binary sequence
n	number of register stages used to generate a p.r.b.s.
$x(t)$	p.r.b.s. of levels +1,0
*	transformation of levels 0 = -1, 1 = +1
$c(t)$	actual system input
b	amplitude of transducer output
λ	clock interval of input sequence
L	number of bits in p.r.b.s.
$y(t)$	linear system output
$z(t)$	measurable output
$p(t)$	modifying sequence
$X(t)$	modified p.r.b.s.
D	delay operator
V	length of p(t)
α	level of U bits in p(t)
β	level of V-U bits in p(t)
$L\alpha$	number of α,α digit pairs
L_β	number of β,β digit pairs
$L\alpha\beta$	number of α,β digit pairs
T	period of p.r.b.s.

$\phi_{x^*z}(\tau)$	crosscorrelation function between unmodified sequence x*(t) and measurable output.
$\phi_{p^*p^*}(\tau)$	autocorrelation function of modifying sequence p*(t)
2^k	dimension of Hadamard matrix
$h(\tau)$	estimate of system impulse response at shift τ
h_i'	ith ordinate of estimated impulse response, dash indicates bias removed.
x_i	ith bit of p.r.b.s.
Δy_i	change in steady state output at time i.
$\Delta_{xy}(\tau_1,t_2)$	departure from steady state correlation function at time t_2, for a shift τ_1.
$u_{xy}(\tau_1,t_2)$	change in $\Delta_{xy}(\tau_1,t_2)$ between t_2 and (t_2+1) at a shift τ_1.
Δh_i	change of ith impulse response estimate
W_i	ith weight
γ	change factor
Gss	steady state gain
a_i	ith coefficient in non-linear characteristic
Q,R	constants
I_i,K_i	ith equations
T_L	elution plus settling time of last eluted component

INTRODUCTION

In Chapter 2 it has been shown that with a careful choice of sample valve, the techniques of crosscorrelation of control theory can be applied to gas analysis. The immediate pay-off has been seen to be an improved signal to noise ratio in the chromatogram. This in itself may not be sufficient motivation for industry to invest capital in implementing the technique. Furthermore, since problems associated with a non-linear detector response can arise, one would like to be able to overcome these. In addition, it has been shown (Chapter 1 - section 2.4.3), that katherometers are not particularly linear devices, and can even prevent successful analyses by conventional chromatography. The possibilities of removing the effects of detector nonlinearities using p.r.b.s. are discussed in this chapter.

This chapter also shows that for straight forward analyses, relatively low cost but special purpose devices, can handle the data analysis required in the p.r.b.s. approach. Moreover it is shown that the technique is capable of analysing samples from several sources simultaneously, with one column, and one detector. The only extra apparatus required would be a sample valve for each sample stream. However, the requirements for data handling equipment are increased.

By a modification of the technique it appears to be possible to analyse samples whose composition varies with

time. Thus continuous chromatography of such sample streams is possible with this method.

The following sections consider each of these aspects.

2. IDENTIFICATION OF A CLASS OF NON-LINEAR SYSTEMS USING PSEUDO-RANDOM BINARY SEQUENCES

It has been noted (Chapter 1, section 2.4.3) that katherometers often behave in a non-linear fashion. The effects of such behaviour on impulse responses estimates obtained using p.r.b.s. has been noted (Chapter 2, section 6.3). Fig. 1 illustrates the situation in terms of system theory. Assuming that the measured output $z(t)$ is related to the output of the linear dynamics by an equation such as

$$z(t) = a_o + a_1 y(t) + a_2 y^2(t) + a_3 y^3(t) + \text{-----higher order terms} \qquad (1)$$

then crosscorrelating between input p.r.b.s. and output $z(t)$ we get

$$\phi_{xz}(\tau) = \frac{a_o}{T} \int_0^T x(t-\tau)dt + \frac{a_1}{T} \int_0^T \int_0^\infty x(t-\tau)c(t-\tau_1)h(\tau_1)d\tau_1 \, dt +$$

$$\frac{a_2}{T} \int_0^T \int_0^\infty \int_0^\infty x(t-\tau)c(t-\tau_1)c(t-\tau_2)h(\tau_1)h(\tau_2)d\tau_1 \, d\tau_2 \, dt +$$

$$\frac{a_3}{T} \int_0^T \int_0^\infty \int_0^\infty \int_0^\infty x(t-\tau)c(t-\tau_1)c(t-\tau_2)c(t-\tau_3)h(\tau_1)h(\tau_2)h(\tau_3)d\tau_1 \, d\tau_2 \, d\tau_3 \, dt$$

$$+ \text{----------} \qquad (2)$$

The presence of the a_o term introduces bias and the a_2 and a_3 terms cause an increase in the variance of the estimates of $h(\tau)$.

The problems of removing the effects of the non-linear terms in (1) has been discussed by Gardiner[1] who shows that by conducting several separate experiments it is possible to derive the linear impulse response estimates. Brown[2] has modified this approach by using inverse repeat sequences whose terms are such that $X^*(t+T) = -X^*(t)$, and have a period 2T. Other treatments have been given by Godfrey[3] and Gyftopoulos[4]. All methods proposed to date of removing the effects of the third and higher order odd power terms in (1), either use multi-level sequences, or are based on repeated experiments with the same sequence but of different predetermined amplitudes. In chromatography neither of these two types of approach is convenient since, unless a special input transducer is designed, one is limited to the states 'ON' and 'OFF' only.

The following subsections consider three possible methods of estimating the linear impulse response using only two levels of input.

2.1 THE USE OF A LINEARISING NETWORK

If the system is assumed to be of the form of Fig. 1, it would be feasible to pass the output $z(t)$ through a non-linear network. This network could be chosen so that its characteristic is the inverse non-linearity to that of of the detector. The overall output would then be linearly related to $y(t)$. The linearising network could be assembled

using diode function generators, multipliers and summers or even digital programming, but requires accurate knowledge of the detector characteristic. This would be difficult to obtain in practice and would vary according to the components of the sample gas, and was not therefore investigated further.

2.2 THE USE OF INVERSE REPEAT SEQUENCES

The results of Chapter 2, section 6.3 show that the variance in the estimates of $h(\tau)$ due to the presence of detector non-linearities is reduced when inverse repeat sequences are used. This was also noted by Godfrey and Devenish[5]. This property relies on the fact that even order autocorrelation functions of inverse repeat sequences are zero everywhere[6]. Thus the even power non-linearities cannot contribute to the input-output crosscorrelation function. However, this is not true for odd power non-linearities and these can contribute significantly to the base-line ripple in a correlogram.

What is not normally appreciated is that for systems whose input levels are (b,0) instead of (±b), the presence of even power terms causes bias in the estimates of the linear impulse response. This situation is detailed in Appendix C.1. where it is shown that for a linear system followed by a non-linearity as in Fig.1, then

$$\phi_{X^*Z}(\tau) = \left[\frac{ba_1}{2} + \frac{G_{ss}^2}{2} b^2 a_2 + \frac{3G_{ss}^2}{8} b^3 a_3 \right] \int_0^\infty \phi_{X^*X^*}(\tau-\tau_1)h(\tau_1)d\tau_1$$

$$+ \frac{b^3 a_3}{8} \int_0^\infty \int_0^\infty \int_0^\infty h(\tau_1)h(\tau_2)h(\tau_3)\phi_3(\tau_1,\tau_2,\tau_3,\tau)d\tau_1\, d\tau_2\, d\tau_3 \qquad (3)$$

where

$$\phi_3(\tau_1,\tau_2,\tau_3,\tau) = \frac{1}{2T} \int_0^{2T} X^*(t-\tau_1)X^*(t-\tau_2)X^*(t-\tau_3)X^*(t-\tau)dt \qquad (4)$$

If a_1, a_2, and a_3 are of different signs then the bias effect can be considerable.

Appendix C.2. shows how to evaluate equation (4) for all values of τ_1, τ_2, τ_3, and τ. Simpson[6] notes some of the properties of ϕ_3. Appendix C.2. shows how to calculate the coordinates (τ_1,τ_2,τ_3) for various τ, of the points at which $|\phi_3| = 1$. The presence of such points causes variance in the estimates of $h(\tau)$ in (3). Note that at some points $|\phi_3| = \frac{1}{L}$, at these points there will be an additional bias term in (3). It was not possible to write this additional bias term in a convenient form, and since it is likely to be of small magnitude, it was not considered further.

Apart from the bias term, the fourth order integral in (3) consists of a number of $h(\tau_1)h(\tau_2)h(\tau_3)$ products multiplied by ± 1. In chromatography the impulse response has considerable transport lag and $h(\tau) \approx 0$ for τ near $(L-1)\lambda$. Thus several $h(\tau)$ will be zero. Inserting the a-priori knowledge of these zero points into the integral of (3), yields some simplification. It may be possible to solve the resulting equation set for the linear impulse response $h(\tau)$.

This procedure was not followed further as a more

convenient approach was developed using Hadamard modified sequences.

2.3 TECHNIQUE USING HADAMARD MODIFIED SEQUENCES

Hadamard matrices[7] are arrays of 1's and 0's, (or using the convention 0 = -1, ± 1's) so chosen that each row is orthogonal to every other row. The first row of such a matrix written in standard form[7] is a sequence of all ones. If this sequence p(t) is used to modify a p.r.b.s. according to

$$X^*(t) = [x(t) \oplus p(t)]^* \qquad (5)$$

then X*(t) will simply be an inverted p.r.b.s. For any other choice of row in the Hadamard matrix as p(t), the resultant X*(t) is an Hadamard modified sequence. Using the properties of Hadamard matrices it is easily shown that a p.r.b.s. and its Hadamard modified form are orthogonal. Appendix C.3. applies this property when identifying the impulse response of the linear dynamics of the class of non-linear systems discussed here.

If similarly to (1), we write

$$z(t) = a_o + a_1\, y(t) + a_2\, y^2(t) + a_3\, y^3(t) + \text{higher order odd power terms}$$

then crosscorrelating between the unmodified p.r.b.s. x*(t) and the output z(t) resulting from an input c(t), we get

$$\phi_{x^*z}(\tau) = \text{Bias term} + Q \int_0^T \int_0^T h(\tau_1)h(\tau_2)\phi_{p^*p^*}(\tau_{12})d\tau_1\, d\tau_2 \qquad (6)$$

where $c(t) = \frac{b}{2}[X^*(t) + 1]$ (7)

and p*(t) is a sequence, taken from the rows (other than the

first) of an eighth order Hadamard matrix.

With such a choice of $p^*(t)$, $\phi_{x^*z}(\tau)$ is a sum of $h(\tau_1)h(\tau_2)$ products each weighted by ± 1 or $\pm\frac{1}{2}$. If we choose $p^*(t) = p_1^*(t)$ the sequence 1,1,1,1,-1,-1,-1,-1 (row 5), then the crosscorrelation of (6) gives $\phi_{x^*z_1}(\tau)$. Performing a second experiment with a sequence $p^*(t)=p_2^*(t)$, and $p_2(t)$ = 1,-1,1,-1,-1,1,-1,1, (row 6), we get $\phi_{x^*z_2}(\tau)$. The sequences $p_1^*,(t)$ and $p_2^*(t)$ have been chosen so that

$$\phi_{p_1^* p_1^*(\tau)} = \phi_{p_2^* p_2}(\tau) = \pm 1 \text{ for } \tau = 0, V\lambda/_2$$

and

$$\phi_{p_1^* p_1}(\tau) = \phi_{p_2^* p_2}(\tau) = \pm \tfrac{1}{2}, \text{ or } 0, \text{ for all other } \tau$$

If this is so, then the sum and difference of $\phi_{x^*z_1}(\tau)$ and $\phi_{x^*z_2}(\tau)$, yields a set of equations in $h(\tau_1)h(\tau_2)$ products, which can be solved to yield the $h(\tau)$, to within a constant factor.

The solution is eased if $h(\tau)$ is zero or approximately zero at several points, e.g. if the system has transport lag or when $h(\tau)$ for τ near $L\lambda$, is small enough to be approximated to zero.

In order to appreciate the applicability of this procedure to chromatography, the contents of Chapter 1, section 2.4.3 are recalled. Here it was noted that the detection characteristics of katherometers can be so non-linear as to contai

certain turning points. Operating in regions of such non-linearity causes the appearance of W or M shaped peaks which are analytically uninterpretable. The use of Hadamard-modified sequences is demonstrated to overcome such behaviour in the following.

2.3.1 THE USE OF HADAMARD-MODIFIED SEQUENCES IN GAS CHROMATOGRAPHY

An example of the non-linear behaviour of katherometer detectors is afforded by the case of hydrogen detection with helium carrier. Published data[8] shows a characteristic which has a maximum at a concentration of approximately 8 mole % hydrogen in helium. A least squares fit of a third order polynomial was seen to be a suitable approximation, as in Fig. 2. The analogue simulation of a column with such a non-linear detector is shown in Fig. 3. The column dynamics in this case was simulated by the function $\frac{1}{(1+S)^5}$. As the input is increased (corresponding to an increase of hydrogen concentration), the detected peaks start to invert and exhibit the behaviour observed with real samples.

By applying the techniques described in this section, the linear impulse response can be obtained to within a constant, and the sample analysed. The details of the solution of (6) are shown in the next section.

2.3.2 ESTIMATION OF THE LINEAR IMPULSE RESPONSE FROM SECOND ORDER WEIGHTS

Equation (6) states that

$$\phi_{x^*z}(\tau) = \text{Bias term} + Q \int_0^T \int_0^T h(\tau_1)h(\tau_2)\phi_{p^*p^*}(\tau_{12})d\tau_1\, d\tau_2$$

the double integral contains second order weights $h(\tau_1)h(\tau_2)$. To obtain $h(\tau)$ separately we need to solve (6).

Now as seen in Appendix C.3.,Fig. 4 shows the coordinates (τ_1,τ_2) and coefficients of the $h(\tau_1)h(\tau_2)$ products which contribute to (6), if $p^*(t) = p_1^*(t)$. Using the simulation of Fig.3, and inserting suitable artificial delay, it is possible to ensure that

$h(\tau) = 0$ for $\tau =$ $(0\text{-}8)\lambda$ inclusive and

$h(\tau) \simeq 0$ for $\tau =$ $(22\text{-}30)\lambda$ inclusive

Performing the experiments suggested in 2.3 we can say that

$$\phi_{x^*z}(\tau) = R + Q \int_0^T \int_0^T h(\tau_1)h(\tau_2)\phi_{p^*p^*}(\tau_{12})d\tau_1\, d\tau_2$$

where R is a bias term.

Hence we can form the following:-

$\frac{1}{2Q}\left[\phi_{x^*z_1}(\tau)+\phi_{x^*z_2}(\tau)\right] - 2R/Q$	τ/λ	Equation No. if used subsequently
$h_{12}\ h_{20}$	0	
$h_{13}\ h_{21}$	1	
0	2	
$-h_9\ \ h_{13}$	3	I_3
$-h_{10}\ h_{14}$	4	I_4
$-h_{11}\ h_{15}$	5	I_5
$-h_{12}\ h_{16}$	6	I_6
$-h_{13}\ h_{17}$	7	I_7
$-h_{14}\ h_{18}$	8	I_8
$-h_{15}\ h_{19}$	9	I_9
$-h_{16}\ h_{20}$	10	I_{10}
$-h_{17}\ h_{21}$	11	
0	12	
0	13	
0	14	
0	15	
0	16	
0	17	
0	18	
0	19	
0	20	
0	21	
0	22	
0	23	
0	24	
0	25	
0	26	
0	27	
$h_9\ \ h_{17}$	28	I_{28}
$h_{10}\ h_{18}$	29	I_{29}
$h_{11}\ h_{19}$	30	I_{30}

and similarly

$1/Q \left[\phi_{x^*z_1}(\tau) - \phi_{x^*z_2}(\tau)\right]$	τ/λ	Equation No. if used subsequently
$h_{17}h_{18}$	0	K_0
$-h_9\ h_{20} + h_{18}\ h_{19}$	1	
$-h_{10}\ h_{21} + h_{19}\ h_{20}\ +h_9\ h_{18}$	2	
$+h_{10}\ h_{19}$	3	K_3
$+h_{11}\ h_{20}$	4	K_4
0	5	
0	6	
0	7	
0	8	
0	9	
0	10	
0	11	
$-h_9\ h_{14}$	12	K_{12}
$-h_{10}h_{15}$	13	K_{13}
$-h_{11}h_{16}\ -h_9\ h_{12}$	14	
$-h_{12}h_{17}\ -h_{10}h_{13}$	15	K_{15}
$-h_{13}h_{18}\ -h_{11}h_{14}$	16	
$-h_{14}h_{19}\ -h_{12}h_{15}$	17	
$-h_{15}h_{20}\ -h_{13}h_{16}$	18	
$-h_{14}h_{17}$	19	K_{19}
$-h_{15}h_{18}$	20	K_{20}
$-h_{16}h_{19}$	21	K_{21}
$-h_{17}h_{20}$	22	K_{22}
$h_9\ h_{10}$	23	K_{23}
$h_{10}h_{11}$	24	K_{24}
$h_{11}h_{12}\ +h_9\ h_{16}$	25	
$h_{12}h_{13}\ +h_{10}h_{17}$	26	K_{26}
$h_{13}h_{14}\ +h_{11}h_{18}$	27	
$h_{14}h_{15}\ +h_{12}h_{19}$	28	
$h_{15}h_{16}\ +h_{13}h_{20}$	29	
$h_{16}h_{17}$	30	K_{30}

Using the equations lettered I_i and K_i we can solve for $h(\tau)$ as in the following :-

$h(\tau)$	=	Expression formed as shown
h_9	=	$(2\times K_{23})/h_{10}$
h_{10}	=	$(2\times K_{24})/h_{11}$
h_{11}	=	$-I_5/h_{15}$
h_{12}		from $2\times K_{26}$ and $-2\times I_{15}$
h_{13}	=	$-I_3/h_9$
h_{14}	=	$-I_4/h_{10}$
h_{15}	=	$\sqrt{I_5\times K_{13}/K_{24}}$
h_{16}	=	$-I_6/h_{12}$
h_{17}	=	I_{28}/h_9
h_{18}	=	I_{29}/h_{10}
h_{19}	=	I_{30}/h_{11}
h_{20}	=	$2\times K_4$

In practice although it is easy to remove the bias term (by examination of those points where

$\phi_{x^*z_1}(\tau) \pm \phi_{x^*z_2}(\tau) = R$), the factor Q is unknown and cannot be calculated easily. It is seen that all estimates of $h(\tau)$ formed using the process described above, contain a multiplicative factor Q. Thus it is necessary to normalise the estimates by dividing by the maximum ordinate.

Proceeding in this manner for the simulation of

Fig. 3 , it is possible to arrive at the normalised impulse response estimates of the linear dynamics, as shown in Fig. 5. For comparison also included are the normalised estimates obtained using a linear detector characteristic, and the normal correlation approach for linear systems.

The parallel case for a minimum in the detector characteristic occurs when detecting acetylene sample in nitrogen carrier, (see Fig. 6). Applying conventional chromatography injection techniques, the detector output is of the simulated form shown in Fig. 7. Inverted peaks are present. Using the identical approach with Hadamard-modified sequences as for the case of hydrogen in helium, the procedures described here give the results of Fig.8.

It is seen that the problem of the anomalous katherometer response (chapter 1, section 2.4.3), can be overcome to a large degree, by the application of the techniques described here. The penalty incurred is an increase of experimenting time. The next section describes attempts to reduce this time.

2.3.3. THE TOTAL EXPERIMENT TIME

In the linearisation procedure of section 2.3

applied in 2.3.1 to chromatographic detection, two experiments with Hadamard modified sequences $X_1(t)$ and $X_2(t)$ each of length $8L\lambda$ are required. The total experimenting time is thus 18λ. This compares with a total time of $6L\lambda$ in the methods of Brown[2] and Gardiner[1]. However, the methods of Brown[2] and Gardiner[1] require a transducer capable of distinguishing four levels of input, those of section 2.3 require just two.

Attempts were made to find other Hadamard sequences of length 8 which would enable the identification of the linear weights in only one experiment. Brauer[9] gives an alternative construction of Hadamard matrices, but as shown in Appendix C.4, these can lead to sequences which are non-antisymmetric. This is shown to be a shortcoming of such sequences in Appendix C.4, and their use is not recommended. No other suitable sequences was found.

Hence it is felt that when applying the proposed procedures, the minimum experimenting time is likely to be $18L\lambda$. Apart from this difference, the methods of Brown[2] and Gardiner[1] can be applied, with some complexity, to systems with any order of non-linearity. The proposed method removes the effects of up to third order non-linearities plus any higher order odd powers. Unfortunately, the presence of even powers greater than two causes extra terms to appear in (6). These may prevent successful identification of $h(\tau)$. However this should not be a serious limitation.

3. MULTI-STREAM ANALYSIS

Briggs and Godfrey[7] have studied the use of delayed pseudo-random binary sequences in multivariable systems analysis. They have shown that by stimulating the various paths of a multivariable system with such pseudo-random binary sequences, each path may be separately identified if the delays between the i^{th} and $(i+1)^{th}$ sequences are chosen to be greater than the settling time of the i^{th} path.

An example of such a multivariable system is a chromatograph column analysing several different samples at once. This type of analysis is not possible with conventional injection techniques, but it is very easily performed using the correlation technique.

Noting that there is considerable transport lag in chromatography, it is relatively easy to shift the impulse response estimates to a convenient absicissae region by simply inserting positive or negative time delays (i.e. delaying or advancing the start of the injection sequence). It is often possible to place a second (or more) sets of impulse response estimates in the regions where the first set are identically or approximately zero.

To appreciate the applications of such a technique, consider the analysis of hydrocarbon mixture(b)*.

---

* Sample (b) composition :- 93.9 vol% Helium, 5.62 vol% Propylene, 0.481 vol% Propane, 0.073 vol% Ethylene.

[Injecting a single 10µl sample into the porapak Q column at 30°C results in Fig.9. The carrier is impure helium, which should give a negative peak at the normal retention time of the impurity (nitrogen). The inverted peak is just visible, but the high noise level prevents qualitative analysis of the sample.]

The mixture was split into two streams, one of which was injected into the column according to the (1,0) logic of a p.r.bs. in 10µl aliquots. A delayed sequence was used to inject the second stream at the same time, in 3µl aliquots into the same column. By choosing the delay carefully, it was possible to analyse both streams in a continuous fashion at the same time, although only one detector was used. This is shown in the results of Fig.10. The inverted peak is clearly evident, and two of the three sample components easily identified. The presence of the inverted peak masked the third component (ethylene) which was eluted soon after the impurity. The significantly reduced noise level is to be noted.

In this case the samples have been derived from the same reservoir. However the technique allows simultaneous analysis of samples from many sources, although the retention times of the samples need to be of the same order. Moreover, the column must be capable of separating the components of both samples.

The extension to multistream analysis is obvious. The analysis is complete in two periods of the m sequence. To achieve the same number of simultaneous analyses with conventional techniques, as many sets of apparatus as samples analysed are required. Using one set of apparatus the conventional approach, (with a second sample injected as the first elutes), would give analyses of two samples at the same time as the proposed method. However as the number of samples increases, the proposed method, with one sample valve for each stream, will give faster analysis.

4. ANALYSIS OF SAMPLES WITH TIME VARYING CONCENTRATIONS

One of the main advantages claimed for the p.r.b.s. approach to chromatography is that since the input is continuous, the correlogram can be obtained continuously. Chapter 2 section 3 shows that although the analyses are always T_L out of date, they can be recomputed every λ units of time. This compares with an updating time of at least (and usually much more than) T_L' for the equivalent case in conventional chromatography.* This observation was first reported by Davies[10]. However, continuous updating requires that the system be stationary. If the component concentration changes and the detector output shows a corresponding change, correlation cannot be begun until one period of data, with the system in a new steady state, has been recorded. This means that after a change in sample composition, a new correlogram cannot be obtained before two elution times have elapsed. This effect is to be seen in the work of Godfrey and Devenish[5], who in the middle of a continuous correlation experiment, switched from oxygen to nitrogen sample. For their particular column (80-100 mesh molecular sieve 5A) and helium carrier gas, the retention characteristics of oxygen and nitrogen are so different that the system dynamics were completely changed. This situation is not particularly realistic however, since in practice, what is more likely to occur, except during catastrophic situations, is a small change in component concentration; i.e. mere gain changes for some of the sample peaks. Even so, if these variations are either discrete or continuous, the correlation technique does not

---

*$T_L' = T_L$ - retention time of air peak, and often $T_L' \approx T_L$ to a good approximation.

give the much vaunted continuous chromatogram.

In such cases it is obvious that some modification of the technique is necessary. Assuming linear operation only, analysis is possible if the data reduction procedures are modified. We assume that the retention characteristics of the sample remain constant, and no new components occur.

The theoretical development for a noise free output is given in Appendix C5, but the main results are summarised here. If a change γ in impulse response ordinates occurs at a time t_2', then the correlogram at shifts τ_i will show a departure $\Delta_{xy}(\tau_i,t_2)$ from the previous steady state correlogram. It is shown that*

$$\left\{\Delta_{xy}(\tau_i,t_2)\right\} = \left\{\frac{1}{L}\sum_{t_j=t_2'}^{t_2} \Delta y_{t_j}\, x_{t_j-\tau_i}\right\} \quad \text{for } i = 0,\rightarrow L-1, \tag{8}$$

where Δy_{t_j} is the change in output y at $t_2 = t_j$ from the value one period before t_2. The change in output y can be expressed in terms of the change in impulse response ordinates, and hence we can write the change in correlogram as

$$\left\{\Delta_{xy}(\tau_i,t_2)\right\} = \frac{1}{L}\left\{\left(\sum_{s=0}^{L-1} \Delta h_s'\, x_{\tau_i-s\lambda}\right) x_{t_2-\tau_i}\right\} + \left\{\Delta_{xy}(\tau_i,t_2-\lambda)\right\} \quad \text{for } i = 0,\rightarrow L-1. \tag{9}$$

Assuming that the change γ is of unit size, (9) can be evaluated for all (τ_i,t_2). Comparing the values obtained

* The curly brackets in the above and Appendix C.5 denote vectors.

from (9), with those obtained in practice, gives the actual change γ. This procedure gives reliable estimates $\hat{\gamma}$ at the first sampling instant after the first change in output has occurred.

This work is believed to be entirely new, and shows that having first calculated a correlogram from one period of output data, variations in peak height can be tracked.

If the output data is contaminated with noise, some averaging process will reduce the variance in the estimate of the gain change. There are two cases of interest here:-

(a) Gain changes which occur at random instants but only once during a period. The change is considered to occur either instantaneously or within a bit interval.

(b) Changes which are either continuous or take place over several bits.

In the case (a) after estimating the change for the first time, further estimates can be made over successive bit intervals. The average over several bits reduces the variance in the initial estimate. A reliable estimate should be available well within one period of the change occurring at the output.

For the case (b) one would reduce the variance by computing an average value of output over one bit. Taking several (e.g. 100) samples and averaging, achieves this.

This process is also applicable in the case (a). By extrapolating to an equivalent 'steady state' in (b) a continuously varying sample concentration could be tracked.

The situation of case(a) in a noise free environment was explored in a simulation using a fifteen bit p.r.b.s. and a 5 point impulse response peak. The gain associated with the peak was changed suddenly from 0.6 to 1.2 in the bit interval between $t_2/_\lambda$ =0(mod L) and $t_2/_\lambda$ =1(mod L). The normal impulse response estimation by correlation(without any compensation of the form described here) is unable to yield a reliable estimate of the new weighting function until one period later. The compensation procedure allows computation of a reliable estimate at $t_2/_\lambda$ =1(mod L) i.e. within a bit of the change occuring. The experimental results are shown in Figs. 11(a) and 11(b). The notation 'C.C.F.' indicates the result of applying the compensation procedures, described here, to update the previous steady state correlogram i.e.

$$\text{C.C.F.} = \hat{\gamma}. \text{ previous steady state values of } \phi_{xy}(\tau).$$

In a second experiment,one bit after the normal uncompensated correlation function reached the steady state, the gain was suddenly reduced from 1.2 to 0.6. Using the compensation procedure a reliable estimate was available at the next sampling instant, whereas, see Fig. 12, the uncompensated procedure was unable to produce a stationary result until one period later. Continuous analysis is seen to be possible if the compensation procedure is applied.

5. THE USE OF A DIGITAL CORRELATOR

The prime object of installing a control scheme in industry is often to reduce the manufacturing cost of the end product. Thus the control scheme itself should be as cheap as possible. In the proposed identification procedure, the need of an on-line computer to handle the data analysis, is stressed. The machine used to date in this work (G.E.C. 90/2 8K online, 1.75 μs cycle time, digital computer) has not been used to its full capacity. This is because we have required only, the calculation of first order correlograms, and generation of p.r.b.s. It was therefore considered in keeping with industrial policy, to replace the computer by other devices which would be capable of the data analysis and signal generation required.

Several pseudo-random binary sequence generators are currently on the market, and recently a digital correlator has become available. The application of this machine (Hewlett Packard 3721A) to system identification has been described recently[11]. In the present case its function is to log the p.r.b.s. input and microkatherometer output. It then correlates them continuously.

Two experiments were conducted in order to evaluate the suitability of the correlator to chromatography. In the first experiment nitrogen was injected into a porapak Q column, using a 10μl injection volume according to the logic of a two second bit interval, 63 bit long sequence. The injection was performed once per "1" bit interval. The carrier used was impure helium at a flowrate of 1/6 ml/sec.

The column was operated at 30°C and a micro katherometer used as detector. Fig.13 shows the result obtained on the correlator which compares satisfactorily with Fig.12 of Chapter 2.

In the second experiment, two samples of nitrogen were injected into the same column at the same time, under the control of delayed sequences. The injection volumes used were 10µl and 3µl. For the first sample, the p.r.b.s. was delayed by 10 bits with respect to a basic sequence, and for the second the delay was 43 bits. Using the same temperature and flow settings as in the first experiment, the two sample experiment yields the result in Fig. 14. Note that the correlator crosscorrelates between the basic (underlayed) sequence and the detector output.

From the results of Figs. 13 and 14 it is obvious that the digital correlator can be used in multi-stream analysis.

6. APPENDICES

APPENDIX C.1.

THE USE OF INVERSE REPEAT SEQUENCES IN CROSS-CORRELATION

Consider the case of a linear system followed by a polynomial gain term as shown in Fig. 1.

If $X(t) = x(t) \oplus p(t)$

where p(t) is a sequence of alternate ones and zeroes, then X(t) is an inverse repeat sequence of period 2T and if the sequence X(t) is transformed so that

$0 = -1, \quad 1 = +1$ to give $X^*(t)$, then

$$X^*(t) = -X^*(t+T).$$

Moreover,

$$\phi_{X^*z}(\tau) \frac{a_o}{2T} \int_0^{2T} X^*(t-\tau)dt + \frac{a_1}{2T} \int_0^{2T}\int_0^{\infty} X^*(t-\tau)c(t-\tau_1)h(\tau_1)d\tau_1\, dt +$$

$$\frac{a_2}{2T} \int_0^{2T}\int_0^{\infty}\int_0^{\infty} X^*(t-\tau)c(t-\tau_1)c(t-\tau_2)h(\tau_1)h(\tau_2)d\tau_1\, d\tau_2\, dt +$$

$$+ \frac{a_3}{2T} \int_0^{2T}\int_0^{\infty}\int_0^{\infty}\int_0^{\infty} X^*(t-\tau)c(t-\tau_1)c(t-\tau_2)c(t-\tau_3)h(\tau_1)h(\tau_2)h(\tau_3)d\tau_1$$

$$d\tau_2\, d\tau_3\, dt + \text{---C.1.(1)}$$

where the actual system input is

$$c(t) = \frac{b}{2}\left[X^*(t) + 1\right]$$

Since $X^*(t)$ is an inverse repeat sequence, we may simplify C.1.(1) as follows:-

$$\frac{1}{2T}\int_0^{2T} X^*(t-\tau)c(t-\tau_1)dt = \frac{b}{4T}\int_0^{2T} X^*(t-\tau)[X^*(t-\tau_1)+1]dt$$

$$= \frac{b}{2}\phi_{X^*X^*}(\tau-\tau_1) \qquad \text{C.1.(2)}$$

$$\frac{1}{2T}\int_0^{2T} X^*(t-\tau)c(t-\tau_1)c(t-\tau_2)dt = \frac{b^2}{8T}\int_0^{2T} X^*(t-\tau)[X^*(t-\tau_1)+1]$$
$$\cdot [X^*(t-\tau_2)+1]dt$$

$$= \frac{b^2}{4}[\phi_{X^*X^*}(\tau-\tau_1)+\phi_{X^*X^*}(\tau-\tau_2)] \qquad \text{C.1.(3)}$$

and

$$\frac{1}{2T}\int_0^{2T} X^*(t-\tau)c(t-\tau_1)c(t-\tau_2)c(t-\tau_3)dt$$

$$= \frac{b^3}{16T}\int_0^{2T} X^*(t-\tau)[X^*(t-\tau_1)+1][X^*(t-\tau_2)+1][X^*(t-\tau_3)+1]dt$$

$$= \frac{b^3}{8}\left[\phi_{X^*X^*}(\tau-\tau_1)+\phi_{X^*X^*}(\tau-\tau_2)+\phi_{X^*X^*}(\tau-\tau_3)\right]+$$

$$\frac{b^3}{16T}\int_0^{2T} X^*(t-\tau)X^*(t-\tau_1)X^*(t-\tau_2)\ X^*(t-\tau_3)dt$$

C.1.(4)

$$\therefore \phi_{X^*Z}(\tau) = \frac{ba_1}{2}\int_0^{\infty}\phi_{X^*X^*}(\tau-\tau_1)h(\tau_1)d\tau_1$$

$$+ \frac{2G_{ss^2}}{4} b^2a_2 \int_0^{\infty} \phi_{X^*X^*}(\tau-\tau_1)h(\tau_1)d\tau_1$$

$$+ \frac{3G_{ss^2}}{8} b^3a_3 \int_0^{\infty}\phi_{X^*X^*}(\tau-\tau_1)h(\tau_1)d\tau_1 +$$

$$\frac{b^3a_3}{8}\int_0^{\infty}\int_0^{\infty}\int_0^{\infty}h(\tau_1)h(\tau_2)h(\tau_3)\phi_3(\tau_1,\tau_2,\tau_3,\tau)d\tau_1\ d\tau_2\ d\tau_3$$

+--------C.1.(5)

where $G_{ss} = \int_0^\infty h(\tau)d\tau$ C.1.(6)

and $\phi_3(\tau_1,\tau_2,\tau_3,\tau) = \frac{1}{2T}\int_0^{2T} X^*(t-\tau_1)X^*(t-\tau_2)X^*(t-\tau_3X^*(t-\tau)dt$

C.1.(7)

APPENDIX C.2.

THIRD ORDER AUTOCORRELATION FUNCTIONS OF INVERSE REPEAT SEQUENCES

The third order autocorrelation function of the inverse repeat sequence $X^*(t)$ formed from

$$X^*(t) = [x(t) \oplus p(t)]^* \text{ is the function}$$

$$\phi_3(\tau_1,\tau_2,\tau_3,\tau) \triangleq \frac{1}{2T}\int_0^{2T} X^*(t-\tau_1)X^*(t-\tau_2)X^*(t-\tau_3)X^*(t-\tau)dt \qquad \text{C.2.(1)}$$

or in summation form

$$\triangleq \frac{1}{2L}\sum_{r=0}^{2L-1} X^*(r\lambda-\tau_1)X^*(r\lambda-\tau_2)X^*(r\lambda-\tau_3)X^*(r\lambda-\tau) \qquad \text{C.2.(2)}$$

If we use the * transformation, Simpson[6] notes that we can write ϕ_3 as

$$\phi_3(\tau_1,\tau_2,\tau_3,\tau) = \frac{1}{2L}\sum_{r=0}^{2L-1} \overline{[X(r\lambda-\tau_1) \oplus X(r\lambda-\tau_2) \oplus X(r\lambda-\tau_3) \oplus X(r\lambda-\tau)]}^* \qquad \text{C.2.(3)}$$

where the bar indicates inversion.

Hence

$$\phi_3(\tau_1,\tau_2,\tau_3,\tau) = \frac{1}{2L}\sum_{r=0}^{2L-1} \overline{[x(r\lambda-\tau_1)\oplus x(r\lambda-\tau_2)\oplus x(r\lambda-\tau_3)\oplus x(r\lambda-\tau)\oplus p'(t)]}^* \qquad \text{C.2.(4)}$$

where $p'(t) = p(t-\tau_1)\oplus p(t-\tau_2)\oplus p(t-\tau_3)\oplus p(t-\tau)$ C.2.(5)

and is a sequence of all 0's or all 1's.

The value of ϕ_3 will be ± 1 or $\pm 1/L$. In this Appendix we wish to calculate the coordinates at which the value is ± 1. For any τ, we attempt to find a τ_3 which will combine with all possible τ_1, τ_2 combinations so that $|\phi_3| = 1$.

The combinations of τ_1, τ_2, and τ_3 which satisfy this condition are recorded in a 2Lx2L matrix. Combinations which do not fit are noted by a blank. The polarity can also be recorded by affixing the appropriate sign to the values of τ_3.

We recognise immediately that $\phi_3 = +1$ at the following points $(\tau_1, \tau_2, \tau_3, \tau)$

(a) $\tau_1 = \tau_2 = \tau_3 = \tau$

(b) $\tau_1 = \tau_2 \neq \tau_3 = \tau$

(c) $\tau_1 = \tau_3 \neq \tau_2 = \tau$

(d) $\tau_1 = \tau \neq \tau_2 = \tau_3$

These points appear as

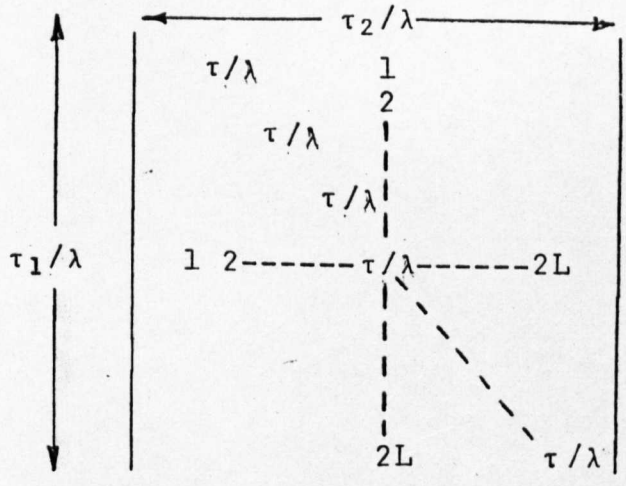

The other points where $|\phi_3| = 1$ are the sets $(\tau_1,\tau_2,\tau_3,\tau)$ satisfying one of the following conditions.

(e) $D^{\tau 1}x \oplus D^{\tau 2}x = D^{\tau a}x$; $D^{\tau 3}x \oplus D^{\tau}x = D^{\tau b}x$

and if $D^{\tau a}x = D^{\tau b}x$ then $\phi_3 = \pm 1$.

(f) $D^{\tau 1} \oplus D^{\tau 3}x = D^{\tau c}x$; $D^{\tau 2}x \oplus D^{\tau}x = D^{\tau d}x$

and if $D^{\tau c}x = D^{\tau d}x$, $\phi_3 = \pm 1$

(g) $D^{\tau 1}x \oplus D^{\tau}x = D^{\tau e}x$; $D^{\tau 2} \oplus D^{\tau 3}x = D^{\tau f}x$

and if $D^{\tau e}x = D^{\tau f}x$, $\phi_3 = 1$.

If $(\tau_1,\tau_2,\tau_3,\tau)$ does not obey any one of the conditions (a) - (g) then $\phi_3 = \pm \frac{1}{L}$.

To calculate the relevant value of τ_3 which ensures abeyance of one of the conditions (a) to (g) for the set $(\tau_1,\tau_2,\tau_3,\tau)$, the following equation is used :-

$$D^{\tau 1}x \oplus D^{\tau 2}x \oplus D^{\tau}x = D^{\tau 3}x \qquad \text{C.2.(6)}$$

The equation C.2.(6) also demonstrates that the solutions τ_3 have a threefold symmetry in (τ_1,τ_2,τ). Thus the matrix of points τ_3 is symmetrical.

For coordinates $(\tau_1,\tau_2,\tau_3,\tau)$ obeying one of (e) to (g) inclusive, the sign of ϕ_3 is readily seen to be positive for $p'(t)$ a sequence of all zeroes, and negative when $p'(t)$ is a sequence of all ones. Since the period of $p(t)$ is two

bit intervals, these conditions are equivalent to examining

$$\tau^1 = \left| \; |\tau_2 - \tau_1| \; - |\tau_3 - \tau| \right| \qquad \text{C.2.(7)}$$

When τ^1 is odd, $p'(t)$ is a sequence of all ones, and ϕ_3 is negative. If τ^1 is even, $p'(t)$ is a sequence of all zeroes and ϕ_3 is positive.

If in equation C.2.(6),

$$D^{\tau 1}x \oplus D^{\tau 2}x = D^{\tau 3}x$$

then for that particular combination of τ_1 and τ_2, there is no sequence $D^{\tau 3}x$ obeying C.2.(6). This situation causes the blanks in the matrix of points τ_3.

Solution of C.2.(6) and C.2.(7) generates the required matrix of points $\tau_3$examples of which for L=15, τ=0 and $\tau=\lambda$ are shown in Figs.15, and 16.
Note that the solutions of C.2.(1) are to be used in solving

$$I = \int_0^\infty \int_0^\infty \int_0^\infty h(\tau_1)h(\tau_2)h(\tau_3)\phi_3(\tau_1,\tau_2,\tau_3,\tau)d\tau_1 \, d\tau_2 \, d\tau_3$$

where $h(\tau_i) \approx 0$ for $\tau_i \geq (L-1)\lambda$. Hence we do not require to solve C.2.(6) for $\tau_i > L\lambda$, and the entries in Fig.15 and Fig.16 are values of τ_i obeying this restriction.

CALCULATION OF THE $(\tau_1,\tau_2,\tau_3,\tau)$ SETS BY THE DIRECT APPROACH

The direct approach to calculation of the coordinates (τ_1,τ_2,τ_3) for all τ is to compute the integral (C.2.(1)) over all t. The combinations at which $\phi_3 = \pm 1$ would then be stored. This is a lengthy process as is shown by some simple calculations :-

To solve for one choice of τ_1,τ_2,τ we require

$$3 \times 2L \times L \text{ multiplications}$$

For the same τ, but all τ_1,τ_2, combinations we need

$$3 \times 2L \times L \times L \times L = 6L^4 \text{ multiplications.}$$

Finally over all τ, the total number of multiplications required would be $6L^5$. On present machines integer multiplication takes approximately 15 μsec. Thus to solve C.2.(1) directly for all τ and L in the region of ≈100 takes at least

$$6 \times 10^{10} \times 15 \times 10^{-6} \text{ sec} = 253\tfrac{1}{2} \text{ hrs !}$$

CALCULATION OF THE $(\tau_1,\tau_2,\tau_3,\tau)$ SETS BY THE INDIRECT APPROACH

Solution of C.2.(1) by the indirect method outlined in this Appendix is much quicker than by the direct evaluation of $\phi_3(\tau_1,\tau_2,\tau_3,\tau)$ as will be demonstrated here.

It is well known that all delays mod L of an m sequence can be generated by modulo-2 additions of the sequences generated at the n register stages.
e.g. for the 'm' sequence

$$D^3x \oplus D^4x = D^0x$$

then $D^5x = D^1x \oplus D^4x.$

We can tabulate the required modulo-2 additions which give all sequence delays in the range (0→L-1).

The tabulation is given in Fig. 17 for L=15.
A 'one' in a column denotes that the sequence output from the particular register stage associated with that column, is to be modulo-2 added to sequences associated with all other columns in which there is a 'one'.
i.e. $D^{10}x = D^1x \oplus D^3x.$
Then since $D^{11}x = D^2 \oplus D^4x$

$$D^{11}x \oplus D^{10}x = D^1x \oplus D^2x \oplus D^3x \oplus D^4x.$$

By inspection $D^7x = D^1x \oplus D^2x \oplus D^3x \oplus D^4x$

i.e. $D^{10}x \oplus D^{11}x = D^7x.$

The application of this technique to the solution of C.2.(6) should be obvious. Hence with the indirect method proposed, one need only scan the table analogous to Fig. 17, to calculate the required $(\tau_1,\tau_2,\tau_3,\tau)$ coordinates. The scan is completed when the required set (if any) is in store. Using this set, the polarity of ϕ_3 at these coordinates is easily obtained from C.2.(7).

[It is of some interest to note that viewed separately, and from bottom to top, each column of connections in Fig. 17 is a p.r.b.s. Taking the last column as the reference sequence, the other columns are the delayed versions shown. Unfortunately, no general formula was found which generated the delay of a given column. However, such a formula would be useful, since this method would be valuable in calculating the required register connections needed to generate a given delayed sequence].

Storing the solutions of C.2.(6) and C.2.(7) in a matrix as in Figs. 15 and 16, the symmetry of the resultant matrices can be used to enable an even faster approach. We list a number of observations :-

(1) Solving C.2.(6) for all τ it is seen that there exist just (L+1) distinct rows in total, from all of the matrices of solutions. Each matrix is made up of L of these (L+1)rows.

(2) For a particular value of τ, the rows of the corresponding matrix are such that the leading diagonal consists entirely of terms $\tau_3=\tau$.

(3) Constructing a matrix from L of the (L+1) rows in such a manner that, without disturbing the order of the elements of any row, the leading diagonal is made up of blanks, we get Fig. 18. This is a symmetrical matrix, with every left to right diagonal consisting of a sequence of natural numbers. The starting points of these sequences are the elements of the first row, and each term is reduced modulo L. This means that (L-1) of the (L+1) district rows can be calculated from the first row.

(4) The row not accounted for in Fig.18 is the sequence of natural numbers beginning at zero.

The procedure for obtaining the matrix of solutions τ_3 to C.2.(1) for a given value of τ, can now be summarized.

i) Obtain the solutions of C.1.(6) for $\tau = \lambda$ $\tau_2 = 0$. This generates one row of the matrix in Fig. 18.

ii) Placing the row generated in (i) in such a manner that the blank occurs on the diagonal of Fig. 18, generate all further terms in Fig. 18 using observation (3) above.

iii) Generate the matrix of solutions τ_3 at any τ from the rows obtained in (ii) and by use of (2) and (4) above.

iv) Evaluate C.2.(7) to find the impulse polarity.

The application of these rules allows a rapid evaluation of $\phi_3(\tau_1,\tau_2,\tau_3,\tau)$ to give the sets $(\tau_1,\tau_2,\tau_3,\tau)$ at which $|\phi_3| = 1$, and also the polarity of ϕ_3. These sets can then be used to calculate

$$I = \int_0^\infty \int_0^\infty \int_0^\infty h(\tau_1)h(\tau_2)h(\tau_3)\phi_3(\tau_1,\tau_2,\tau_3,\tau)d\tau_1\, d\tau_2\, d\tau_3.$$

the importance of which is discussed in Chapter 3, section 2.2.

APPENDIX C.3.

THE USE OF HADAMARD MODIFIED 'M' SEQUENCES TO REMOVE THE EFFECTS OF NON-LINEARITIES ON PROCESS CROSSCORRELATIONS

Consider the case of a linear system followed by a polynomial gain as shown in Fig. 1. The input transducer is assumed to be such that the system input is the modified sequence X*(t)

i.e. $C(t) = X^*(t)$.

Where X*(t) is a sequence generated by modifying an 'm' sequence x(t) of length L with a sequence p chosen from the rows (other than the first) of an Hadamard matrix written in standard form[7] and of dimension 2^k where k = 3.

i.e. $X(t) = x(t) \oplus p(t)$ C.3.(1)

and X(t) is transformed to X*(t) according to

$0^* = -1$, $1^* = 1$.

Then

$$\frac{1}{8T}\int_0^{8T} X^*(t-\tau)dt = \frac{1}{8T}\int_0^{8T} X^*(t-\tau_1)x^*(t-\tau)dt$$

$$= \frac{1}{8T}\int_0^{8T} X^*(t-\tau_1)X^*(t-\tau_2)X^*(t-\tau_3)x^*(t-\tau)dt = 0 \qquad \text{C.3.(2)}$$

$$\therefore \phi_{X^*z}(\tau) = \frac{a_2}{8T}\int_0^{8T}\int_0^{\infty}\int_0^{\infty}\int_0^{\infty} h(\tau_1)h(\tau_2)X_1^*(t-\tau_1)X_1^*(t-\tau_2)x^*(t-\tau)d\tau_1 d\tau_2 dt$$

$$+ \frac{a_0}{8T}\int_0^{8T} x^*(t-\tau)dt \qquad \text{C.3.(3)}$$

where $h(\tau)$ is the linear system impulse response.

Let $I = \frac{1}{8T}\int_0^{8T} X^*(t-\tau_1)X^*(t-\tau_2)x^*(t-\tau)dt$,

then $I = \frac{1}{8T}\int_0^{8T} \overline{[D^{\tau 1}x \oplus D^{\tau 2}x \oplus D^{\tau}x \oplus D^{\tau 1}p \oplus D^{\tau 2}p]}^* dt$ C.3.(4)

where the bar indicates inversion.

thus $I = \frac{1}{8T}\int_0^{8T} \overline{[D^{\tau 1}x \oplus D^{\tau 2}x \oplus D^{\tau}x]}^* [\overline{D^{\tau 1}p \oplus D^{\tau 2}p}]^* dt$ C.3.(5)

which for p of period 8 bits is equivalent to

$$I = \phi_{p^*p^*}(|\tau_1-\tau_2|_{\text{mod } 8}) \cdot \phi_{x^*x^*}(\alpha-\tau) \qquad \text{C.3.(6)}$$

where α is such that

$$D^{\tau 1}x \oplus D^{\tau 2}x = D^{\alpha}x \qquad \text{C.3.(7)}$$

As τ_1 and τ_2 vary there are two cases of interest in C.3.(6)

(i) $\alpha = \tau$

then $I = \phi_{p^*p^*}|\tau_1-\tau_2|_{\text{mod } 8} = \pm 1, \pm\frac{1}{2}, 0$

For a non-zero value the following conditions must hold jointly

A1: $D^{\tau 1}x \oplus D^{\tau 2}x = D^{\tau}x$

A2: $\tau_{12} = |\tau_1-\tau_2|_{\text{mod } 8}$ is such that

$$\phi_{p^*p^*}(\tau_{12}) = \pm 1 \text{ or } \pm\tfrac{1}{2}.$$

(ii) $\alpha \neq \tau$

then $I = \frac{-1}{L}\phi_{p^*p^*}(\tau_{12})$

this term gives rise to a constant bias in $\phi_{x^*z}(\tau)$.

Thus in general

$$\phi_{x^*z}(\tau) = \frac{(L+1)}{L}\left[a_2 \int_0^T\int_0^T h(\tau_1)h(\tau_2)\phi_{p^*p^*}(\tau_{12})d\tau_1\, d\tau_2\right]\delta_{\alpha\tau} \qquad \text{C.3.(8)}$$

+ bias term

where the bias term $= -\frac{a_2}{L}\int_0^T\int_0^T h(\tau_1)h(\tau_2)\phi_{p^*p^*}(\tau_{12})d\tau_1\, d\tau_2$

$$+\frac{a_o}{L}$$

and $\delta_{\alpha\tau} = 1$ if $\alpha = \tau$, zero otherwise.

hence $\phi_{x^*z}(\tau)$ is a sum of $h(\tau_1)h(\tau_2)$ products each weighted by ± 1 or $\pm\frac{1}{2}$, together with a bias term.

One sequence p_1 of period 8 bits obtained from the eighth order Hadamard matrix is the sequence 1,1,1,1,-1,-1, -1,-1,(row 5). If we use this sequence to modify x(t) we get the sequence $X_1(t)$ according to $X_1(t) = x(t) \oplus p_1(t)$. The resulting expression for C.3.(8) is

$$\phi_{x^*z_1}(\tau) = a_2' \int_0^T \int_0^T h(\tau_1)h(\tau_2)\phi_{p_1^*p_1^*}(\tau_{12})d\tau_1\, d\tau_2\, \delta_{\alpha\tau} \qquad \text{C.3.(9)}$$

+ bias term

The solution of C.3.(9) to give the linear impulse response ordinates $h(\tau)$ is eased if a second experiment is performed with another modifying sequence p_2 of the same length V. p_2 is chosen to be such that

$$\phi_{p_1^*p_1^*}(\tau) = \phi_{p_2^*p_2^*}(\tau) = \pm 1 \text{ for } \tau = 0, V\lambda/2$$

$$\phi_{p_1^*p_1^*}(\tau) = -\phi_{p_2^*p_2^*}(\tau) = \pm \tfrac{1}{2} \text{ or } 0, \text{ for all other } \tau.$$

The sum and difference of $\phi_{x^*z_1}(\tau)$ and $\phi_{x^*z_2}(\tau)$ yields a simplified set of equations in $h(\tau_1)h(\tau_2)$, from which it is relatively easy to determine $h(\tau)$. The solution is further simplified if $h(\tau)$ has zero value at several points, e.g. if the system has inherent transport lag, or where $h(\tau)$, for values of τ near L is small enough to be considered equal to zero. Alternatively, an artificial delay can be inserted either before or after the system dynamics.

N.B. $a_2' = \frac{(L+1)}{L} a_2$.

The modifying Hadamard sequences with the described properties do not exist for Hadamard matrices of dimension less than eight. Modifying sequences of length greater than eight may be used, but the equation set is increased significantly. Using row 5 as p_1, a suitable choice for p_2 would be the row 6, such that p_2 = 1,-1,1,-1,-1,1,-1,1. The autocorrelation functions of these sequences are shown in Fig. 19. Note that the only other rows of this matrix which have a period of eight bits are rows 7 and 8, and are merely shifted versions of row 5 and 6.

For the sequence $D^0x = D^5x \oplus D^6x$, Fig. 20 shows those values of τ_2 which satisfy condition A1 for various combinations of (τ_1,τ). Note that for some (τ_1,τ) there is no solution τ_2. The matrix is symmetrical and each of the left to right diagonals consist of terms in a natural number sequence reduced modulo L.

Hence the matrix of Fig.20 is particularly easy to construct having first calculated the terms of the first row using the condition A1.

Using the values of τ_1 and τ_2 for various τ in Fig.20, τ_{12} can be calculated from the requirement of condition A2. Using $p(t) = p_1(t)$, Fig.4 shows the coordinates of the $h(\tau_1)h(\tau_2)$ products which contribute to C.3.(9), and the sign and magnitude of $\phi_{p_1p_1}(\tau_{12})$ for all τ, if p_1 = 1,1,1,1,-1,-1,-1,-1, and L = 31. Thus for example

$$\phi_{x^*z_1}(0) = a_2'\left[h_{12}\,h_{20} - h_{11}\,h_{23} - h_6\,h_{10} + \tfrac{1}{2}(h_{17}\,h_{18} + h_{15}\,h_{22} + h_{13}\,h_{30} + h_9\,h_{24} + h_7\,h_{16} - h_1\,h_{14} - h_4\,h_{25} - h_8\,h_{19} - h_{26}h_{29})\right] + \text{bias term} \quad \text{C.3.(10)}$$

and using $p(t) = p_2(t) = 1,-1,1,-1,-1,1,-1,1$

$$\phi_{x^*z_2}(0) = a_2'\left[h_{12}\,h_{20} - h_{11}\,h_{23} - h_6h_{10} - \tfrac{1}{2}(h_{17}\,h_{18} + h_{15}\,h_{22} + h_{13}\,h_{20} + h_9\,h_{24} + h_7\,h_{16} - h_1\,h_{14} - h_4\,h_{25} - h_8\,h_{19} - h_{26}\,h_{29})\right] + \text{bias term} \quad \text{C.3.(11)}$$

$$\therefore \phi_{x^*z_1}(0) + \phi_{x^*z_2}(0) = 2a_2'\left[h_{12}\,h_{20} - h_{11}\,h_{23} - h_6\,h_{10}\right] + 2\,(\text{bias term}) \quad \text{C.3.(12)}$$

$$\phi_{x^*z_1}(0) - \phi_{x^*z_2}(0) = a_2'\left[h_{17}\,h_{18} + h_{15}\,h_{22} + h_{13}\,h_{20} + h_9\,h_{24} + h_7\,h_{16} - h_1\,h_{14} - h_4\,h_{25} - h_8\,h_{19} - h_{26}\,h_{29}\right] \quad \text{C.3.(13)}$$

and similarly for all other τ in the range $(0 \rightarrow L-1)\lambda$.

Inserting a priori knowledge regarding the position of zero ordinates in the impulse response function, some of the terms corresponding to C.3.(12) and C.3(13) are zero.

e.g. if $h(\tau) = 0$ for $\tau = 0$ to 8λ inclusive and
$h(\tau) = 0$ for $\tau = 21\lambda$ to 30λ inclusive

$$\phi_{x^*z_1}(0) + \phi_{x^*z_2}(0) = 2a_2'\,h_{12}\,h_{20} + \text{bias term}$$

$$\phi_{x^*z_1}(0) - \phi_{x^*z_2}(0) = a_2'\,h_{17}\,h_{18}$$

etc. for all τ. The resultant non-linear equation set can

be solved for the $h(\tau)$ to within a constant.

A fuller example of the application of this technique is given in shapter 3 section 2.3. The analysis so far has assumed that the system input is $X^*(t)$. If the input transducer produces $c(t)$ such that

$c(t) = \frac{b}{2}\left[X^*(t) + 1\right]$ then some modification is necessary to C.3.(8).

$$\text{i.e. } \phi_{x^*z}(\tau) = \left[\frac{b^2 a_2}{4} + \frac{3b^3 a_3}{8} Gss\right] \int_0^T\int_0^T h(\tau_1)h(\tau_2)\phi_{p^*p^*}(\tau_{12}) \cdot \phi_{x^*x^*}(\alpha-\tau)d\tau_1 d\tau_2$$

$$+ \frac{a_o}{L} - \left[\frac{b\, a_1\, Gss}{2L} + \frac{b^2\, a_2 Gss^2}{4L} + \frac{b^3 a_3\, Gss^3}{8L}\right] \qquad \text{C.3.(14)}$$

$$\therefore \quad \phi_{x^*z}(\tau) = \text{Bias term} + Q \int_0^T\int_0^T h(\tau_1)h(\tau_2)\phi_{p^*p^*}(\tau_{12})d\tau_1\, d\tau_2 \qquad \text{C.3.15)}$$

where Q is a constant.

C.3.(15)is similar to C.3.(8) and the same procedure to obtain the linear impulse response estimates applies. The bias term in C.3.(15) as in C.3.(8) is best removed by examining the shifts τ at which the sum of the $h(\tau_1)h(\tau_2)$ products is zero. The residual is then the bias term.

APPENDIX C.4.

ALTERNATIVE MODIFYING SEQUENCES

Appendix C.3. considers the use of sequences p_1 and p_2 from an Hadamard matrix of dimension 2^k in identification studies. These matrices are constructed from a core matrix of $\begin{vmatrix} 1 & 1 \\ 1 & -1 \end{vmatrix}$ by kronecker multiplication. Bell[12] notes that other constructions due to Brauer[9] give alternative matrices. The binary matrix of dimension eight resulting from the Brauer construction is

row 1	0	0	1	0	1	1	0	1
row 2	0	0	0	1	1	0	1	1
row 3	1	0	0	0	0	1	1	1
row 4	1	1	0	0	1	0	0	1
row 5	0	1	1	0	0	0	1	1
row 6	1	0	1	1	0	0	0	1
row 7	0	1	0	1	0	1	0	1
row 8	1	1	1	1	1	1	1	1

C.4.(1)

The properties of Hadamard matrices are unaltered by interchanging rows or columns or by inverting every bit in a row or column. Using such operations, the above matrix may be transformed into C.4.(2).

i.e.

row 1	1	1	1	1	1	1	1	1
row 2	1	0	1	0	1	0	1	0
row 3	1	1	0	1	1	0	0	0
row 4	1	0	1	1	0	0	0	1
row 5	1	1	1	0	0	1	0	0
row 6	1	0	0	0	1	1	0	1
row 7	1	1	0	0	0	0	1	1
row 8	1	0	0	1	0	1	1	0

C.4.(2)

This is to be compared with the matrix obtained by kronecker multiplication of the core matrix

$$\begin{vmatrix} 1 & 1 \\ 1 & -1 \end{vmatrix}$$, in which all -1's are replaced by 0's.

This is the matrix of C.4.(3).

$$p_1 = \begin{vmatrix} 1 & 1 & 1 & 1 & 1 & 1 & 1 & 1 \\ 1 & 0 & 1 & 0 & 1 & 0 & 1 & 0 \\ 1 & 1 & 0 & 0 & 1 & 1 & 0 & 0 \\ 1 & 0 & 0 & 1 & 1 & 0 & 0 & 1 \\ 1 & 1 & 1 & 1 & 0 & 0 & 0 & 0 \\ 1 & 0 & 0 & 1 & 0 & 1 & 1 & 0 \\ 1 & 1 & 0 & 0 & 1 & 1 & 0 & 0 \\ 1 & 0 & 0 & 1 & 0 & 1 & 1 & 0 \end{vmatrix} \qquad p_2 = \qquad \text{C.4.(3)}$$

Compared with C.4.(3), it is evident that rows 3,4,5 and 6 of the transformed Brauer matrix have no counterpart in C.4.(3).

If either of the rows 3,4,5 or 6 of the Brauer matrix is used to modify a pseudo-random binary sequence as in Appendix C.3, then it is found that

$$\frac{1}{8T}\int_0^{8T} X_1^*(t-\tau_1)X_1^*(t-\tau_2)X_1^*(t-\tau_3)x^*(t-\tau)dt \neq 0 \qquad \text{C.4.(4)}$$

For successful application of the techniques of Appendix C.3. in systems with odd power non-linearities, it is essential however that C.4.(4) be zero everywhere. Thus the application of Hadamard-Brauer sequences is not recommended here. We can examine their shortcomings in the following.

THE ANTISYMMETRIC REQUIREMENT

In the sequences p_1 and p_2 of C.4.(3), the first half of the sequence is the inverse of the second half. We

say that the sequences are 'antisymmetric'. The rows of interest in the Hadamard-Brauer matrix (3,4,5 and 6) do not possess this property. To demonstrate that C.4(4) is zero everywhere, only if the modifying sequences have the 'anti-symmetric' property, we invoke a notation due to Stapleton and Hollo[13]. This notation is illustrated with an example :-

Example : To calculate $\phi_{pp}(0)$

In a V bit sequence p(t) assume that U bits are of level α and V-U bits are of level β. Thus

$$V\phi_{pp}(\tau) = \sum_{V=1}^{V} p_j p_{j-\tau} \qquad \text{C.4.(5)}$$

In ϕ_{pp}, the number of times an α is paired with another α spaced τ digits apart in one period, is called the number of (α,α) digit pairs and is denoted by $L_\alpha(\tau)$. Similarly $L_\beta(\tau)$ is the number of (β,β) digit pairs, and $L_{\alpha\beta}(\tau)$ the number of (α,β) digit pairs. Now every α to β transition is matched by a β to α transition, thus $L_{\alpha\beta}(\tau)$ is also the number of (β,α) digit pairs.

As j varies from 1 to V

(i) $p_j\, p_{j-\tau} = \alpha^2$ occurs $L_\alpha(\tau)$ times

(ii) $p_j\, p_{j-\tau} = \beta^2$ occurs $L_\beta(\tau)$ times and

(iii) $p_j\, p_{j-\tau} = \alpha\beta$ occurs $2L_{\alpha\beta}(\tau)$

$$\therefore\ V.\phi_{pp}(\tau) = \alpha^2 L_\alpha(\tau) + \beta^2 L_\beta(\tau) + 2\alpha\beta L_{\alpha\beta}(\tau) \qquad \text{C.4.(6)}$$

Now for all τ

$$L_\alpha(\tau) + L_{\alpha\beta}(\tau) = U$$

$$L_\beta(\tau) + L_{\alpha\beta}(\tau) = V-U$$

Thus since $L_{\alpha\beta}(0) = 0$

then $$V\phi_{pp}(0) = \alpha^2 U + \beta^2(V-U) \qquad \text{C.4.(7)}$$

To apply this notation to C.4.(4) we note that in C.4.(4)

$$\frac{1}{8T}\int_0^{8T} X^*(t-\tau_1)X^*(t-\tau_2)X^*(t-\tau_3)x^*(t-\tau)dt$$

$$= \frac{1}{8T}\int_0^{8T} \overline{[D^{\tau 1}\, X \oplus D^{\tau 2}\, X \oplus D^{\tau 3}\, X \oplus D^{\tau} x]^*}\, dt$$

$$= \frac{1}{8T}\int_0^{8T} \overline{[D^{\tau 1}\, x \oplus D^{\tau 2}\, x \oplus D^{\tau 3}\, x \oplus D^{\tau}\, x \oplus D^{\tau 1}\, p \oplus D^{\tau 2}\, p \oplus D^{\tau 3}\, p]^*}\, dt$$

$$= I$$

where the sequence $X^*(t) = [x(t) \oplus p(t)]^*$

$$\therefore\ I = \frac{1}{8T}\int_0^{8T} [D^{\tau 1}\, x \oplus D^{\tau 2}\, x \oplus D^{\tau 3} \oplus D^{\tau}\, x][D^{\tau 1}\, p \oplus D^{\tau 2} p \oplus D^{\tau 3} p]^* dt$$

C.4.(8)

To establish the necessity of the antisymmetric property in the modifying sequences p(t) for the work of Appendix C.3., we note that since C.4.(4) and C.4.(8) are equivalent, then the latter should be zero everywhere. Thus we can consider the case when $D^{\tau 1}\, x \oplus D^{\tau 2}\, x \oplus D^{\tau 3}\, x \oplus D^{\tau}\, x = 0$,

$$\text{then } I = \frac{1}{8T}\int_0^{8T} [D^{\tau 1} p \oplus D^{\tau 2} p \oplus D^{\tau 3} p]^* dt \qquad \text{C.4.(9)}$$

The equivalent expression for I in summation form is

$$I = \sum_{j=1}^{V} P_j\, P_{j-\mu}\, P_{j-\psi} \qquad \text{C.4.(10)}$$

where $\mu = \tau_2 - \tau_1$, $\psi = \tau_3 - \tau_1$.

We can evaluate C.4.(10) by a similar approach to that used in the earlier example.

Thus as j varies from 1 to V

(i) $p_j\ p_{j-\mu}\ p_{j-\psi} = \alpha^3$ occurs L_α times

(ii) $p_j\ p_{j-\mu}\ p_{j-\psi} = \beta^3$ occurs L_β times

(iii) $p_j\ p_{j-\mu}\ p_{j-\psi} = \alpha^2\beta$ occurs $L_{\alpha\beta\alpha}$ times

(iv) $p_j\ p_{j-\mu}\ p_{j-\psi} = \alpha\beta^2$ occurs $L_{\beta\alpha\beta}$ times

$$\therefore\ I = \alpha^3 L_\alpha(\tau') + \alpha^2\beta L_{\alpha\beta\alpha}(\tau') + \alpha\beta^2 L_{\beta\alpha\beta}(\tau') + \beta^3 L_\beta(\tau')$$

where $\tau' = (\mu+\psi) - j$

For antisymmetric sequences only

$$L_{\beta\alpha\beta} = L_{\alpha\beta\alpha} = L' \qquad \text{C.4.(11)}$$

and

$$U = L_\alpha(\tau') + L'(\tau')$$

$$V-U = L_\beta(\tau') + L'(\tau')$$

We have equal numbers of α's and β's in any one sequence p(t).

$$\therefore\ L_\alpha(\tau') + L'(\tau') = L_\beta(\tau') + L'(\tau') \qquad \text{C.4.(12)}$$

Then if $\beta = -\mu$,

$$I = \alpha^3 L_\alpha(\tau') - \alpha^3 L'(\tau') + \alpha^3 L'(\tau') - \alpha^3 L_\beta(\tau')$$

$$= 0 \text{ for all } \tau' \qquad \text{C.4.(13)}$$

If the sequences p are not antisymmetric, then $L_{\beta\alpha\beta} \neq L_{\alpha\beta\alpha}$ in general. Thus $I \neq 0$ in general and C.4.(4) is non-zero. We thus see that a necessary requirement of the sequence p(t) in Appendix C.3. is that they be antisymmetric.

APPENDIX C.5.

CONTINUOUS UPDATING OF A TIME VARYING SYSTEM USING P.R.B.S.

Consider the case of a system initially in the steady state. Assume also a noise free output (the treatment is extended to systems contaminated with noise at the end of this appendix).

Let the d.c. bias in the correlogram be removed. Consider the case of the maximum ordinate changing by an unknown factor (greater or less than one), at some instant t_2' reduced modulo L. All other ordinates are assumed to change by the same fraction, at the same time. If the departures from the steady state correlogram at τ_i are denoted by the vector $\{\Delta_{xy}(\tau_i, t_2)\}$, where t_2 is measured from the origin of the p.r.b.s., then

$$\{\Delta_{xy}(\tau_i, t_2)\} = \left\{\frac{1}{L} \sum_{r=t_2'}^{t_2} \Delta y_r \, x_{r-\tau_i}\right\} \qquad \text{C.5.(1)}$$

for $i = 0, \rightarrow L-1$.

We may compute values of $L\Delta_{xy}(\tau_i, t_2)$ for all (τ_i, t_2) from the matrix of C.5.(2).

In C.5.(2) note that

Δy_{t_j} = difference of y (at $t_2 = t_j$) from the previous steady state value; and that in this case we have set $t_2' = 0 (\text{mod } L)$, this does not affect the generality of the technique.

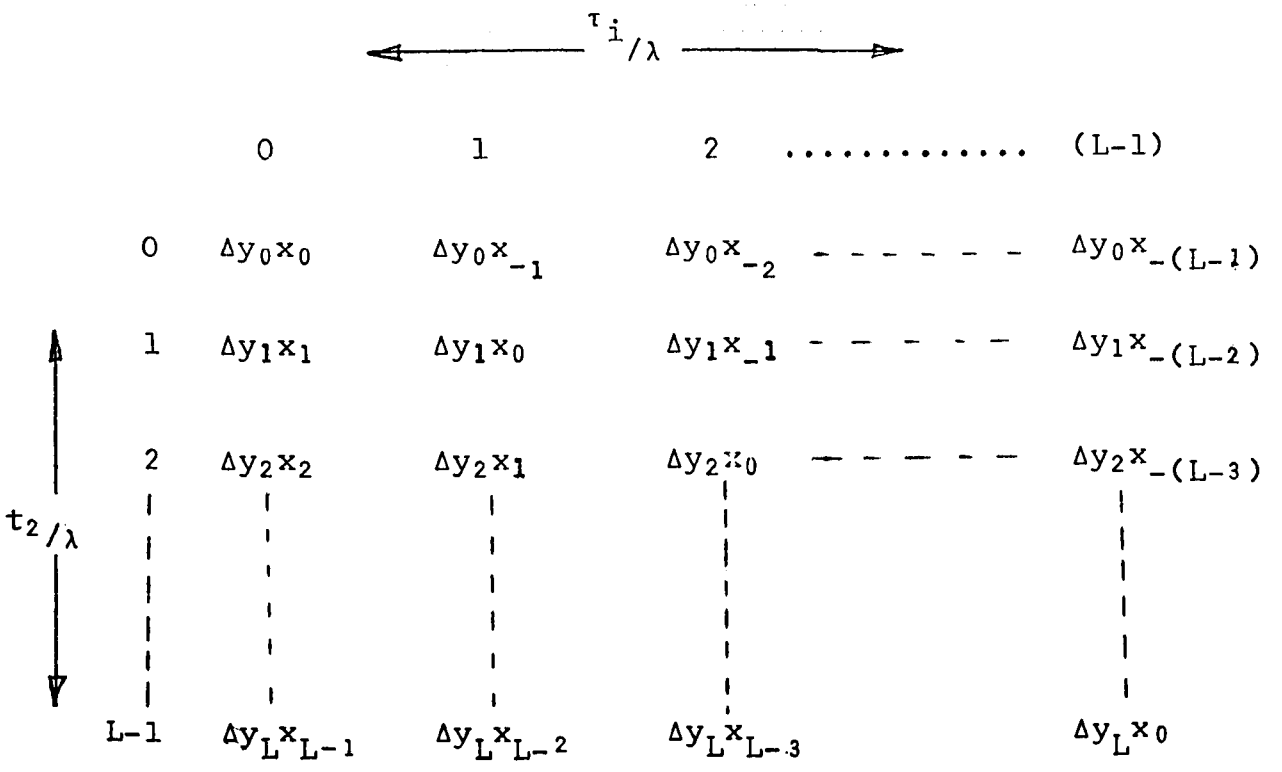

C.5.(2)

One row (t_2=const.) of C.5.(2) can be expressed as the vector

$$\left\{U_{xy}(\tau_i,t_2)\right\} = \left\{\Delta y_{t_2} x_{t_2-\tau_i}\right\} \qquad \text{for } i = 0,\rightarrow L-1$$

$$\text{then} \quad \left\{\Delta_{xy}(\tau_i,t_2)\right\} = \left\{\frac{1}{L}\sum_{t_j=t_2'}^{t_2} \Delta y_{t_j}\, x_{t_j-\tau_i}\right\} \quad \text{for } i = 0,\rightarrow L-1$$

C.5.(3)

If h_s' is $h(\tau)$ obtained using p.r.b.s. at $\tau=s\lambda$ with the d.c. bias removed

$$\text{then} \quad \Delta y_r = \sum_{s=0}^{L-1} \Delta h_s' \, x_{r-s\lambda} \qquad \text{C.5.(4)}$$

Expressing the change in impulse response as a set of ordinates W_i then

$$\Delta y_r = \sum_{i=0}^{L-1} W_i x_{r-i\lambda} \qquad \text{C.5.(5)}$$

$$\therefore \quad \left\{U_{xy}(\tau_i, t_2)\right\} = \left\{\left(\sum_{k=0}^{L-1} W_k x_{t_2-k\lambda}\right) x_{t_2-\tau_1}\right\}$$

for i = 0, L-1 C.5.(6)

From C.5.(3) and C.5.(6)

$$\left\{\Delta xy(\tau_i, t_2)\right\} = \frac{1}{L}\left\{\left(\sum_{k=0}^{L-1} W_k x_{t_2-k\lambda}\right) \cdot x_{t_2-\tau_i}\right\} + \left\{\Delta xy(\tau_i, t_2-\lambda)\right\}$$

for i = 0,L-1 C.5.(7)

Consider the case for L=15, let all impulse response ordinates change by a fraction γ at a time t_2'.

If initially, (i.e. before the change),

$h_0' = 1$, $h_1' = 3$, $h_2' = 2$, $h_3' \rightarrow h_{14}'$ inclusive $= 0$, then

$$\left\{U_{xy}(\tau_i, t_2)\right\} = \left\{\gamma\left[h_0' x_{t_2} + h_1' x_{t_2-\lambda} + h_2' x_{t_2-2\lambda}\right] x_{t_2-\tau_i}\right\}$$

for i = 0 → L-1 C.5.(8)

Note that C.5.(8) is the product of the column vector $\left\{h_0' x_{t_2} + h_1' x_{t_2-\lambda} + h_2' x_{t_2-2\lambda}\right\}$ a row vector $\left\{x_{t_2-\tau_i}\right\}$, and an unknown scalar γ. The column vector can be expressed as :-

	0	γ	-1	$+3\gamma$	1	$+2\gamma$	-1	$=\gamma$	0			
	1		-1		-1		1		-2			
	2		1		-1		-1		-4			
	3		1		1		-1		2			
	4		-1		1		1		4			
	5		1		-1		1		0			
	6		-1		1		-1		0			
t_2/λ	7		1		-1		1		0			C.5.(9)
	8		1		1		-1		2			
	9		1		1		1		6			
	10		1		1		1		6			
	11		-1		1		1		4			
	12		-1		-1		1		-2			
	13		-1		-1		-1		-6			
	14		1		-1		-1		-4			

Using C.5.(9) and C.5.(8), the departures from the steady state correlation function at instants t_2, can be calculated in terms of γ for all shifts τ_i.

The departures can be calculated from the values of $\{U_{xy}(\tau_i, t_2)\}$ shown in Fig. 21 (for L=15, γ=1, and the column vector of C.5.(9)), by use of C.5.(7).

Also shown are the respective column totals at values of τ_j, of the equivalent to the matrix of C.5.(2). The original disturbance occurs after $t_2 = 4\lambda$ and before $t_2 = 5\lambda$. The column

totals are evaluated one period later at $t_2 = \lambda \times 19 (\text{mod } 15) = 5\lambda$. Hence the vector of column totals is the overall change from the initial to the new steady state for a change $\gamma = 1$, in impulse response ordinates.

Removing the bias from the column totals and dividing by (L+1) we get the vector {1,3,?,0,0,0,0,0,0,0,0,0,0,0,0,}, which for $\gamma = 1$ is what we would expect. The column totals could be calculated at intermediate values of t_2 to give solutions of C.5.(7).

In practice changes γ will not always be unity. To obtain estimates of γ at instants t_2 before the correlogram settles at the new steady state (one period after the change), the following calculation is made :-

$$\hat{\gamma} = \frac{\phi_{xy}(\tau_1, t_2) - \phi_{xy}(\tau_1, t_2-\lambda)}{\Delta_{xy}(\tau_1, t_2) - \Delta_{xy}(\tau_1, t_2-\lambda)} \qquad \text{C.5.(10)}$$

This procedure is indeterminate whenever the denominator is zero, as occurs in Fig. 21 for the first three rows of the matrix. This results from the presence of zeroes in the column vector of C.5.(9). In general, solution of C.5.(10) gives a reliable estimate of γ at the first sampling instant after the first change in output has occurred. From the knowledge of the previous state and $\hat{\gamma}$, extrapolation to the new steady state is possible.

To estimate γ in a noisy environment, the average

of a number of estimations at various t_2 may be taken. Alternatively, if we wish to track a continuously varying impulse response, several output samples can be logged at one t_2 and averaged. $\hat{\gamma}$ may be calculated at each t_2, and extrapolation to the new 'equivalent' steady state is possible if the last 'equivalent' steady state is known.

7. REFERENCES

1. Gardiner, A.B., Elimination of the Effect of Non-Linearities on Process Crosscorrelations, Electronics Letters, May 1966, Vol.2, No.5, pp 164-165.

2. Brown, R.F., Goodwin,G.C., Simplified Method of Eliminating the Effect of Non-Linearities on Process Crosscorrelations, Electronics Letters, Dec.1966, Vol.2, No.12, pp 453-454.

3. Godfrey, K.R., Three Level m Sequences, Electronics Letters, July 1966, Vol.2, No.7, pp 241-243.

4. Gyftopoulos, E.P., Hooper, R.J., 'Signals for Transfer Function Measurements in Non-Linear Systems'. Proc. of Symposium, (Noise Analysis in Nuclear Systems) at Univ. of Florida 4-6 Nov.1964, U.S.Atomic Energy Commission, Report TID - 7679.

5. Godfrey, K.R., Devenish, M., An Experimental Investigation of Continuous Gas Chromatography using Pseudo-Random Binary Sequences, Measurement and Control,1969, 2, pp 228-233.

6. Simpson, H.R., Statistical Properties of a Class of Pseudo-Random Sequences, Proc. I.E.E., Vol.113, No.12, Dec.1966.

7. Briggs, P.A.N., Godfrey, K.R., Pseudo-Random Signals For the Dynamic Analysis of Multivariable Systems, Proc. I.E.E., Vol.113, No.7, July 1966, pp 1259-1267.

8. Schmauch, L.J., Dinnerstein, R.A., Response of Thermal Conductivity Cells in Gas Chromatography, Anal.Chem., Vol.32, No.3, March 1960.

9. Brauer, A., On a New Class of Hadamard Determinants, Math.Zeit., 1953, 58, p 219.

10. Davies, W.D.T., The Use of Chain Codes in On-Line Process Chromatography. Inst. Practice, March 1968.

11. Dack, D., System Identification by On-Line Correlation, Control Engineering, March 1970, Vol.17, No.3.

12. Bell, D.A., Walsh Functions and Hadamard Matrices, Electronics Letters, Sept.1966, Vol.2, No.9, p 340.

13. Schmauch, L.J., Dinnerstein, R.A., Response of Thermal Conductivity Cells in Gas Chromatography, Anal. Chem., Vol.32, No.3, March 1960.

8. ILLUSTRATIONS FOR CHAPTER 3

Fig.1 System with Non-Linear Output Transducer

Fig.2 The Detection of Hydrogen with Helium Carrier.

Fig.3. Pulse Response of Simulated Hydrogen Detection System with Helium Carrier.

Fig.4 Impulse Sign and Coordinates (τ_1,τ_2) in $h(\tau_1)h(\tau_2)$ products For L = 31.

Fig.5 Removal of the Effect of Non-Linearities for Hydrogen Detection with Helium Carrier (Simulated).

Fig.6 The Detection of Acetylene with Nitrogen Carrier.

Fig.7 Pulse Response of Simulated Acetylene Detection System with Nitrogen Carrier.

Fig.8 Removal of the Effect of Non-Linearities For Acetylene Detection with Nitrogen Carrier(Simulated).

Fig.9 Conventional Injection of Hydrocarbon Mixture (b).

Fig.10. Multi Sample Analysis Using Hydrocarbon Sample.

Fig.11(a) } Updating a Correlogram after an
Fig.11(b) } Increase in Gain.

Fig.12 Updating of Impulse Response After a Decrease in Gain.

Fig.13 Nitrogen Analysis Using Digital Correlator.

Fig.14 Multi-Sample Analysis Using Digital Correlator.

Fig.15 Solutions τ_3/λ of $D^{\tau 1}\, x \oplus D^{\tau 2}\, x \oplus D^{\tau}\, x = D^{\tau 3}\, x$

Fig.16 for $\tau = 0$ and $\tau = \lambda$.

Fig.17 Register Connections For a Given Delay.

Fig.18 Matrix Constructed From L of (L+1) Rows of Solutions τ_3/λ to $D^{\tau 1}\, x \oplus D^{\tau 2}\, x \oplus D^{\tau}\, x = D^{\tau 3}\, x$ So That Blanks Lie on Main Diagonal.

Fig.19 Autocorrelation Function Of Modifying Sequences.

Fig.20 Solutions τ_2/λ of $D^{\tau 1} x \oplus D^{\tau} x = D^{\tau 2} x$ For L=31.

Fig.21 Departures From Steady State Correlogram After Change $\gamma = 1$

SYSTEM WITH NON-LINEAR OUTPUT TRANSDUCER

FIG. 1

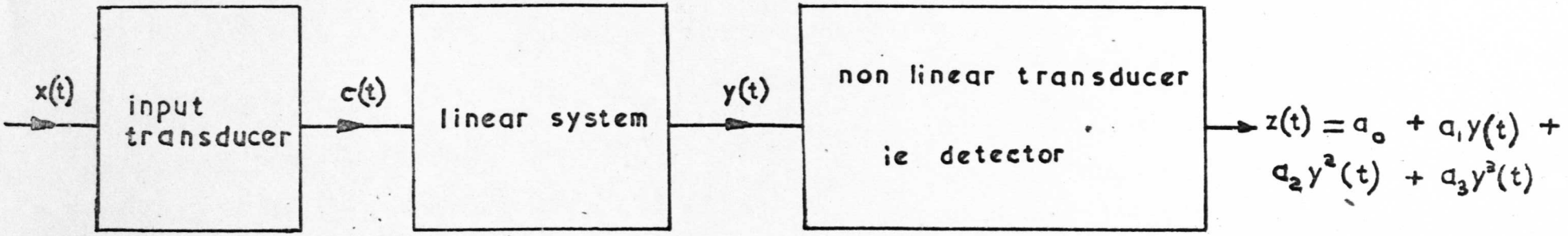

THE DETECTION OF HYDROGEN WITH HELIUM CARRIER.

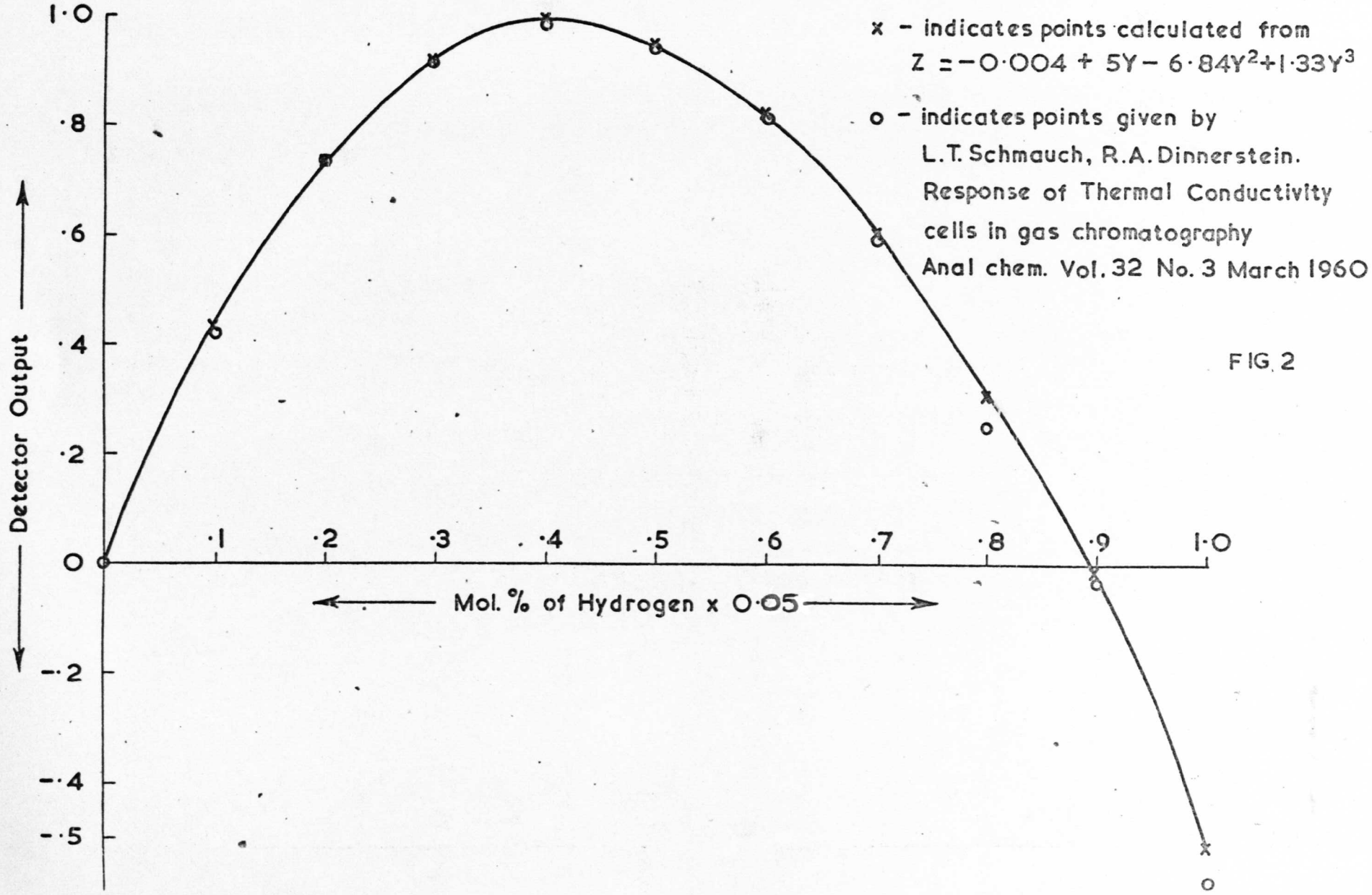

x - indicates points calculated from
$Z = -0{\cdot}004 + 5Y - 6{\cdot}84Y^2 + 1{\cdot}33Y^3$

o - indicates points given by
L.T. Schmauch, R.A. Dinnerstein.
Response of Thermal Conductivity
cells in gas chromatography
Anal chem. Vol. 32 No. 3 March 1960

FIG. 2

PULSE RESPONSE OF SIMULATED HYDROGEN DETECTION SYSTEM WITH HELIUM CARRIER.

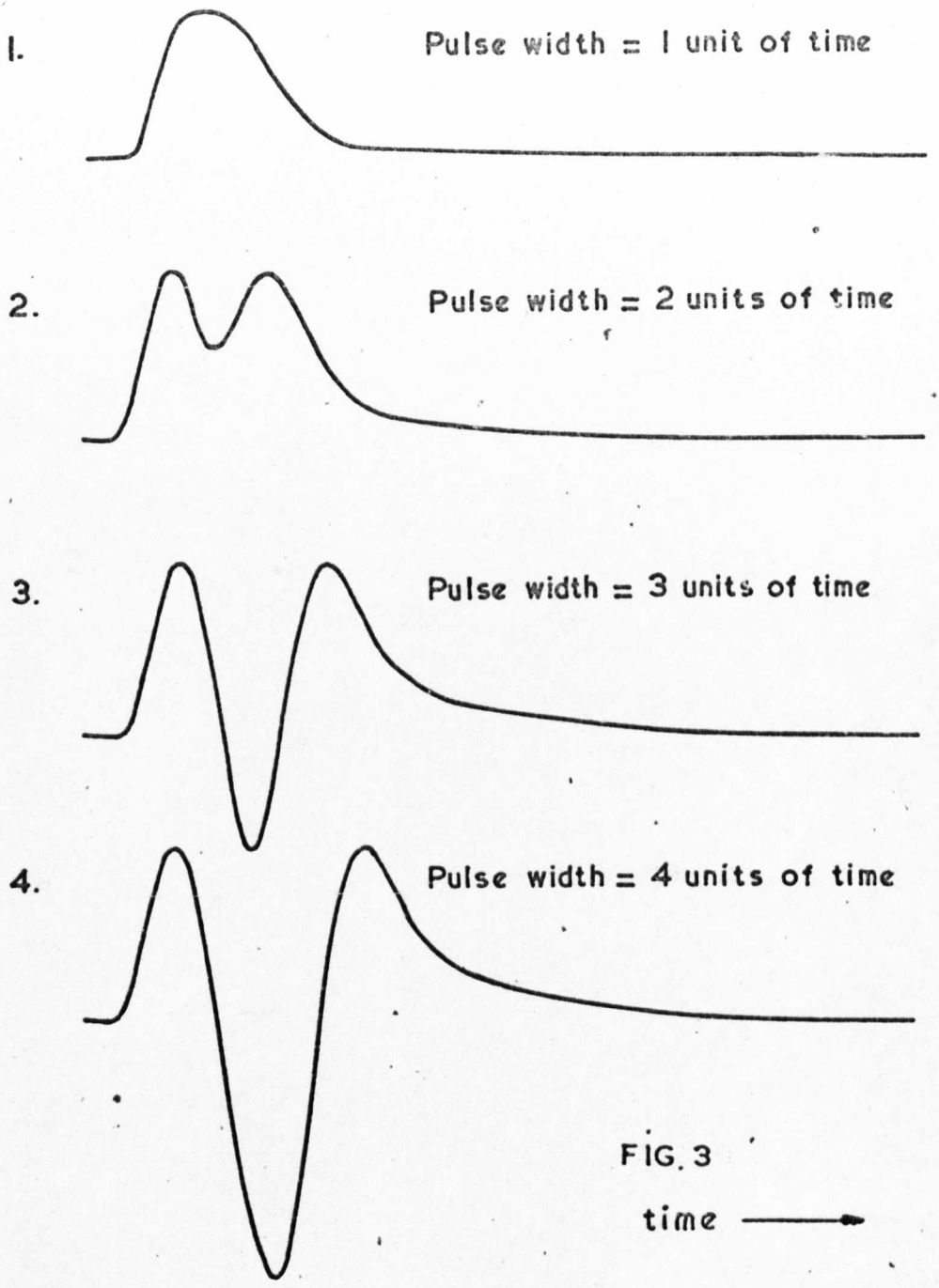

FIG. 3

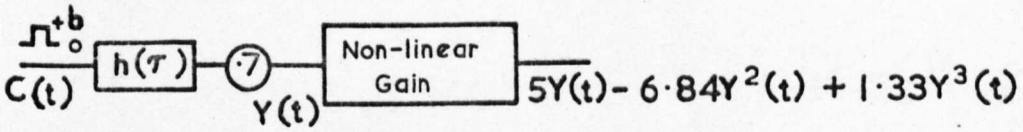

C(t) is pulse input +b to O

FIG. 4.

IMPULSE SIGN AND COORDINATES (τ_1,τ_2) IN $h(\tau_1)\,h(\tau_2)$ PRODUCTS FOR L = 31

0	-1,14	4,25	7,16	-8,19	9,24		15,22	17,18	13,30	-26,29	-6,10	-11,23	12,20		
1	-2,15	5,26	8,17	-9,20	10,25		16,23	18,19		-27,30	-7,11	-12,24	13,21		
2	-3,16	6,27	9,18	-10,21	11,26		17,24	19,20			-8,12	-13,25	14,22		-0,28
3	-4,17	7,28	10,19	-11,22	12,27	-0,5	18,25	20,21			-9,13	-14,26	15,23		-1,29
4	-5,18	8,29	11,20	-12,23	13,28	-1,6	19,26	21,22	0,25		-10,14	-15,27	16,24		-2,30
5	-6,19	9,30	12,21	-13,24	14,29	-2,7	20,27	22,23	1,26	-0,3	-11,15	-16,28	17,25		
6	-7,20		13,22	-14,25	15,30	-3,8	21,28	23,24	2,27	-1,4	-12,16	-17,29	18,26		
7	-8,21		14,23	-15,26		-4,9	22,29	24,25	3,28	-2,5	-13,17	-18,30	19,27	0,16	
8	-9,22		15,24	-16,27	-0,19	-5,10	23,30	25,26	4,29	-3,6	-14,18		20,28	1,17	
9	-10,23		16,25	-17,28	-1,20	-6,11		26,27	5,30	-4,7	-15,19	0,24	21,24	2,18	
10	-11,24		17,26	-18,29	-2,21	-7,12		27,28		-5,8	-16,20	1,25	22,30	3,19	
11	-12,25	0,23	18,27	-19,30	-3,22	-8,13		28,29		-6,9	-17,21	2,26		4,20	
12	-13,26	1,24	19,28		-4,23	-9,14		29,30		-7,10	-18,22	3,27		5,21	-0,20
13	-14,27	2,25	20,29		-5,24	-10,15				-8,11	-19,23	4,28		6,22	-1,21
14	-15,28	3,26	21,30		-6,25	-11,16		0,1		-9,12	-20,24	5,29		7,23	-2,22
15	-16,29	4,27			-7,26	-12,17		1,2		-10,13	-21,25	6,30		8,24	-3,23
16	-17,30	5,28			-8,27	-13,18	0,7	2,3		-11,14	-22,26			9,25	-4,24
17		6,29			-9,28	-14,19	1,8	3,4		-12,15	-23,27			10,26	-5,25
18		7,30			-10,29	-15,20	2,9	4,5	0,17	-13,16	-24,28			11,27	-6,26
19					-11,30	-16,21	3,10	5,6	1,18	-14,17	-25,29		0,8	12,28	-7,27
20						-17,22	4,11	6,7	2,19	-15,18	-26,30	-0,12	1,9	13,29	-8,28
21	-0,27					-18,23	5,12	7,8	3,20	-16,19		-1,13	2,10	14,30	-9,29
22	-1,28				0,15	-19,24	6,13	8,9	4,21	-17,20		-2,14	3,11		-10,30
23	-2,29			-0,11	1,16	-20,25	7,14	9,10	5,22	-18,21		-3,15	4,12		
24	-3,30		0,9	-1,12	2,17	-21,26	8,15	10,11	6,23	-19,22		-4,16	5,13		
25			1,10	-2,13	3,18	-22,27	9,16	11,12	7,24	-20,23	-0,4	-5,17	6,14		
26	-0,29		2,11	-3,14	4,19	-23,28	10,17	12,13	8,25	-21,24	-1,5	-6,18	7,15		
27	-1,30	-0,21	3,12	-4,15	5,20	-24,29	11,18	13,14	9,26	-22,25	-2,6	-7,19	8,16		
28		-1,22	4,13	-5,16	6,21	-25,30	12,19	14,15	10,27	-23,26	-3,7	-8,20	9,17		
29		-2,23	5,14	-6,17	7,22		13,20	15,16	11,28	-24,27	-4,8	-9,21	10,18		
30	-0,13	-3,24	6,15	-7,18	8,23		14,21	16,17	12,29	-25,28	-5,9	-10,22	11,19		

IMPULSE HEIGHT = 0.5 | IMPULSE HEIGHT = 1.0

N.B. Magnitude of contribution for each (τ_1,τ_2) pair is 2 x impulse height x $h(\tau_1)h(\tau_2)$

N.B. $D^0x(t) = D^3x(t) \oplus D^5x(t)$

REMOVAL OF THE EFFECT OF NON-LINEARITIES FOR HYDROGEN DETECTION WITH HELIUM CARRIER (SIMULATED).

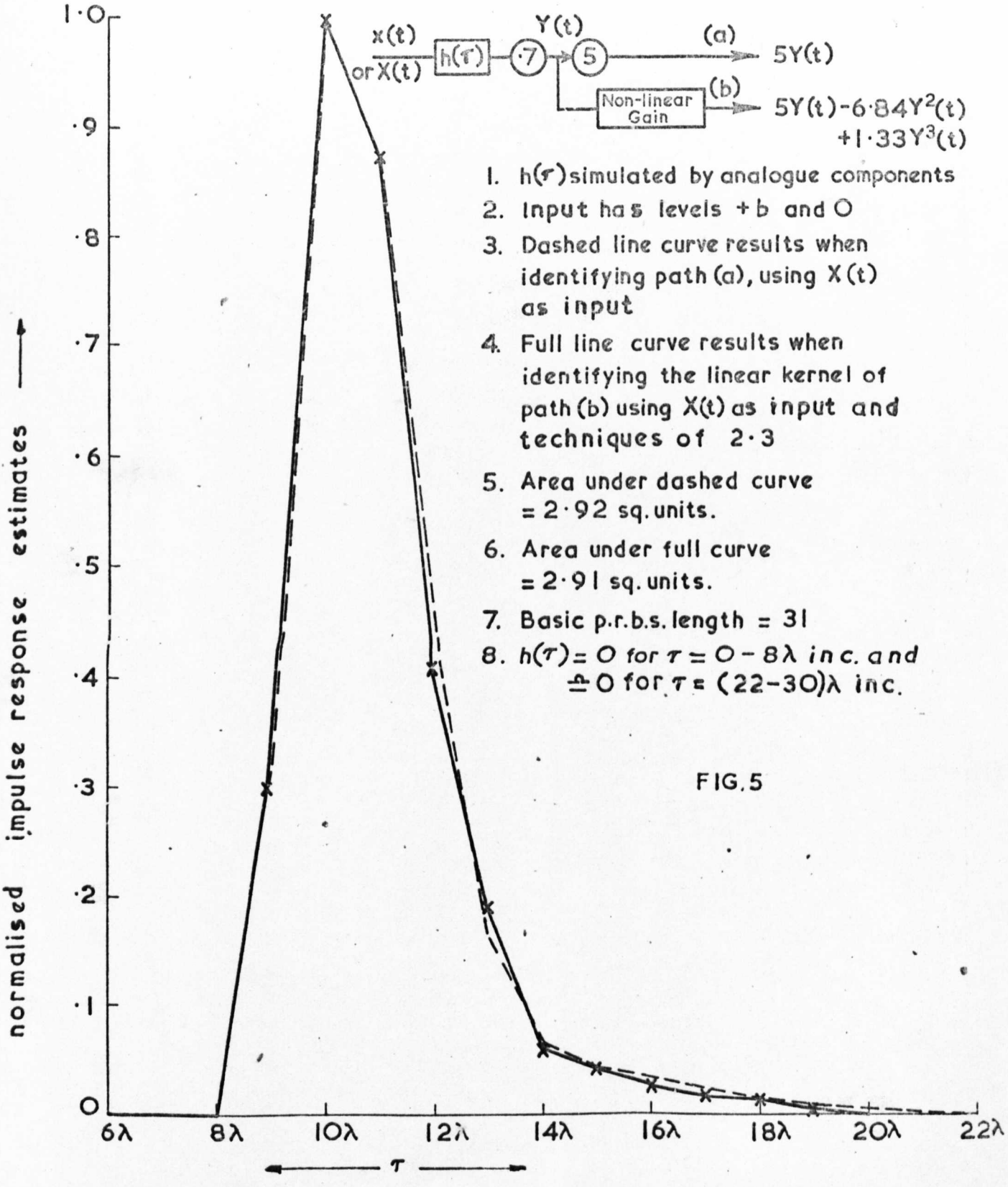

FIG. 5

THE DETECTION OF ACETYLENE WITH NITROGEN CARRIER

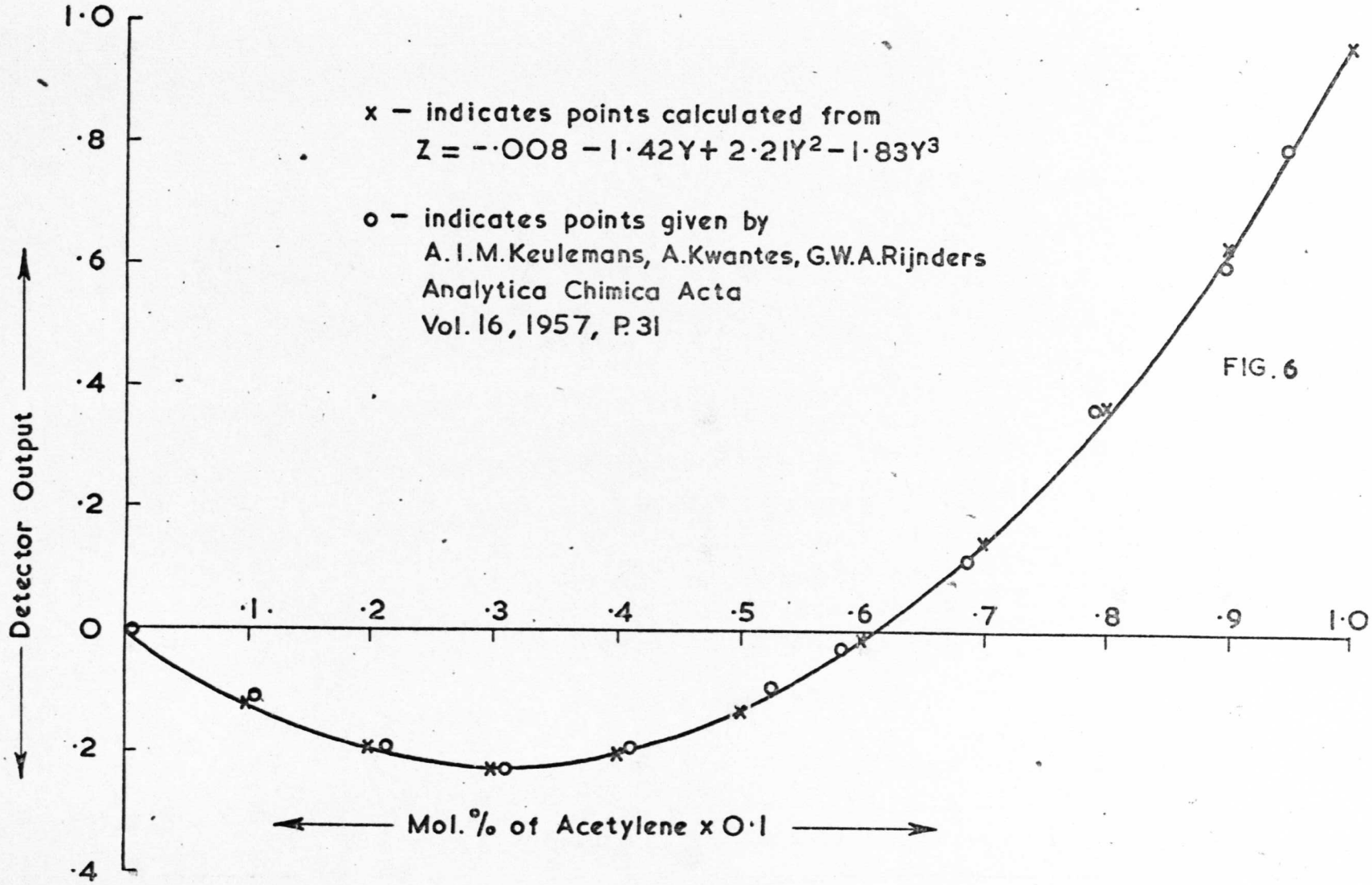

FIG. 6

PULSE RESPONSE OF SIMULATED ACETYLENE DETECTION SYSTEM WITH NITROGEN CARRIER

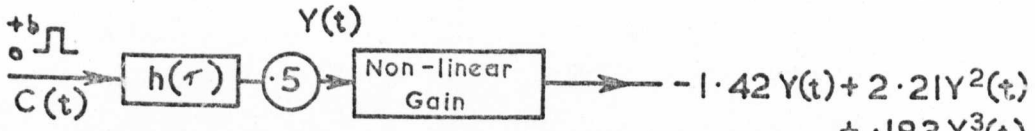

C(t) is pulse input + b, O.

FIG. 7

Pulse width = 5 units of time

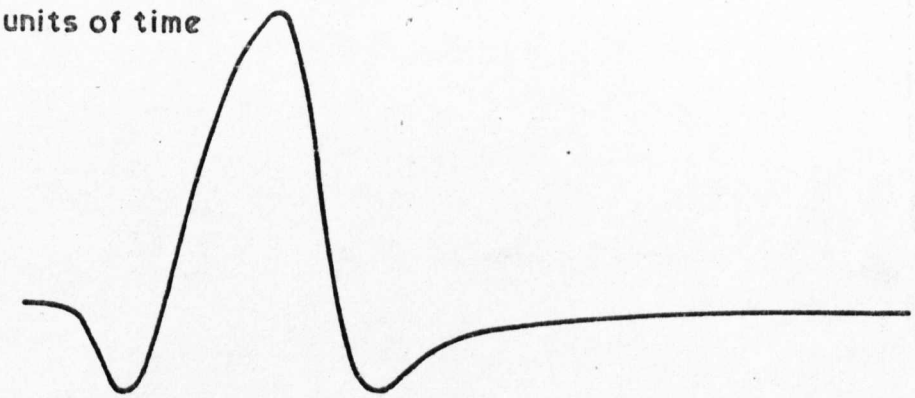

Pulse width = 3 units of time

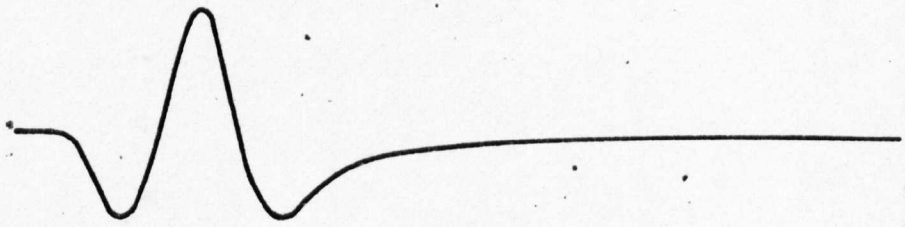

Pulse width = 1 unit of time

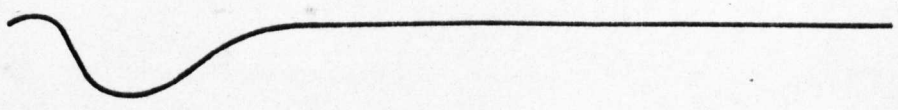

time →

REMOVAL OF THE EFFECT OF NON-LINEARITIES FOR ACETYLENE DETECTION WITH NITROGEN CARRIER (SIMULATED)

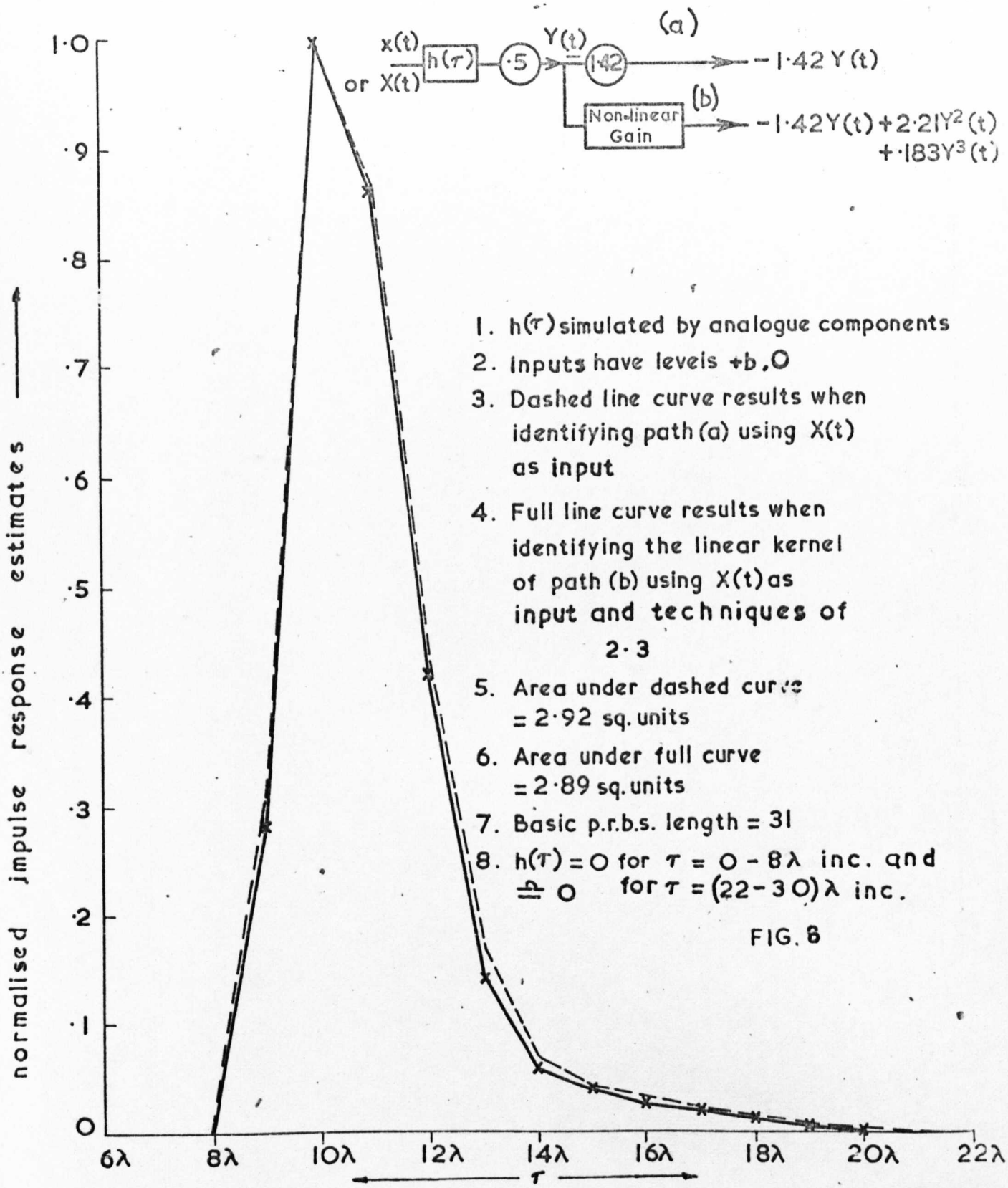

FIG. 8

CONVENTIONAL INJECTION OF HYDROCARBON MIXTURE (b)

CARRIER = HELIUM (IMPURE)
FLOW RATE = 1/6 ml/SEC.
TEMPERATURE = 30°C
SLIDER VOLUME = 10μl
FILTER IN
Y SENSITIVITY = ·5 VOLT/cm
X SENSITIVITY = 5 SECS/cm
INJECTION TIME = ·64 SEC.
BRIDGE VOLTAGE SUPPLY = 7·0 VOLTS
AMPLIFIER GAIN = 10^4

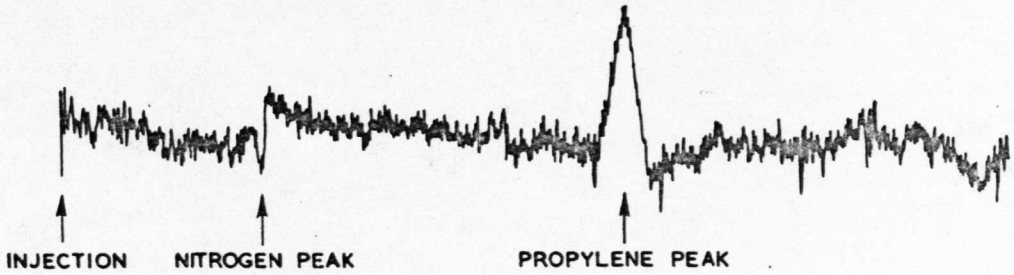

FIG. 9

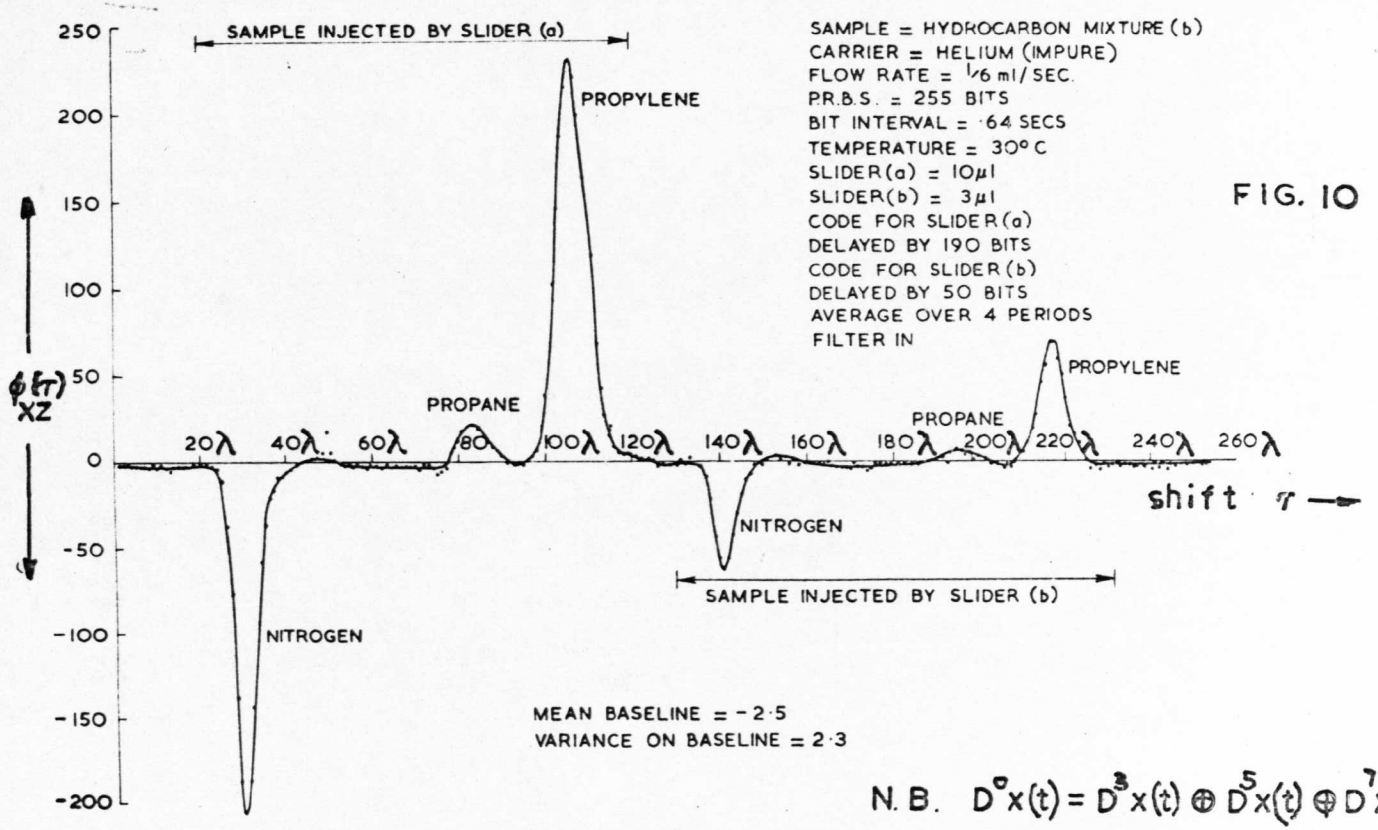

FIG. 10

N.B. $D^0x(t) = D^3x(t) \oplus D^5x(t) \oplus D^7x(t) \oplus D^8x(t)$.

FIG. 11a UPDATING A CORRELOGRAM AFTER AN INCREASE IN GAIN

Gain = 0·6, Correlogram shown below output after steady state reached.

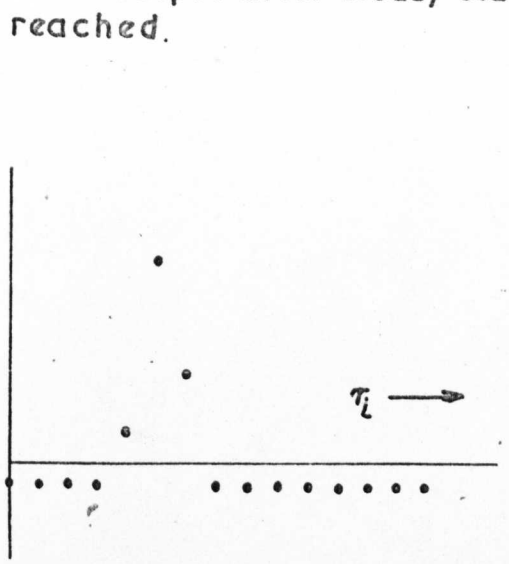

$\phi_{xy}(\tau_i, 0)$

Gain changed to 1·2 during next Bit. Correlogram shown below output at next sampling instant. after using compensation procedure.

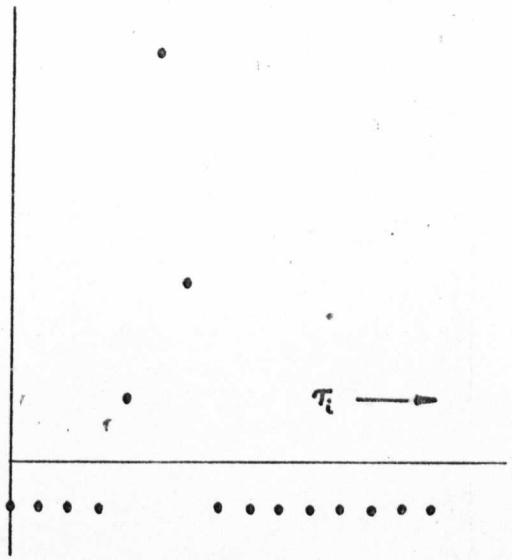

CCF (τ_i, λ)

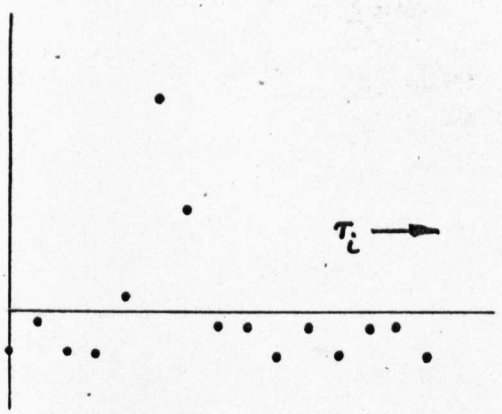

$\phi_{xy}(\tau_i, 1\lambda)$ - No Compensation

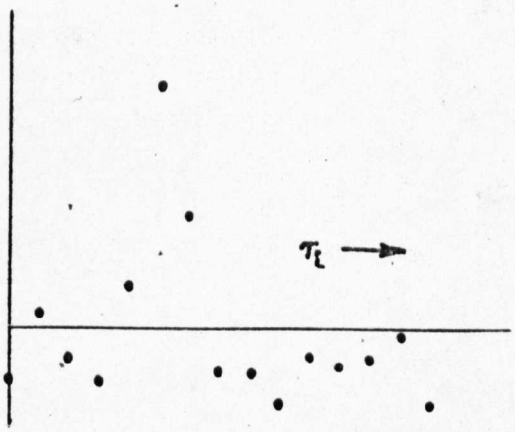

$\phi_{xy}(\tau_i, 3\lambda)$ No Compensation

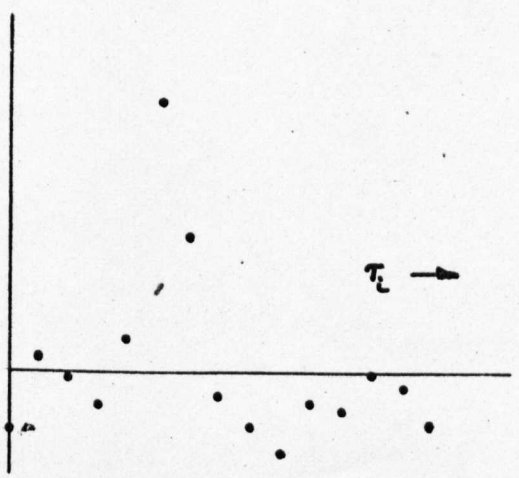

$\phi_{xy}(\tau_i, 5\lambda)$ - No Compensation

$\phi_{xy}(\tau_i, 7\lambda)$ No Compensation

FIG 11b UPDATING A CORRELOGRAM AFTER AN INCREASE IN GAIN (cont)

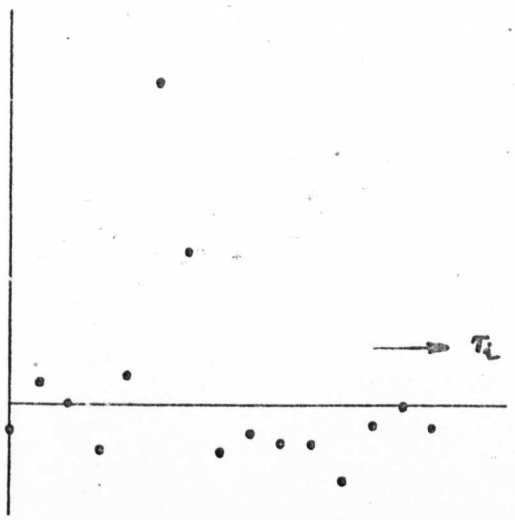

$\phi_{xy}(\tau_i, 9\lambda)$ - No Compensation

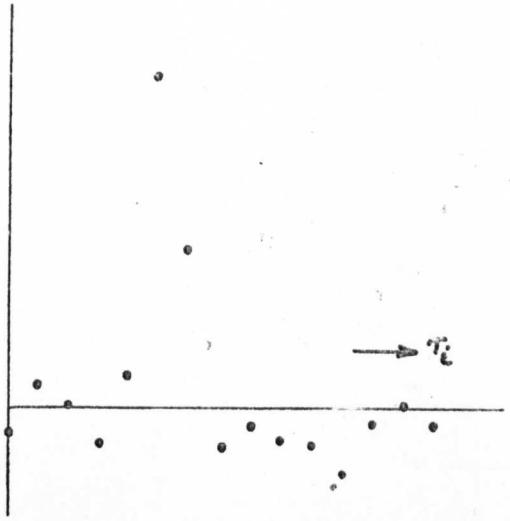

$\phi_{xy}(\tau_i, 11\lambda)$ No Compensation

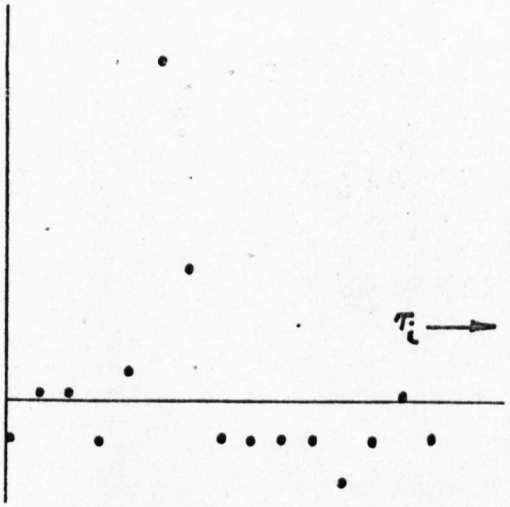

$\phi_{xy}(\tau_i, 13\lambda)$ - No Compensation

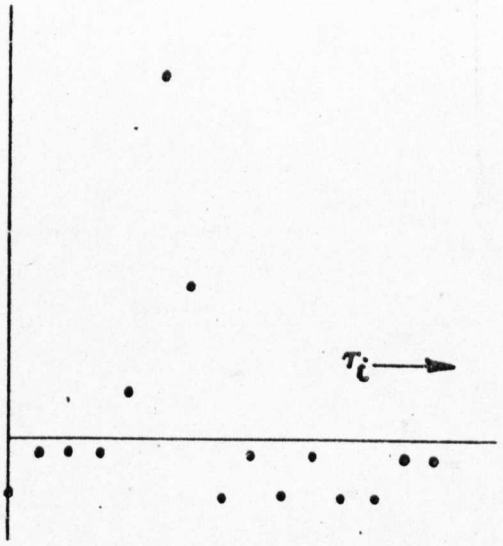

$\phi_{xy}(\tau_i, 14\lambda)$ - No Compensation

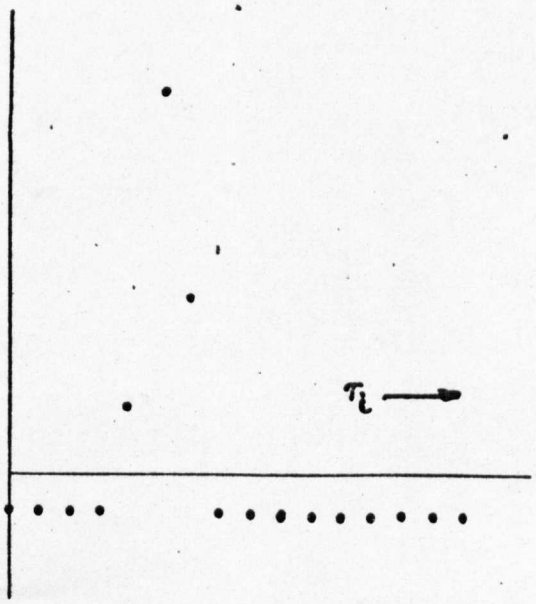

Correlation in new steady state

$\phi_{xy}(\tau_i, 15\lambda)$ - No Compensation

Gain changed from 1·2 to 0·6 one Bit after steady state. reached. The Correlogram shown below was output at the next sampling instant, after using compensation procedure.

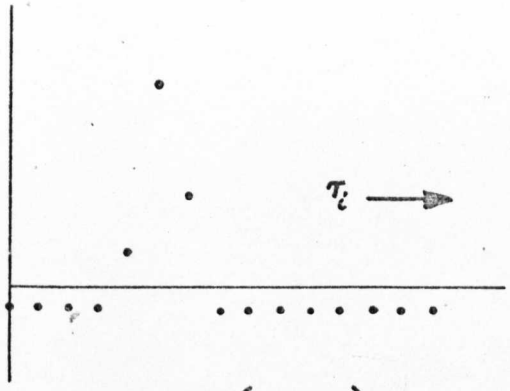

C.C.F $(\tau_i, 17\lambda)$

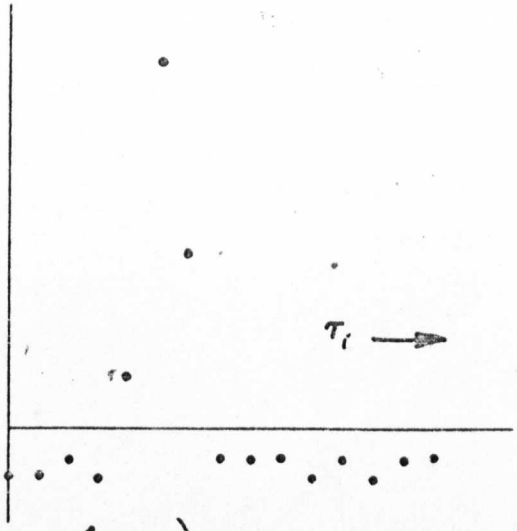

$\phi_{xy}(\tau_i, 17\lambda)$ No Compensation

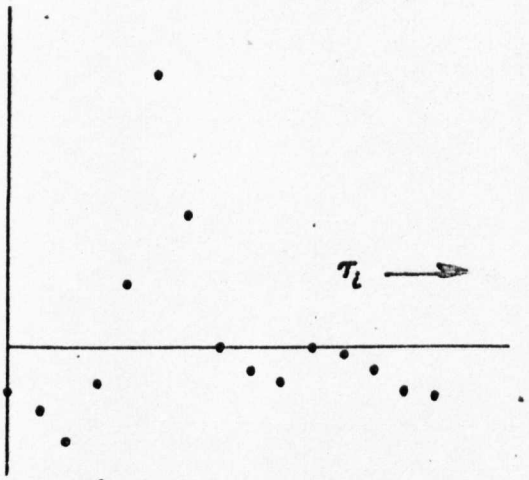

$\phi_{xy}(\tau_i, 26\lambda)$ No Compensation

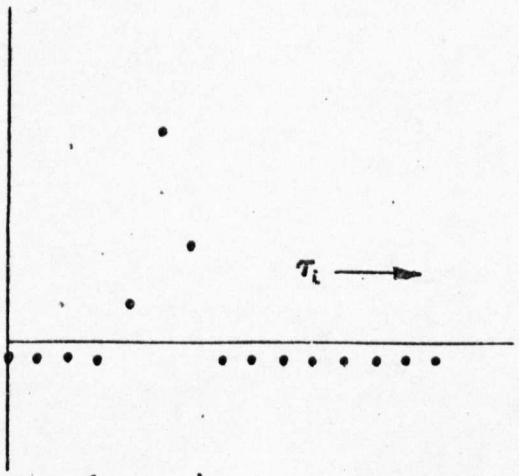

$\phi_{xy}(\tau_i, 30\lambda)$ No Compensation
Correlation in new steady state.

FIG. 12. UPDATING A CORRELOGRAM AFTER A DECREASE IN GAIN

NITROGEN ANALYSIS USING DIGITAL CORRELATOR

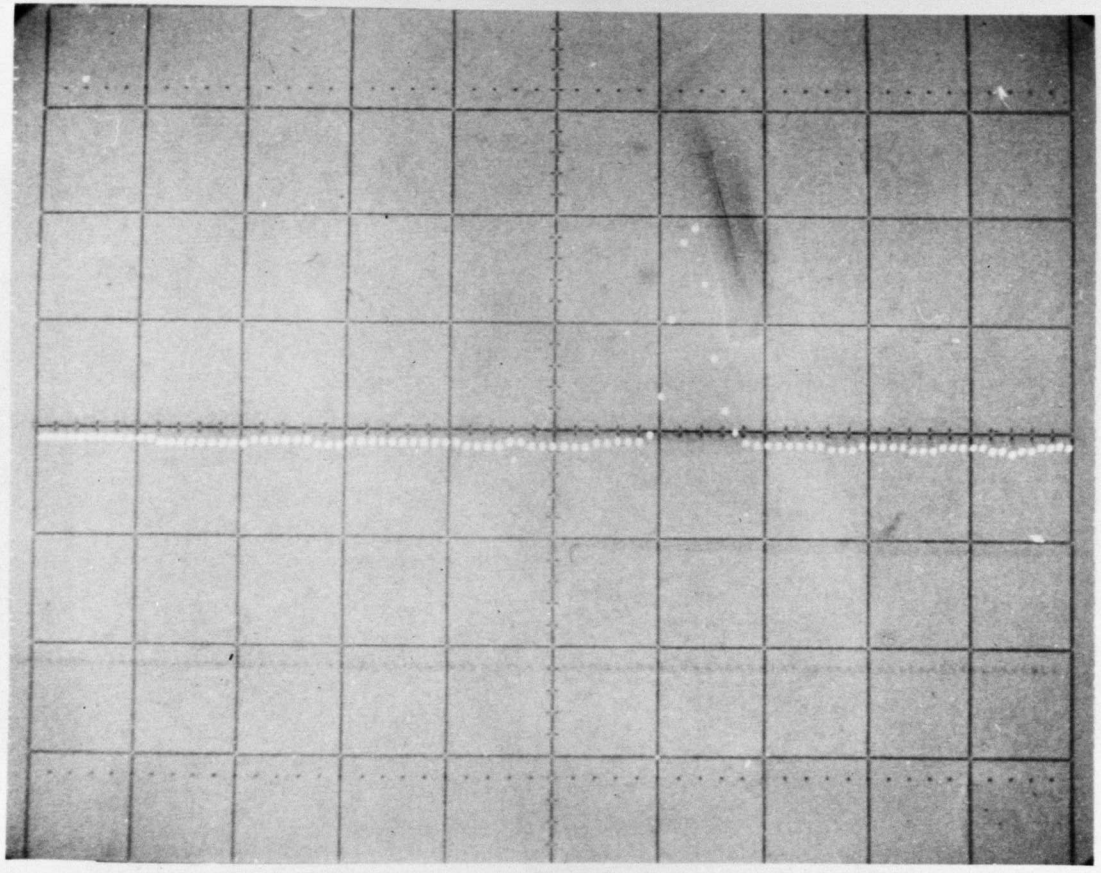

FIG. 13

MULTI—SAMPLE ANALYSIS USING DIGITAL CORRELATOR

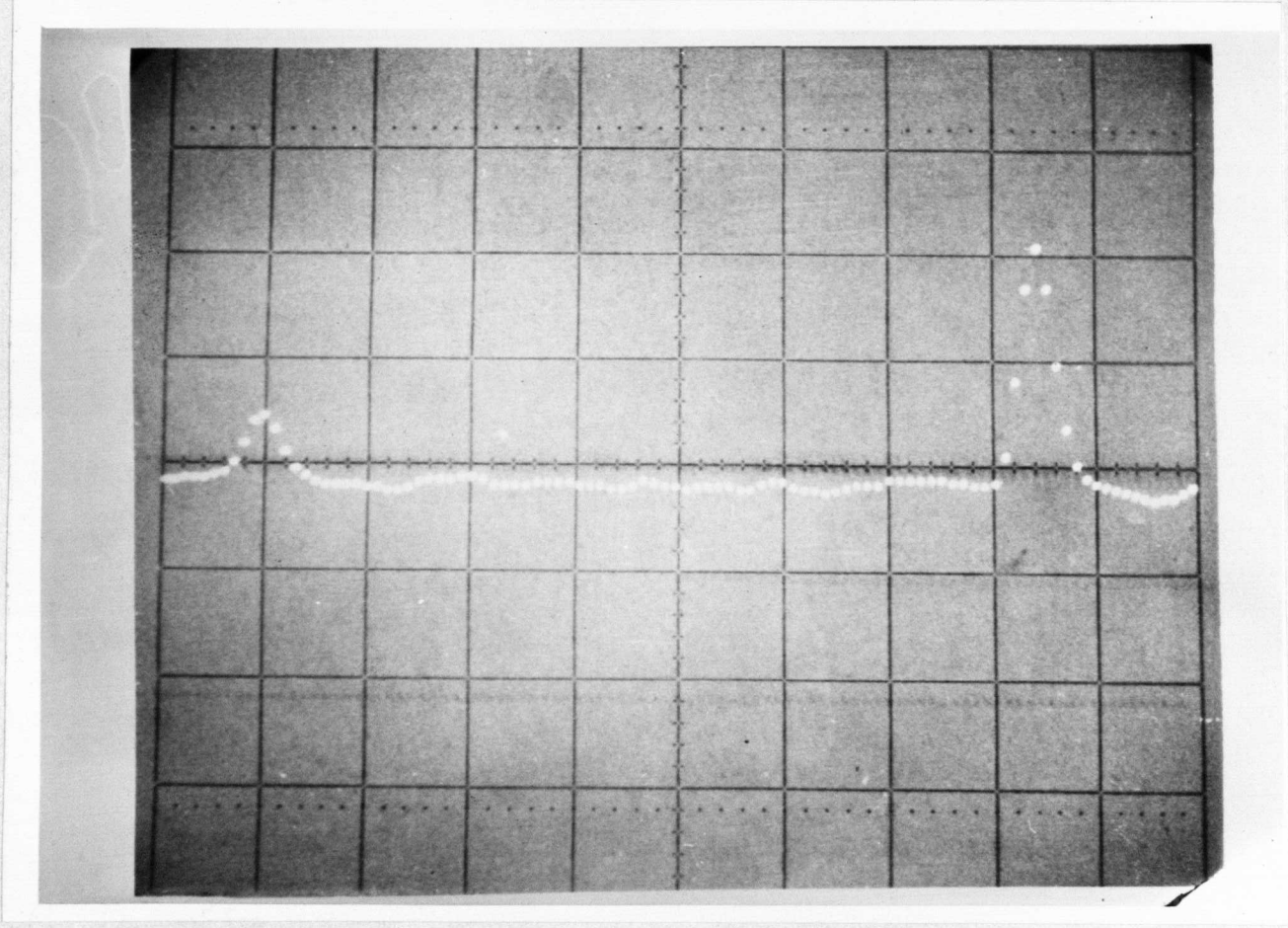

FIG. 14

FIG. 15

$\tau = 0$

$L = 15$

τ_2/λ \ τ_1/λ	0	1	2	3	4	5	6	7	8	9	10	11	12	13	14
0	0	1	2	3	4	5	6	7	8	9	10	11	12	13	14
1	1	0	7	-5	-10	-3	-14	2	11	-13	-4	8		-9	-6
2	2	7	0	11	14	-8	10	1	-5		6	3	-13	-12	4
3	3	-5	11	0		-1	13	8	7	14	-12	2	-10	6	9
4	4	-10	14		0	-12	-7	-6	-13	11	-1	9	-5	-8	2
5	5	-3	-8	-1	-12	0	9	-11	-2	6		-7	-4	14	13
6	6	-14	10	13	-7	9	0	-4		5	2	-12	-11	3	-1
7	7	2	1	8	-6	-11	-4	0	3	12	-14	-5	9		-10
8	8	11	-5	7	-13	-2		3	0	-10	-9	1	14	-4	12
9	9	-13		14	11	6	5	12	-10	0	-8	4	7	-1	3
10	10	-4	6	-12	-1		2	-14	-9	-8	0	13	-3	11	-7
11	11	8	3	2	9	-7	-12	-5	1	4	13	0	-6	10	
12	12		-13	-10	-5	-4	-11	9	14	7	-3	-6	0	-2	8
13	13	-9	-12	6	-8	14	3		-4	-1	11	10	-2	0	5
14	14	-6	4	9	2	13	-1	-10	12	3	-7		8	5	0

FIG. 16

$\tau = 1\lambda$

$L = 15$

τ_2/λ \ τ_1/λ	0	1	2	3	4	5	6	7	8	9	10	11	12	13	14
0	1	0	7	-5	-10	-3	-14	2	11	-13	-4	8		-9	-6
1	0	1	2	3	4	5	6	7	8	9	10	11	12	13	14
2	7	2	1	8	-6	-11	-4	0	3	12	-14	-5	9		-10
3	-5	3	8	1	12	-0	-9	11	2	-6		7	4	-14	-13
4	-10	4	-6	12	1		-2	14	9	8	-0	-13	3	-11	7
5	-3	5	-11	-0		1	-13	-8	-7	-14	12	-2	10	-6	-9
6	-14	6	-4	-9	-2	-13	1	10	-12	-3	7		-8	-5	-0
7	2	7	0	11	14	-8	10	1	-5		6	3	-13	-12	4
8	11	8	3	2	9	-7	-12	-5	1	4	13	0	-6	10	
9	-13	9	12	-6	8	-14	-3		4	1	-11	-10	2	-0	-5
10	-4	10	-14		-0	12	7	6	13	-11	-1	-9	5	8	-2
11	8	1	-5	7	-13	-2		3	0	-10	-9	1	14	-4	12
12		12	9	4	3	10	-8	-13	-6	2	5	14	1	-7	11
13	-9	13		-14	-11	-6	-5	-12	10	-0	8	-4	-7	1	-3
14	-6	14	-10	-13	7	-9	-0	4		-5	-2	12	11	-3	1

N.B. FIG. 15 & FIG. 16 SHOW SOLUTIONS τ_3/λ OF

$$D^{\tau 1}x \oplus D^{\tau 2}x \oplus D^{\tau}x = D^{\tau 3}x.$$

AND ALSO THE SIGN OF $\phi_3(\tau_1, \tau_2, \tau_3, \tau)$

FIG.17

	← REGISTER CONNECTIONS FOR A GIVEN DELAY →				
	1	2	3	4	
0	0	0	1	1	
1	1	0	0	0	$D^0x = D^3x \oplus D^4x$
2	0	1	0	0	L = 15
3	0	0	1	0	
4	0	0	0	1	
5	1	0	0	1	i.e. $D^5x = D^1x \oplus D^4x$
6	1	1	0	1	
7	1	1	1	1	
8	1	1	1	0	
9	0	1	1	1	
10	1	0	1	0	
11	0	1	0	1	
12	1	0	1	1	
13	1	1	0	0	
14	0	1	1	0	
	↑	↑	↑	↑	
	$D^{14}x$	$D^{13}x$	$D^{12}x$	D^0x	

Sequence delay ↑ ↓

L = 15 FIG.18

	12	9	4	3	10	8	13	6	2	5	14	1	7	11
12		13	10	5	4	11	9	14	7	3	6	0	2	8
9	13		14	11	6	5	12	10	0	8	4	7	1	3
4	10	14		0	12	7	6	13	11	1	9	5	8	2
3	5	11	0		1	13	8	7	14	12	2	10	6	9
10	4	6	12	1		2	14	9	8	0	13	3	11	7
8	11	5	7	13	2		3	0	10	9	1	14	4	12
13	9	12	6	8	14	3		4	1	11	10	2	0	5
6	14	10	13	7	9	0	4		5	2	12	11	3	1
2	7	0	11	14	8	10	1	5		6	3	13	12	4
5	3	8	1	12	0	9	11	2	6		7	4	14	13
14	6	4	9	2	13	1	10	12	3	7		8	5	0
1	0	7	5	10	3	14	2	11	13	4	8		9	6
7	2	1	8	6	11	4	0	3	12	14	5	9		10
11	8	3	2	9	7	12	5	1	4	13	0	6	10	

MATRIX CONSTRUCTED FROM L OF (L+1) ROWS OF SOLUTIONS $\tau_{3/\lambda}$ TO

$$D^{\tau_1}x \oplus D^{\tau_2}x \oplus D^{\tau}x = D^{\tau_3}x,$$

SO THAT BLANKS LIE ON MAIN DIAGONAL.

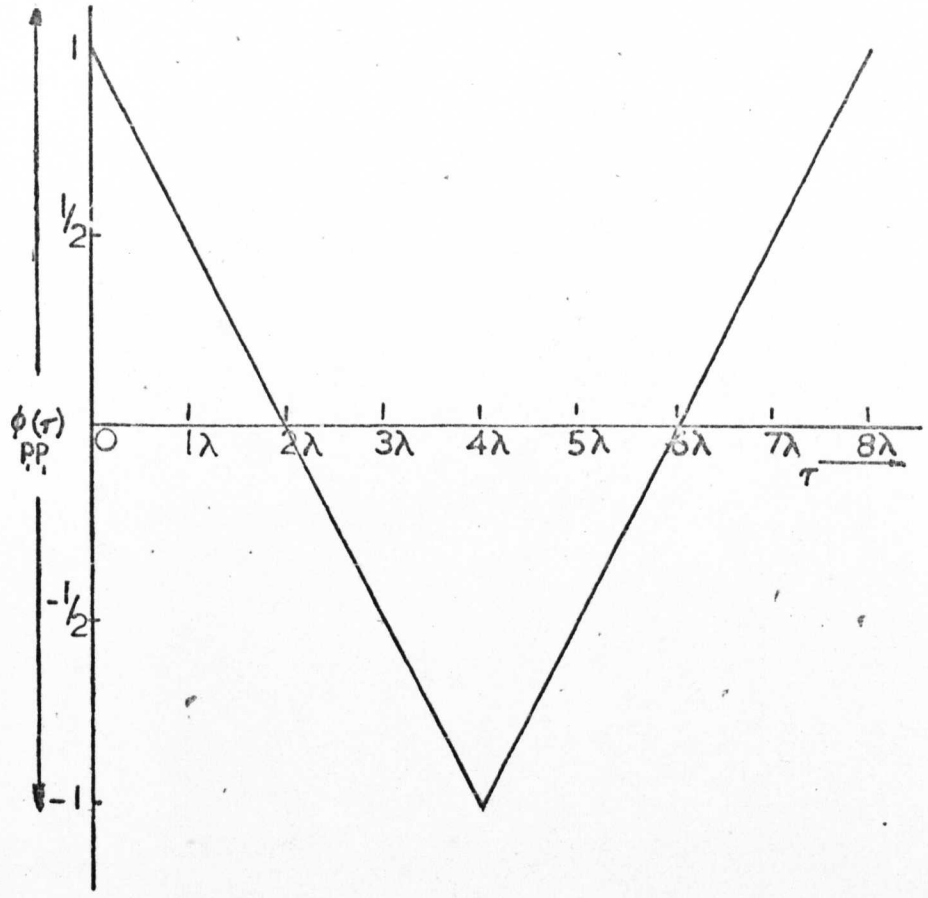

FIG. 19a

AUTOCORRELATION FUNCTIONS OF MODIFYING SEQUENCES

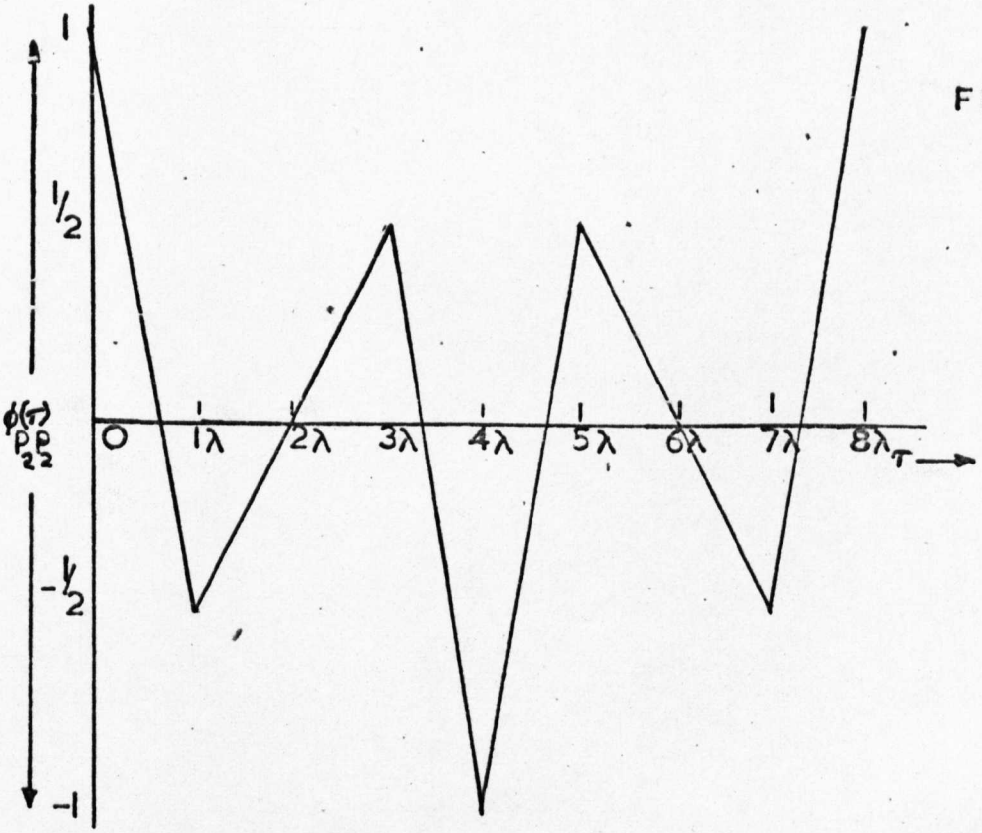

FIG. 19b

FIG. 20

τ_2/λ \ τ_1/λ	0	1	2	3	4	5	6	7	8	9	10	11	12	13	14	15	16	17	18	19	20	21	22	23	24	25	26	27	28	29	30
0		14	28	5	25	3	10	16	19	24	6	23	-20	30	1	22	7	18	17	8	12	27	15	11	9	4	29	21	2	26	13
1	14		15	29	6	26	4	11	17	20	25	7	24	21	0	2	23	8	19	18	9	13	28	16	12	10	5	30	22	3	27
2	28	15		16	30	7	27	5	12	18	21	26	8	25	22	1	3	24	9	20	19	10	14	29	17	13	11	6	0	23	4
3	5	29	16		17	0	8	28	6	13	19	22	27	9	26	23	2	4	25	10	21	20	11	15	30	18	14	12	7	1	24
4	25	6	30	17		18	1	9	29	7	14	20	23	28	10	27	24	3	5	26	11	22	21	12	16	0	19	15	13	8	2
5	3	26	7	0	18		19	2	10	30	8	15	21	24	29	11	28	25	4	6	27	12	23	22	13	17	1	20	16	14	9
6	10	4	27	8	1	19		20	3	11	0	9	16	22	25	30	12	29	26	5	7	28	13	24	23	14	18	2	21	17	15
7	16	11	5	28	9	2	20		21	4	12	1	10	17	23	26	0	13	30	27	6	8	29	14	25	24	15	19	3	22	18
8	19	17	12	6	29	10	3	21		22	5	13	2	11	18	24	27	1	14	0	28	7	9	30	15	26	25	16	20	4	23
9	24	20	18	13	7	30	11	4	22		23	6	14	3	12	19	25	28	2	15	1	29	8	10	0	16	27	26	17	21	5
10	6	25	21	19	14	8	0	12	5	23		24	7	15	4	13	20	26	29	3	16	2	30	9	11	1	17	28	27	18	22
11	23	7	26	22	20	15	9	1	13	6	24		25	8	16	5	14	21	27	30	4	17	3	0	10	12	2	18	29	28	19
12	20	24	8	27	23	21	16	10	2	14	7	25		26	9	17	6	15	22	28	0	5	18	4	1	11	13	3	19	30	29
13	30	21	25	9	28	24	22	17	11	3	15	8	26		27	10	18	7	16	23	29	1	6	19	5	2	12	14	4	20	0
14	1	0	22	26	10	29	25	23	18	12	4	16	9	27		28	11	19	8	17	24	30	2	7	20	6	3	13	15	5	21
15	22	2	1	23	27	11	30	26	24	19	13	5	17	10	28		29	12	20	9	18	25	0	3	8	21	7	4	14	16	6
16	7	23	3	2	24	28	12	0	27	25	20	14	6	18	11	29		30	13	21	10	19	26	1	4	9	22	8	5	15	17
17	18	8	24	4	3	25	29	13	1	28	26	21	15	7	19	12	30		0	14	22	11	20	27	2	5	10	23	9	6	16
18	17	19	9	25	5	4	26	30	14	2	29	27	22	16	8	20	13	0		1	15	23	12	21	28	3	6	11	24	10	7
19	8	18	20	10	25	6	5	27	0	15	3	30	28	23	17	9	21	14	1		2	16	24	13	22	29	4	7	12	25	11
20	12	9	19	21	11	27	7	6	28	1	16	4	0	29	24	18	10	22	15	2		3	17	25	14	23	30	5	8	13	26
21	27	13	10	20	22	12	28	8	7	29	2	17	5	1	30	25	19	11	23	16	3		4	18	26	15	24	0	6	9	14
22	15	28	14	11	21	23	13	29	9	8	30	3	18	6	2	0	26	20	12	24	17	4		5	19	27	16	25	1	7	10
23	11	16	29	15	12	22	24	14	30	10	9	0	4	19	7	3	1	27	21	13	25	18	5		6	20	28	17	26	2	8
24	9	12	17	30	16	13	23	25	15	0	11	10	1	5	20	8	4	2	28	22	14	26	19	6		7	21	29	18	27	3
25	4	10	13	18	0	17	14	24	26	16	1	12	11	2	6	21	9	5	3	29	23	15	27	20	7		8	22	30	19	28
26	29	5	11	14	19	1	18	15	25	27	17	2	13	12	3	7	22	10	6	4	30	24	16	28	21	8		9	23	0	20
27	21	30	6	12	15	20	2	19	16	26	28	18	3	14	13	4	8	23	11	7	5	0	25	17	29	22	9		10	24	1
28	2	22	0	7	13	16	21	3	20	17	27	29	19	4	15	14	5	9	24	12	8	6	1	26	18	30	23	10		11	25
29	26	3	23	1	8	14	17	22	4	21	18	28	30	20	5	16	15	6	10	25	13	9	7	2	27	19	0	24	11		12
30	13	27	4	24	2	9	15	18	23	5	22	19	29	0	21	6	17	16	7	11	26	14	10	8	3	28	20	1	25	12	

N.B. $D^0x(t) = D^3x(t) \oplus D^5x(t)$

Solutions τ_2/λ of $D^{\tau_1} \oplus D^{\tau}x = D^{\tau_2}x$ for L=31

FIG. 21

DEPARTURES FROM STEADY STATE CORRELOGRAM AFTER CHANGE $\gamma = 1$

t_2/λ \ τ_i/λ	0	1	2	3	4	5	6	7	8	9	10	11	12	13	14
5	0	0	0	0	0	0	0	0	0	0	0	0	0	0	0
6	0	0	0	0	0	0	0	0	0	0	0	0	0	0	0
7	0	0	0	0	0	0	0	0	0	0	0	0	0	0	0
8	2	2	-2	2	-2	2	2	-2	-2	2	-2	-2	-2	2	2
9	6	6	6	-6	6	-6	6	6	-6	-6	6	-6	-6	-6	6
10	6	6	6	6	-6	6	-6	6	6	-6	-6	6	-6	-6	-6
11	-4	4	4	4	4	-4	4	-4	4	4	-4	-4	4	-4	-4
12	2	2	-2	-2	-2	-2	2	-2	2	-2	-2	2	2	-2	2
13	6	6	6	-6	-6	-6	-6	6	-6	6	-6	-6	6	6	-6
14	-4	4	4	4	-4	-4	-4	-4	4	-4	4	-4	-4	4	4
0	0	0	0	0	0	0	0	0	0	0	0	0	0	0	0
1	2	2	-2	2	2	2	-2	-2	-2	-2	2	-2	2	-2	-2
2	-4	4	4	-4	4	4	4	-4	-4	-4	-4	4	-4	4	-4
3	2	2	-2	-2	2	-2	-2	-2	2	2	2	2	-2	2	-2
4	-4	4	4	-4	-4	-4	4	-4	-4	4	4	4	4	-4	4

$L = 15$

Each row contains the members of $U_{xy}(\tau_i, t_2)$

COLUMN TOTALS ARE

=	10	42	26	-6	-6	-6	-6	-6	-6	-6	-6	-6	-6	-6	-6	= $L.\Delta_{xy}(\tau_i, 5\lambda)$

The matrix of rows $U_{xy}(\tau_i, t_2)$ has a disturbance occurring between $t_2 = 4\lambda$ and $t_2 = 5\lambda$.

CHAPTER 4 - CONCLUSIONS

1. CONCLUSIONS

It was seen that there exists an exact parallel between conventional chromatography and impulse testing. Mindful of this, a scheme to analyse gas or liquid samples using pseudo-random injections has been developed. Cross-correlation between input and output yields the chromatogram. Since correlation is capable of considerable noise rejection, this approach filters detector outputs. This eases the problem of identification of trace components which are normally buried in the detector noise.

By extending the technique with extra sample valves, simultaneous analysis of several independent sample streams is possible with only one column and detector. Using conventional chromatography this would be impossible. Conventional techniques are also unhelpful when certain specific detector non-linearities give rise to anomalies. By a modification of the proposed scheme, the effects of detector non-linearities can be circumvented and linear analysis is possible. Other modifications allow removal of the effects of base-line drift, and continuous analysis of samples with time varying concentrations. This latter could be of importance in closed loop schemes using chromatograph outputs as control data, since it eliminates many of the inherent time delays of the conventional approach.

To implement the scheme one requires some carefully chosen conventional equipment, plus an injection sequence generator, and some means of data analysis. This latter is amply provided by either a low cost computer or a digital correlator.

2. SUGGESTIONS FOR FURTHER WORK

In the available time it was impossible to exhaustively evaluate every conceivable application of the proposed technique. Certain procedures would be difficult to implement (e.g.temperature programming, column switching, heart cut), but using pseudo-random binary sequences, other procedures (e.g. trace and continuous analysis) appear to benefit. Hence further research into the proposed technique would be justified. Certain specific areas are most attractive in view of this and these are enumerated in the following.

Recently a Dutch analytical chemist Smit[1] tentatively explored the possibilities of applying the correlation technique (using p.r.b.s.) to trace analysis. As he points out, one normally has extreme difficulty in identifying trace peaks because they are buried in noise. Using 3µl liquid samples (liquid n pentane)and vapourising by infra-red heating, a peak not visible in the resultant detector output for a conventional injection, becomes easily identifiable when using p.r.b.s. The noise rejection properties of p.r.bs. have also been emphasised in the work of Chapter 2. Since it appears that there would be commercial interest in the application of such properties to trace analysis, it would appear useful to explore the possibilities further.

Although some of Smit's results were based on averages over 16 sequence lengths, the appropriate correlograms still contain a certain amount of base-line uncertainty. The reproducibility of these results is not quoted, but the detector output appears to contain drift components of up to at least

second order. Chapter 2 has discussed the effects of such drift on impulse response estimates. By application of one of the methods for drift removal quoted in Appendix B.2., the results of Smit[1] might well be improved. Further research is needed to establish more fully the best drift removal procedure to use, not only in trace analysis, but in other analyses where noise levels are lower.

Under certain experimental conditions, katherometers have been seen to exhibit a non-linear response. Chapter 3 has discussed several methods of removing the effects of output non-linearities on impulse response estimates. The work on Hadamard-modified sequences needs to be examined to see if it would be possible to determine the coefficients of the polynomial describing the non-linearity. These could be used to design a linearising network as described in Chapter 3, section 2.1. Subsequent analyses would then be possible using unmodified m sequences, since the effective measured output would now be linearised.

The ability of the technique developed to follow time varying concentrations has only been studied, for practical reasons, with simple simulations. The situation where there is considerable output noise might impose limitations which need to be evaluated (e.g. smallest detectable change). In addition, the case of several sample peaks which can change independently of each other needs to be studied before this technique can be

widely applied. Since the basic technique is quite general, it should be possible to apply it in situations other than Chromatography, as long as the impulse response peaks do not change in shape or location.

Lastly, the research, for economic reasons, was conducted solely using katherometric detection. Since there are other detectors available, each having an area of particular application, some work is necessary to establish whether or not other detectors can be used satisfactorily in the proposed technique. It may also be valuable to examine the lower limit of detection (for each detector) in the light of the noise rejection properties of correlation.

3. REFERENCES

1. Smit, H.C., Chromatographia, 3, 1970.

ADDENDUM

Paper presented at Conference on Laboratory Automation, Middlesex Hospital Medical School, 10-12 November 1970, organised by I.E.R.E.

CONTINUOUS GAS CHROMATOGRAPHY.

By K.C.Ng* B.Sc., Ph.D. and G.C.Moss*

Summary:
The paper describes an application of the well-known correlation technique of control systems theory to the on-line continuous chromatographic analysis of gases. The accuracy of the analysis compares well with that of general purpose conventional gas chromatographs. The most important cause of inaccuracy is the non-linearity of the detector and means of minimizing the errors are discussed. Extension of the basic system to the simultaneous analysis of several samples using a single column is described.

1. Introduction

In conventional gas chromatography a single plug of sample gas is injected into the carrier gas stream flowing into a packed column. The packing adsorbs the sample gas components and retains them for a certain time before releasing them back to the gas stream. This process of adsorption and release continues down the column. Since some components are more strongly adsorbed than others, they gradually separate. By choosing the flow rate and column length properly, it is possible to obtain complete separation at the column exit.

The various components in the sample gas are detected by monitoring a suitable physical property of the column effluent, such as density, ionisation potential or thermal conductivity. The detector will respond in sympathy with variations in effluent composition. The delay (or elution) time between injection and each response peak is characteristic of the component giving rise to the peak and is also dependent on the experimental conditions. The peak area is indicative of the percentage concentration of the component. Figure 1 shows the schematic of the conventional chromatograph and a typical detector response. The elution time T_L is often of the order of tens of minutes giving rise to stability problems in automatic process control schemes. Izarwa[1] suggested that the essentially batch process of conventional gas chromatography can be made continuous by applying the well-known identification technique of cross-correlation[2].

2. Continuous Analysis

In the continuous approach[1,3] samples are introduced into the carrier stream according to the 1,0 (gas, no gas) logic of a pseudo-random binary sequence (p.r.b.s.). The resulting detector response takes the form shown in Figure 2. The period T of the p.r.b.s. is generally a little longer than the longest elution time of the gas sample components.

*School of Engineering Science, University of Warwick.

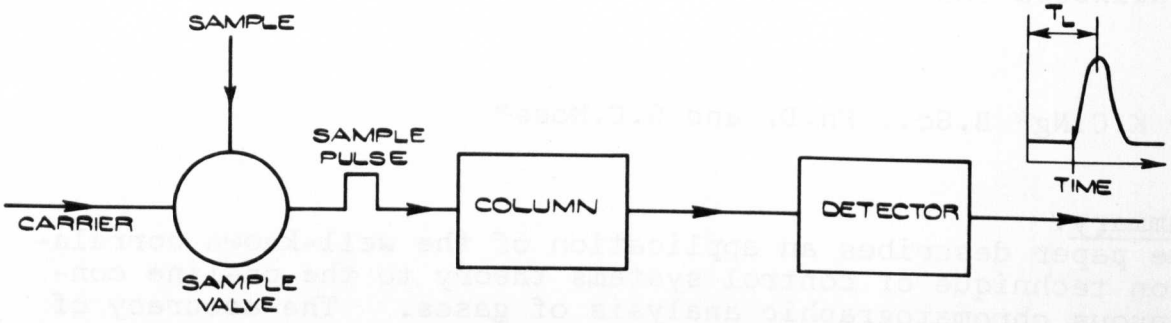
SAMPLE
SAMPLE PULSE
CARRIER
SAMPLE VALVE
COLUMN
DETECTOR
T_L
TIME

FIG. 1

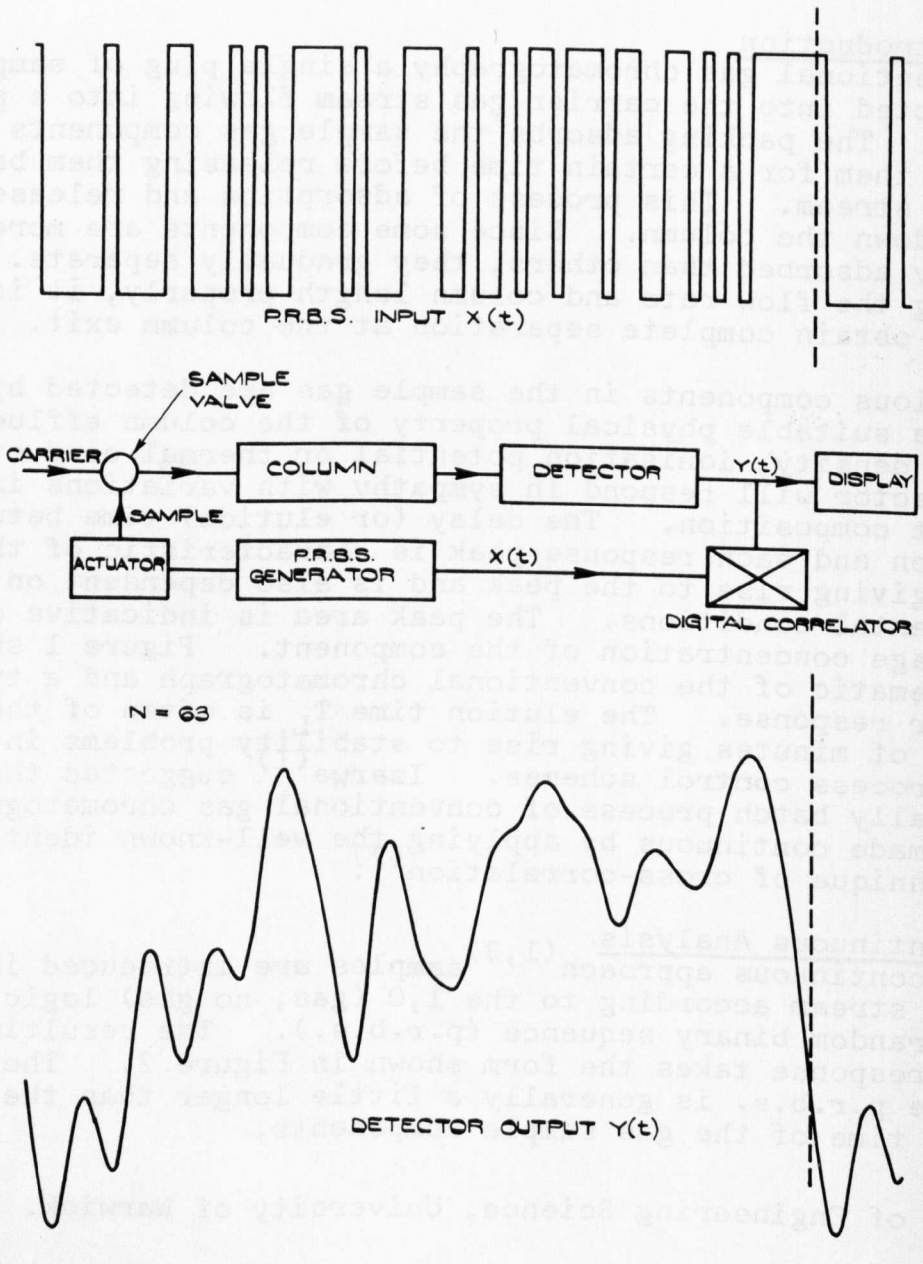
P.R.B.S. INPUT X(t)
SAMPLE VALVE
CARRIER
COLUMN
DETECTOR
Y(t)
DISPLAY
SAMPLE
ACTUATOR
P.R.B.S. GENERATOR
X(t)
DIGITAL CORRELATOR
N = 63
DETECTOR OUTPUT Y(t)

FIG. 2.

By correlating the detector response with the p.r.b.s., and noting that the chromatogram of Figure 1 is essentially a plot of the impulse response of the gas-column-detector combination, we obtain the chromatogram as the cross-correlation function $\Phi_{xy}(t)$ defined as

$$\Phi_{xy}(t) \triangleq \int_0^\infty \Phi_{xx}(t-\tau)\, h(\tau)\, d\tau$$

where $h(\tau)$ is the true impulse response (or true correlogram) and $\Phi_{xx}(\lambda)$ is the auto-correlation function of the p.r.b.s. If $\Phi_{xx}(\lambda)$ is an impulse function then $\Phi_{xy}(t)$ is exactly the desired chromatogram. Of course $\Phi_{xx}(\lambda)$ for the p.r.b.s. is only a very good approximation to an impulse and the effect of this deviation can be made small (and readily accounted for) by proper choice of the sequence parameters.

2.1 Problems of the Continuous Technique

Izawa[4] followed up his original suggestion but little was reported on the practical problems of this approach to gas analysis. The most common problems encountered in gas chromatography are those of base-line drift and of noise in the detector output. The correlation technique has good noise rejection properties and this has been confirmed in this application. Methods of minimizing the effects of base-line drift in the correlation technique are well-known and will not be dealt with in this paper.

The more serious problem, not peculiar to this method of analysis, is that the overall system can become non-linear. The effect of non-linearities is an increased level of base-line ripple and the presence of additional peaks which may be wrongly identified as the presence of unknown components.

Non-linear behaviour can be attributed to two elements in the gas chromatograph. The injection or sampling valve can exhibit non-linear behaviour in the form of unequal switching delays and switching times. This type of non-linearity gives rise to an additional peak at only one point in the correlogram[5]. Although such a response was initially observed, the choice of the sampling valves subsequently used in the apparatus eliminated this source of non-linear error.

In the course of the experiment, non-linearity (due to saturation)in the column was clearly shown to be non-existent, at least at the level of concentration of gas used or likely to be used with such an apparatus.

The source of most severe non-linear behaviour is the detector which in this case is a katherometer. Regarding linearity of response of the katherometer, one should note the following:

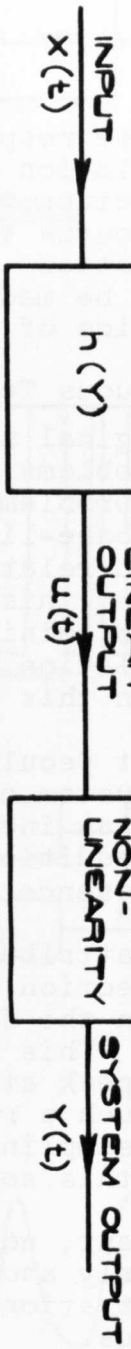
INPUT
x(t)
LINEAR
DYNAMICS
h(Y)
LINEAR
OUTPUT
u(t)
NON-
LINEARITY
SYSTEM OUTPUT
Y(t)

FIG. 3.

(i) the carrier and sample gas components should have widely different thermal conductivities.

(ii) Linearity is best with hydrogen or helium as the carrier gas. Nitrogen is a very poor carrier in this respect.

(iii) Low mole concentrations should be used. (It has been suggested by some workers that a typical concentration of sample gas in carrier gas be about 0.5 mole percent. In the continuous mode of operation the concentration is generally likely to be greater than this figure.)

(iv) The thermal conductivity of a mixture of gases is generally a non-linear function of the concentrations. Many functions are quoted in the literature. A typical one is

$$k_o = \frac{k_s}{1 + A_{cs}\left(\frac{\alpha_c}{\alpha_s}\right)} + \frac{k_c}{1 + A_{sc}\left(\frac{\alpha_s}{\alpha_c}\right)}$$

where α_s, α_c are the respective mole fractions of sample and of carrier in the mixture; k_s, k_c are the respective thermal conductivities of the sample and the carrier; k_o is the overall thermal conductivity and A_{cs}, A_{sc} are Constants for a given carrier and sample mixture.

The range of concentrations over which such non-linear descriptions apply is narrow. In some not uncommon cases, the detector output versus concentration characteristic can show a turning point (maximum or minimum). The result of operation at or near this turning point is that the conventional chromatograph becomes distorted. Although interpretation of the chromatograph for the case of hydrogen in helium carrier has been attempted, the analysis is impossible, in general, without extensive calibration of the detector. By a two-test approach[6], it is possible in the correlation technique to extract the desired chromatogram to within a constant factor.

3. Removal of the Effects of Non-linearities

The model of the system chosen for the development of techniques of eliminating the effect of non-linearity is shown in Figure 3. The authors assumed the system to be noise-free and drift-free. Further, the linear (frequency dependent) and non-linear (concentration dependent) parts are separable, the non-linearity following the linear part.

An investigation of the non-linear characteristic of the detector shows that a very close approximation to the characteristic is afforded by the general cubic function

$$y = a_o + a_1 u + a_2 u^2 + a_3 u^3 .$$

where a_s, a_1, a_2, a_3 are constants for the particular gas mixture. u is the concentration at the input to the detector and y is the detector response. The desired term is the linear term $a_1 u$.

Now using a p.r.b.s. x(t) to modulate the input to the column with sample gas, the input to the detector is

$$u(t) = \int_o^\infty h(\tau)\, x\,(t-\tau)\, d\tau$$

Then $y(t) = a_o + a_1 \int_o^\infty h\,(\tau)\, x\,(t-\tau)\, d\tau +$

$$a_2 \int_o^\infty \int_o^\infty h(\tau_1)\, h\,(\tau_2)\, x\,(t-\tau_1)\, x\,(t-\tau_2)\, d\tau_1\, d\tau_2 +$$

$$a_3 \int_o^\infty \int_o^\infty \int_o^\infty h(\tau_1)h(\tau_2)h(\tau_3)x(t-\tau_1)x(t-\tau_2)x(t-\tau_3)d\tau_1\, d\tau_2\, d\tau_3$$

Finally,

$$\Phi_{xy}(\lambda) = a_1 \int_o^\infty h(\tau)\Phi_{xx}(\tau-\lambda)d\tau + a_2 \int_o^\infty \int_o^\infty h(\tau_1)h(\tau_2).$$

$$m_3(\tau_1,\tau_2,\lambda)\, d\tau_1\, d\tau_2 .$$

$$+ a_3 \int_o^\infty \int_o^\infty \int_o^\infty h(\tau_1)h(\tau_2)h(\tau_3).$$

$$m_4\,(\tau_1,\tau_2,\tau_3,\lambda)\, d\tau_1\, d\tau_2\, d\tau_3$$

where $m_i(\tau_1,\tau_2,\ldots\tau_{i-1},\lambda)$ is the ith moment of the p.r.b.s.

It is seen that $\Phi_{xy}(\lambda)$ is contaminated with the result of the quadratic and cubic terms and the chromatogram obtained can be very difficult to interpret.

There are several techniques available for removing the effects of non-linear terms, all relying on multiple tests with the same binary sequence but of differing amplitudes, (see e.g. ref.7). Other techniques use multi-level sequences. In chromatography, however, simplicity of operation and speed of analysis restricts the use of these techniques. The use of inverse repeat binary sequences (3) does remove the second order non-linear effects but can in-

troduce at the same time additional linear terms of the form $c_2 a_2 \int_0^\infty h(\tau)\, \Phi_{xx}(\tau-\lambda)d\lambda$ and $c_3 a_3 \int_0^\infty h(\tau)\, \Phi_{xx}(\tau-\lambda)d\lambda$, each of which is proportional to the constant of the quadratic and cubic terms. c_2, c_3 are constants. This makes the calibration procedure more difficult.

The authors have been working on a technique [6] which will extract the linear term (to within a constant factor) from a general cubic from the results of two tests with a modified p.r.b.s. Initial results are encouraging and future work will aim at determining the linear term exactly and in combining the two tests into one.

4. Experimental Results

A series of experiments were conducted, using two sets of apparatus, in the study of continuous chromatography.

Set 1 consists of a slowly operating pneumatic sliding plate valve, the column and a microkathemometer enclosed in an unthermostatted box.

Set 2 consists of a fast operating micro sliding plate sampling valve with selectable sample volumes. The column and katherometer used were of the same type, but the latter is enclosed in a box which can be thermostatically controlled.

4.1. Experiments with set 1.

In these experiments, nitrogen is used as the sample gas with helium as the carrier. Two injection techniques can be used.

(i) The sample gas is injected for the whole of each of the "1" bits of the p.r.b.s. The volume of sample gas introduced per bit is thus determined by the flow rate and by the bit interval.

(ii) The sample gas volume is determined by an external loop. At each "1" bit, the carrier gas sweeps through this loop transporting a fixed volume sample into the column, irrespective of the flow rate of the carrier gas.

The second method is preferred as it is easier to control the exact amount of sample gas injected into the carrier stream and since it is desirable that the concentration of the sample in the column be low.

Using a sample volume of 40μℓ and a flow rate of 1/6 mℓ/sec., the mole percentage of nitrogen at the column entry is 23 per cent. Figure 4a shows the correlogram obtained when a 63 bit p.r.b.s. is used. The nitrogen peak is clearly identifiable but there is considerable base-line ripple(approximately ± 7 per cent of peak height).

An inverse repeat sequence obtained from the 63 bit p.r.b.s. is now used to control the sample injection. The other parameters are as in the last experiment. The resulting chroma-

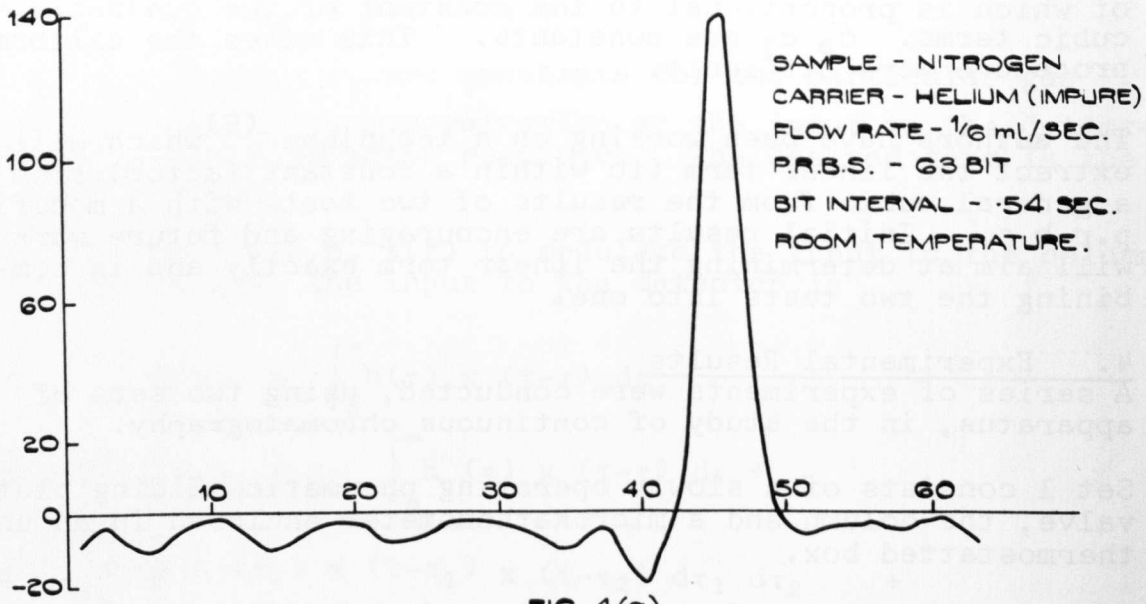
140
100
60
20
0
-20
10
20
30
40
50
60
SAMPLE - NITROGEN
CARRIER - HELIUM (IMPURE)
FLOW RATE - 1/6 mL/SEC.
P.R.B.S. - 63 BIT
BIT INTERVAL - ·54 SEC.
ROOM TEMPERATURE.

FIG. 4(a)

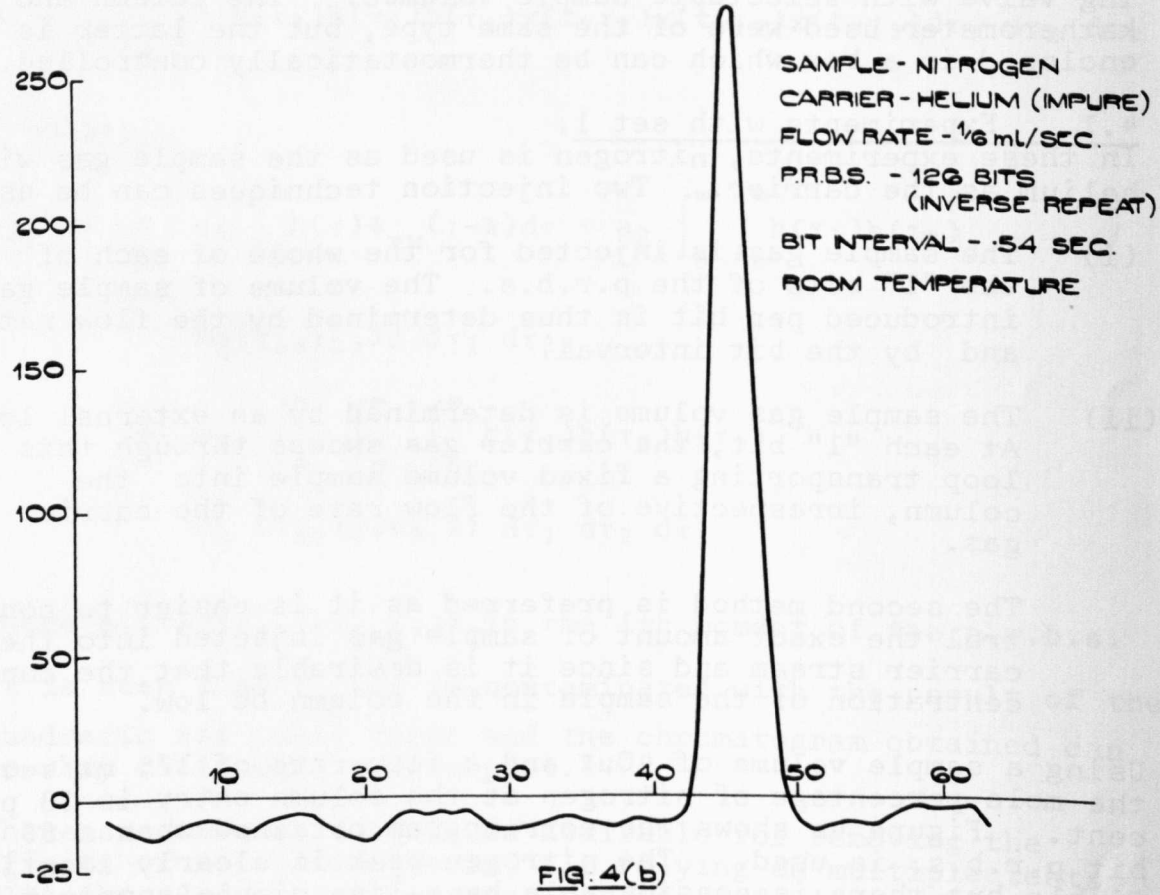
250
200
150
100
50
0
-25
10
20
30
40
50
60
SAMPLE - NITROGEN
CARRIER - HELIUM (IMPURE)
FLOW RATE - 1/6 mL/SEC.
P.R.B.S. - 126 BITS
(INVERSE REPEAT)
BIT INTERVAL - ·54 SEC.
ROOM TEMPERATURE

FIG. 4(b)

togram, shown in Figure 4B, shows considerable reduction in base-line ripple (approximately ± 2% of peak height). This indicates the presence of quite severe even-power non-linearity in the system.

The sample gas nitrogen is not adsorbed by the column packing. Thus we can rule out saturation of the packing material. Significant non-linearity of the sampling valve can be ruled out as the characteristics of errors due to this source are not consistent with those observed. The conclusion is that the detector is heavily non-linear. To confirm this requires the use of the second set of apparatus as the first sampling valve is not capable of delivering very small volumes of gas.

4.2. Experiments with set 2

In this apparatus, the sample volume can be one of five values 0.3, 1.0, 3.0, 10 or 20μℓ. For a 1.0 μℓ slider with four injections per "1" bit interval and with nitrogen as the sample gas and helium carrier at the flow rate of 1/6 mℓ/sec. the mole percentage of sample at the column entry is 0.6 per cent. Using the same unmodified 63 bit p.r.b.s. the base line ripple of the chromatogram is reduced to less than ± 0.5 per cent of peak height(see Figure 5). The sampling valve is known to be linear. The ripple is due to the residual non-linear effects and possibly due to quantization errors in the digital correlator.

An analysis of a representative sample of hydrocarbons in helium is shown in Figure 6. The composition of the gas sample is known to be as follows :- Helium 99%, Propylene 0.9%, Propane 0.08%, Ethane 0.02%. A 10μℓ slider is used in this case. Note that the oven temperature is controlled at 60^{0}. Operation at 30^{0} does not affect the noise content but slows down the response so that the elution time is increased by approximately 10 per cent.

4.3. Simultaneous Analysis of Several Samples

A property of the p.r.b.s. is that the signal is uncorrelated with a delayed version of itself for delays not identically equal to multiples of the period T. With the continuous analysis technique, it is therefore possible to use a single column-detector-correlator system for the simultaneous analyses of two or more samples. In this extension, a sample valve is used for each sample to be analysed, the sample valves being actuated by suitably delayed versions of the same p.r.b.s. The delay time between any two sampling valve actuation signals is chosen to be just longer than the difference between the longest elution time for the first of these two samples and the shortest of the second.

The period of the p.r.b.s. is approximately (but longer) than the sum of the delays and the longest elution time of the last sample. The number of bits in the sequence is determined by the resolution required between successive points of each correlogram.

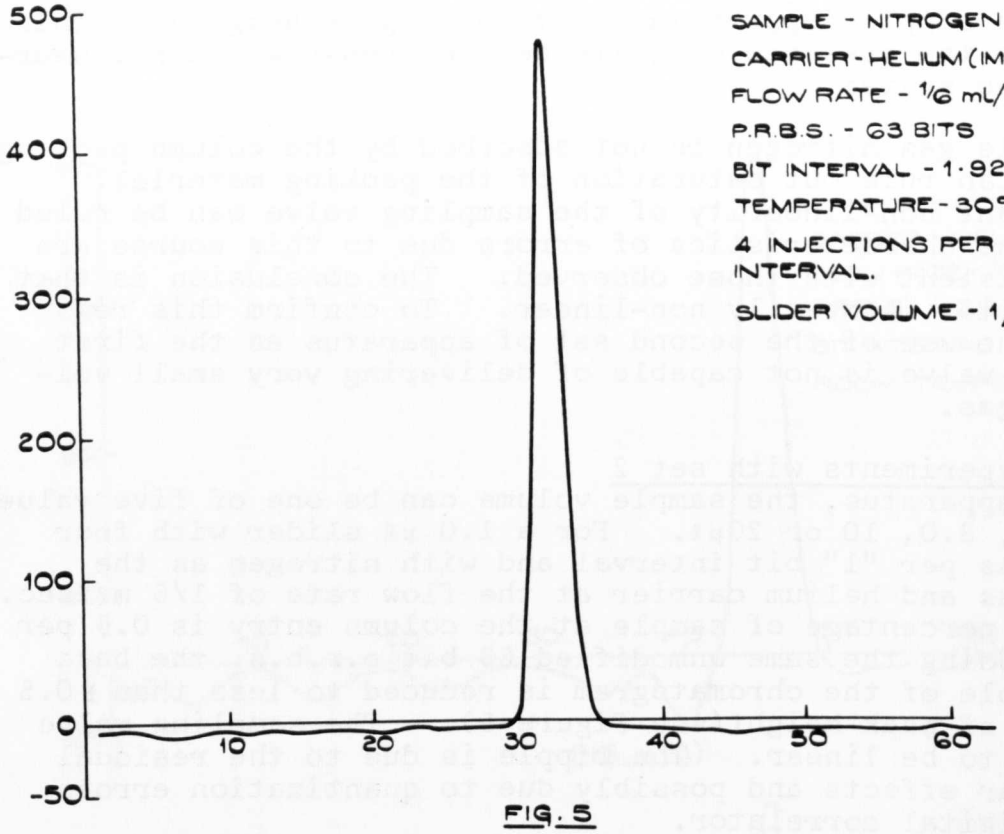

FIG. 5

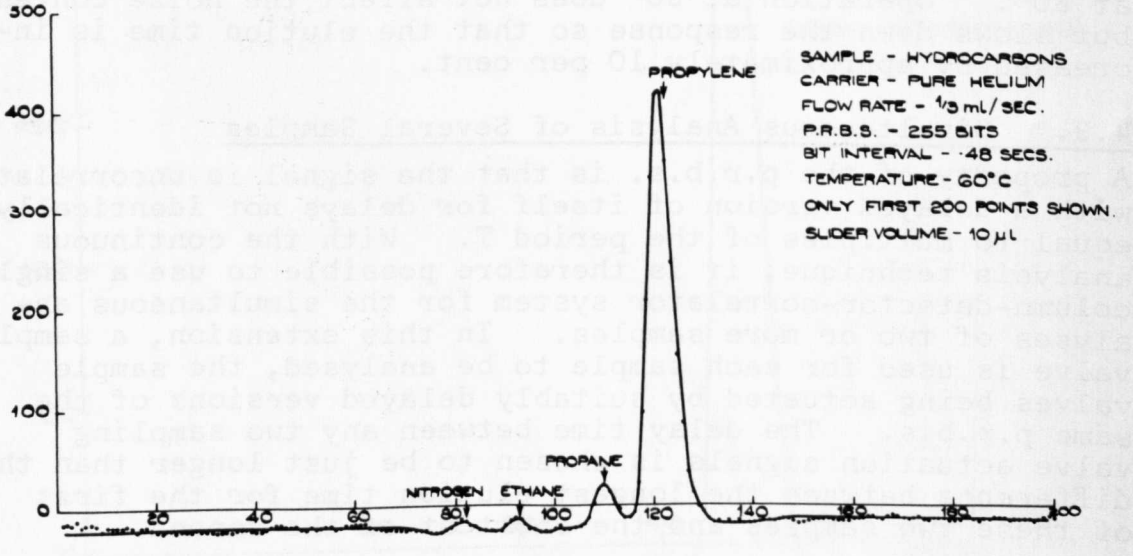

VARIANCE OF POINTS 1-70 AND 141-255 = 4·82
MEAN BASELINE AT 16·9

FIG.6

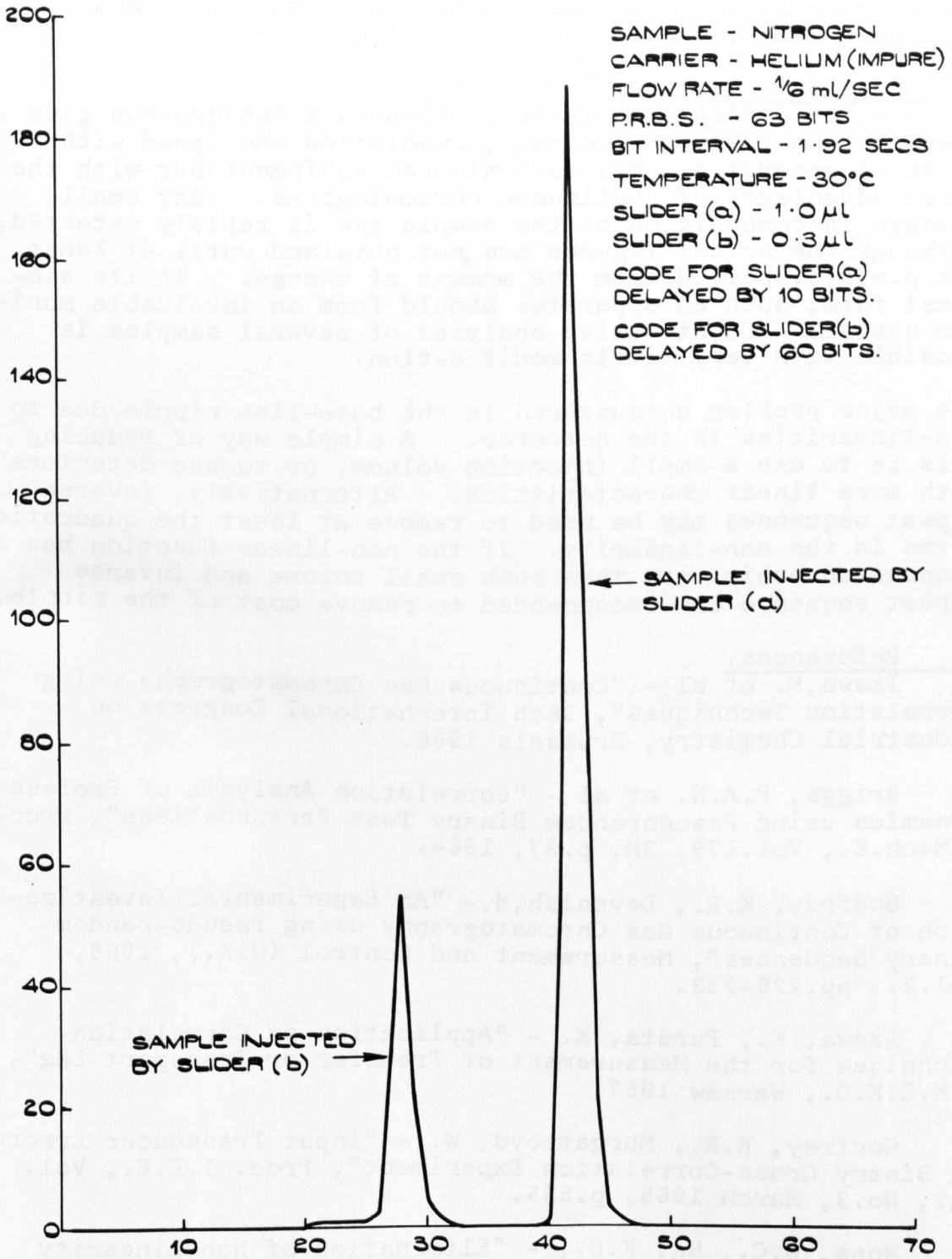
SAMPLE - NITROGEN
CARRIER - HELIUM (IMPURE)
FLOW RATE - 1/6 ml/SEC
P.R.B.S. - 63 BITS
BIT INTERVAL - 1·92 SECS
TEMPERATURE - 30°C
SLIDER (a) - 1·0 µl
SLIDER (b) - 0·3 µl
CODE FOR SLIDER(a) DELAYED BY 10 BITS.
CODE FOR SLIDER(b) DELAYED BY 60 BITS.
SAMPLE INJECTED BY SLIDER (a)
SAMPLE INJECTED BY SLIDER (b)
200
180
160
140
120
100
80
60
40
20
0
10
20
30
40
50
60
70

FIG. 7

An initial test has been conducted with nitrogen as the gas in each of two samples and the result is in Figure 7.

This application has obvious importance in the cost-effectiveness considerations of the continuous technique. It is certainly much faster than the conventional sequential analysis of several samples using a single column.

5. Conclusions.

The results indicate that the continuous technique can give results comparable in accuracy, resolution and speed with those of general purpose conventional equipment but with the added advantages of continuous chromatograms. Any small changes in composition of the sample gas is rapidly detected, although the actual figures are not obtained until at least one p.r.b.s. period from the moment of change. In its simplest form, such an apparatus should form an invaluable monitor system. Quantitative analyses of several samples is possible with very little modification.

The major problem encountered is the base-line ripple due to non-linearities in the detector. A simple way of reducing this is to use a small injection volume, or to use detectors with more linear characteristics. Alternatively, inverse repeat sequences may be used to remove at least the quadratic terms in the non-linearity. If the non-linear function has a pronounced cubic term then both small volume and inverse repeat sequence are recommended to remove most of the ripple.

6. References.

1. Izawa,K. et al - "Continuous Gas Chromatography using Correlation Techniques", 36th International Congress on Industrial Chemistry, Brussels 1966.

2. Briggs, P.A.N. et al - "Correlation Analysis of Process Dynamics using Pseudorandom Binary Test Perturbations", Proc. I.Mech.E., Vol.179, 3H, p.37, 1964.

3. Godfrey, K.R., Devenish,M.- "An Experimental Investigation of Continuous Gas Chromatography using Pseudo-random Binary Sequences", Measurement and Control (U.K.), 1969, vol.2., pp.228-233.

4. Izawa, K., Furuta, K. - "Application of Correlation Technique for the Measurement of Transfer or Transport Lag", I.M.E.K.O., Warsaw 1967.

5. Godfrey, K.R., Murgatroyd, W. - "Input Transducer Errors in Binary Cross-Correlation Experiment", Proc. I.E.E., Vol. 112, No.3, March 1965, p.565.

6. Moss, G.C., Ng, K.C., - "Elimination of Non-Linearity Effects in Binary Cross-Correlation". To be published.

7. Gardiner, A.B. - "Elimination of the Effects of Non-linearities on Process Correlations", Electronic Letters, May 1966, Vol.2, No.5.

ADDENDUM 2

TO COMPARE THE CONVENTIONAL AND PROPOSED INJECTION TECHNIQUES FOR COLUMNS OPERATING JUST WITHIN THE LIMITS OF LINEARITY

1 INTRODUCTION

The application of pseudo random binary sequences to chromatography has been discussed in part with reference to the noise rejection properties of the correlation technique. It has been shown, (Appendix B 1), that if repeated injections each of the same size as normally used in a single shot analysis, are made according to the logic of a p.r.b.s., an improvment of $[\sqrt{Tb_n}]/2$ in signal to noise ratio results from correlation between input and output. In practice, since there will be $[L+1]/2$ injections, more sample will be injected with a p.r.b.s. than with the equivalent single shot method, and it is to be noted that the signal to noise ratio of a single shot analysis could be improved simply by increasing the sample size. However, sample size cannot be increased indefinetly.

Apart from the requirement of linear detector operation, the allowable limit on the maximum sample size is often set by considering column linearity. In Chapter 1 it has been seen that columns behave linearly up to a limiting sample component concentration, beyond which the partition coefficient varies with concentration, and the column is non-linear as a consequence. Thus this limiting concentration controls the maximum allowed sample size, and it is therefore of some interest to estimate its value. However this is often impractical because of the dependence of absolute values on a number of factors viz:-

(i) Carrier flow rate

(ii) Sample size

(iii) Specific surface area of stationary phase

(iv) Temperature

(v) Pressure

(vi) Nature of Sample

However a very rough 'guesstimate' of the allowed concentrations is the range 0-5 mole % and beyond this column can be expected to overload. This being the situation, it is possible to postulate the case of a single injection conventional gas chromatograph operating just on the limit of the range of column linearity. What then is the comparative maximum allowable size of each injection in the p.r.b.s. approach so that linear column operation is ensured? If it is possible to deduce a relationship between the maximum sample sizes, the noise rejection properties of correlation can be more realistically interpreted.

PRACTICAL INVESTIGATION

Some simulated, lumped column dynamics $\left[\frac{1}{(1+S)^5}\right]$ were perturbed by an m sequence. Arranging five, first order systems in cascade it was possible to consider the column as a set of interconnected lags, and the output of each could be monitored. This gave some indication of the passage of the m sequence down the column, (for a single sample component). FIG 1 shows the overall system response to an impulse of strength 10 volts * 100 msec = 1 volt sec. Plotted on a different scale, FIG 2a shows a 63 bit, (100 msec clock interval) m sequence of levels +10 and 0 volts used to stimulate the system. FIG 2b shows the result of pertubing the input with the signal of FIG 2a, in a set of traces (i) to (v); (i) is the overall system output and the remainder of the traces are the outputs from the column segments indicated. FIG 2c is the impulse response of Fig 1 plotted to the same scale. The results show that as expected, highest concentrations occur at the beginning of the column $[\frac{1}{1+S}]$, and the concentrations at the column exit (detector input) are somewhat lower. Moreover, the maximum concentrations are directly attributable to the run of n 'ones' in the m sequence. FIG 3 show the name test but with the sequence length increased to 127.

RESULTS

Noting that each of the m sequence injections are the same size as an equivalent single shot injection, then from FIGS 1 and 2 it is seen that, for one component

$$\frac{\text{max. conc. due to an m sequence of length 63}}{\text{conc. due to single shot}} = \frac{9.0}{1.7} = 5.3$$

and again from FIGS 1 and 3

$$\frac{\text{max. conc. due to an m sequence of length 127}}{\text{conc. due to a single shot}} = \frac{9.2}{1.7} = 5.4$$

DISCUSSION

It has been seen that using m sequences the maximum concentration occurs after a run of 'n' ones in the sequence. Thus it appears that empirically, each m sequence injection should be $\leq \frac{1}{n}$ of that which just allows linear operation of the column for single shot analysis. The simulation exercise judged this to be a pessimistic estimate, but useful as a rule of thumb guide. Thus comparing the best, (assuming linear operation of column), possible results from single shot analysis and the p.r.b.s. approach, the improvement in signal to noise ratio using m sequences becomes $[\sqrt{Tb_n}]$ or greater. It is important to note however that the experiment dealt only with one sequence of length 63 and of length 127. The particular sequences chosen were only one of many possible choices for the sequence length of interest. Everett[1] notes that for an 'm' sequence of length L, then there are $\frac{1}{n}\phi(L)$ possible choices of sequence, where $\phi(L)$ is the Euler totient function denoting the number of integers less than and relatively prime to the integer L. Davies[2] gives a convenient table showing the possible numbers of sequence of a given length. The particular sequence chosen may possess long runs of ones relatively close together, thus the concentration resulting from the string of n 'ones' alone may not give rise to the maximum concentration. This means that the particular sequence of length L used in an application, must be chosen with its internal structure in mind Lindholm's[3] paper would be of value in this respect.

REFERENCES

1 Everett, D., Periodic Digital Sequences with Pseudo noise Properties, G.E.C. Journal, Vol. 33, No. 3, 1966

2 Davies, W.D.T., Using the Binary Maximum Length Sequence For the Identification of System Dynamics. Proc. I.E.E., Vol. 114, No. 10, Oct 1967, pp 1582-1584

3 Lindholm, J.H., An Analysis of the Pseudo-Randomness Properties of Subsequences of Long m-sequences, I.E.E.E. Trans On Information Theory, July 1968, Vol. IT-14, No.4, pp 569-576

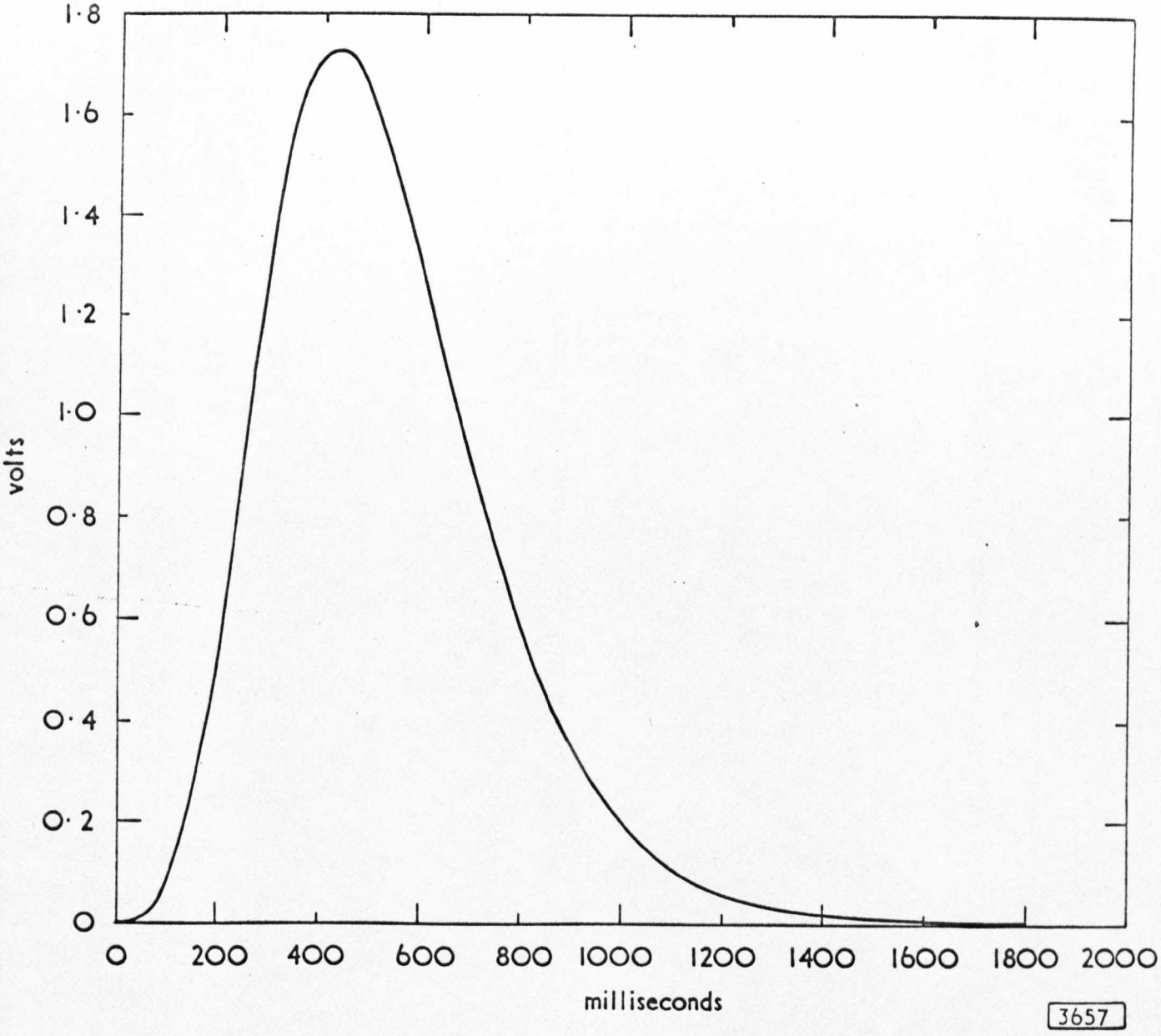

FIG.1 IMPULSE RESPONSE OF SIMULATED COLUMN DYNAMICS $\frac{1}{(1+S)^5}$

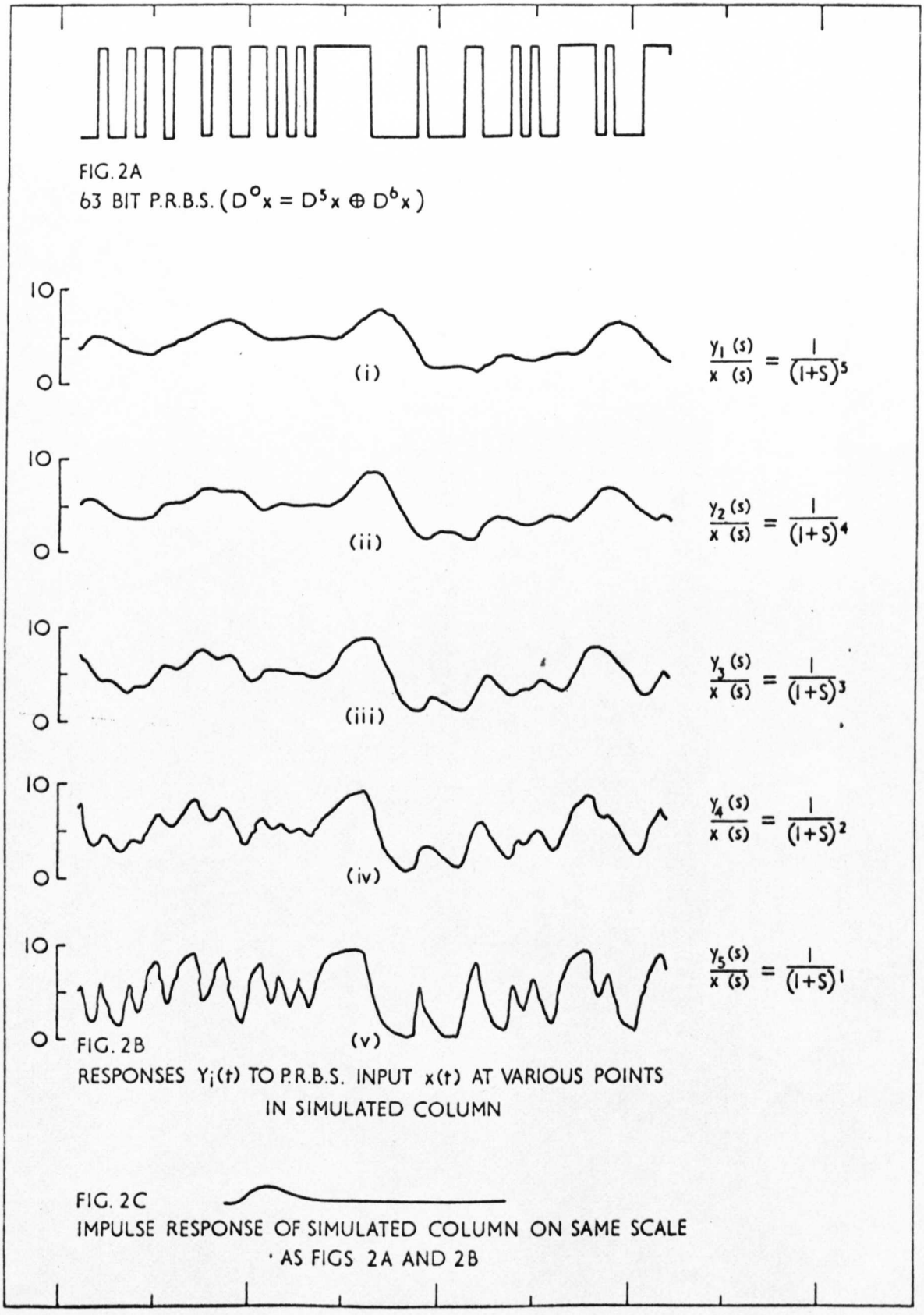
FIG. 2A
63 BIT P.R.B.S. ($D^0x = D^5x \oplus D^6x$)
10
0
(i)
$\frac{y_1(s)}{x(s)} = \frac{1}{(1+S)^5}$
10
0
(ii)
$\frac{y_2(s)}{x(s)} = \frac{1}{(1+S)^4}$
10
0
(iii)
$\frac{y_3(s)}{x(s)} = \frac{1}{(1+S)^3}$
10
0
(iv)
$\frac{y_4(s)}{x(s)} = \frac{1}{(1+S)^2}$
10
0
(v)
$\frac{y_5(s)}{x(s)} = \frac{1}{(1+S)^1}$
volts
FIG. 2B
RESPONSES $Y_i(t)$ TO P.R.B.S. INPUT $x(t)$ AT VARIOUS POINTS IN SIMULATED COLUMN
FIG. 2C
IMPULSE RESPONSE OF SIMULATED COLUMN ON SAME SCALE AS FIGS 2A AND 2B
0 1 2 3 4 5 6 7 8 9
TIME, seconds.
3658

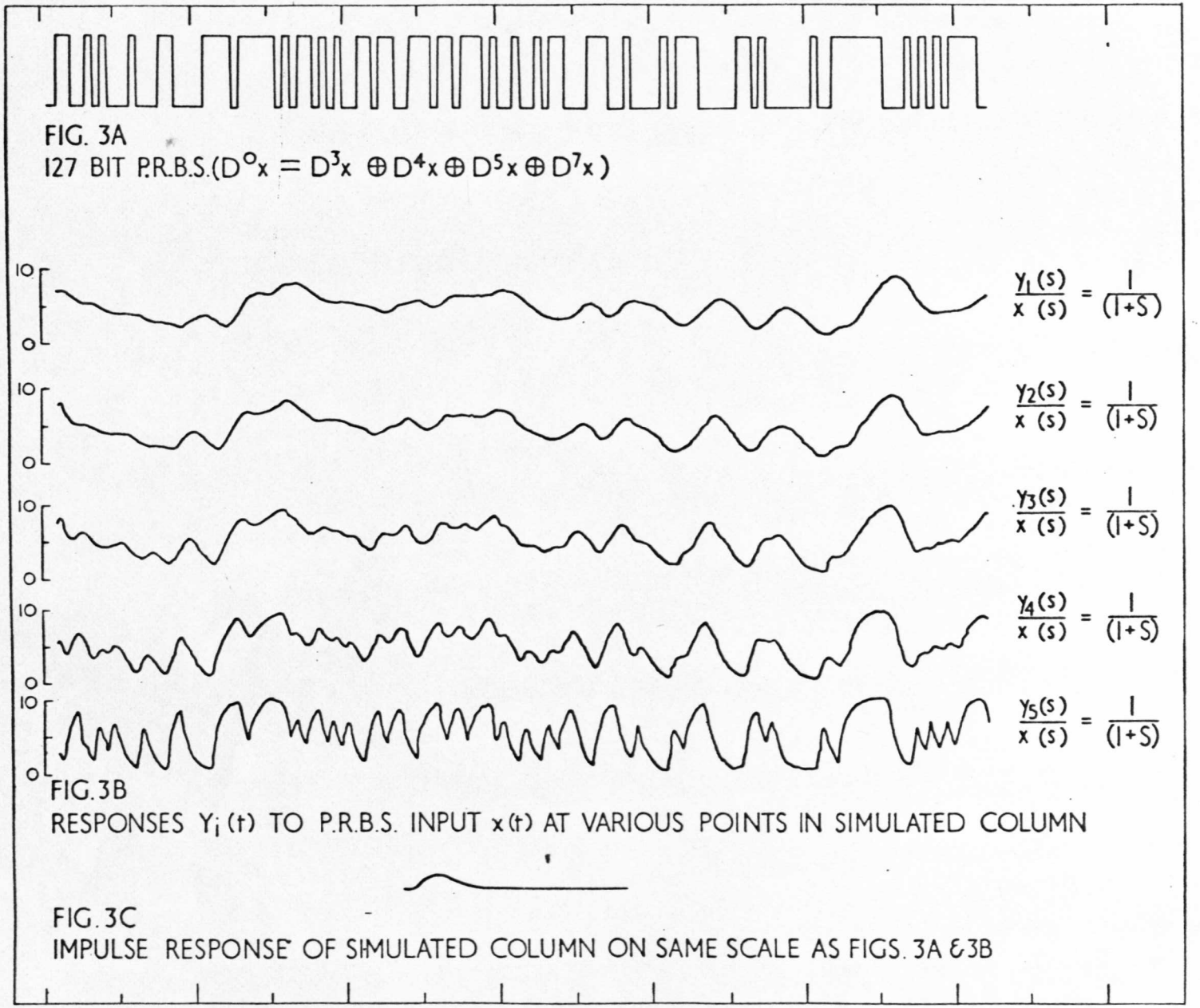
FIG. 3A
127 BIT P.R.B.S.($D^0x = D^3x \oplus D^4x \oplus D^5x \oplus D^7x$)
volts
10
0
$\frac{Y_1(s)}{x(s)} = \frac{1}{(1+S)}$
$\frac{Y_2(s)}{x(s)} = \frac{1}{(1+S)}$
$\frac{Y_3(s)}{x(s)} = \frac{1}{(1+S)}$
$\frac{Y_4(s)}{x(s)} = \frac{1}{(1+S)}$
$\frac{Y_5(s)}{x(s)} = \frac{1}{(1+S)}$
FIG. 3B
RESPONSES $Y_i(t)$ TO P.R.B.S. INPUT $x(t)$ AT VARIOUS POINTS IN SIMULATED COLUMN
FIG. 3C
IMPULSE RESPONSE OF SIMULATED COLUMN ON SAME SCALE AS FIGS. 3A & 3B
0 1 2 3 4 5 6 7 8 9 10 11 12 13 14 15
TIME, seconds.
3659